



UNIVERSITÀ
DEGLI STUDI
DI PADOVA

Sede Amministrativa: Università degli Studi di Padova

Dipartimento di *Ingegneria Civile, Edile ed Ambientale*

SCUOLA DI DOTTORATO DI RICERCA IN: Scienze dell'Ingegneria Civile ed Ambientale

CICLO XXV

**Seismic risk analysis of Revenue Losses, Gross Regional Product and
transportation system.**

Direttore della Scuola: Ch.mo Prof. Stefano Lanzoni

Supervisore: Ch.mo Prof. Carlo Pellegrino

Dottorando: Federico Carturan

CONTENTS

1	INTRODUCTION	1
1.1	Historical earthquakes	2
1.1.1	1989 Loma Prieta	2
1.1.2	1994 Northridge	3
1.1.3	Losses connected with earthquakes	6
1.2	State of the art	6
1.3	Objective and Scope	9
1.3.1	Known and Unknown	9
1.4	Organization of the Thesis	10
2	BACKGROUND	13
2.1	Statement of the problem	15
2.1.1	Seismic risk analysis for distributed systems	16
2.1.2	Seismic risk assessment for transportation network: Kiremidjian et al. approach	18
2.2	Earthquake modeling	19
2.2.1	Deterministic Seismic Hazard Analysis	20
2.2.2	Probabilistic Seismic Hazard Analysis	20
2.2.3	Earthquake source characterization	21
2.2.4	Spatial uncertainty	21
2.2.5	Size uncertainty	21
2.2.6	Gutenberg-Richter Recurrence Law	21
2.2.7	Characteristic earthquake recurrence law	22
2.2.8	Ground Motion Predictive relationships	23
2.2.9	Temporal uncertainty	23
2.3	Indirect losses	24
2.4	RiskUe projects	25
2.4.1	Procedure to define the risk in lifeline systems	26
2.4.2	Transportation system	28
2.4.3	Bridges vulnerability	28
2.5	Redars	29
2.6	Models	29
2.6.1	Bridges damage	29
2.6.2	Businesses damage	34
2.6.3	Residual functionality	34
2.6.4	Damage to transportation network	35
2.6.5	Post earthquake transportation demand	36
2.7	Transportation modeling	37
2.7.1	Supply model	38
2.7.2	Demand model	38
2.7.3	Equilibrium models	39
2.7.4	Topological model	39
2.7.5	Transportation network	39
2.7.6	Incidence matrix: links-paths	40
2.7.7	Link cost functions: B.P.R.	40
2.7.8	Frank and Wolfe algorithm	41
2.8	Monte Carlo method	44
2.8.1	General notes on the method	44
2.9	Testbed	47

Contents

3	MATERIALS, METHOD AND RESULTS	49
3.1	Earthquake scenarios	49
3.1.1	Previous study: Sleijko and Rebez 2002	51
3.1.2	Previous study: Peresan et al. 2009	52
3.1.3	Proposed methodology	52
3.2	Input data	53
3.2.1	Seismogenic sources	53
3.2.2	Recurrence law	54
3.2.3	Attenuation relationships	55
3.3	Earthquake scenario generation	56
3.3.1	Filtering scenarios	58
3.4	Loss of productivity	61
3.4.1	Fragility curves	63
3.4.2	Residual functionality	65
3.4.3	Computing Business damage scenario	66
3.4.4	Indirect economic losses	68
3.5	Time domain analysis	69
3.5.1	Recovery model	70
3.6	Cost benefit analysis	72
3.7	Relation Businesses–transportation system	74
3.7.1	Hypotheses	75
3.8	General loss model	76
3.9	Notes on parallelization	77
4	DISCUSSION	81
4.1	Conclusions	81
4.2	Future work	82

LIST OF FIGURES

Figure 1.1	The Richter magnitude 7.5 Messina earthquake and related tsunami caused up to 200'000 casualties on December 28, 1908 in Sicily and Calabria[4].	1
Figure 1.2	The San Francisco-Oakland Bay bridge suffered relatively minor damage. A 76-by-60-foot (23m x 15m) section of the upper deck on the eastern cantilever side crashed onto the deck below. The quake caused the Oakland side of the bridge to shift 7in (18cm) to the east. The quake caused the bolts of one section to shear off, sending the 250-short-ton (230t) section of roadbed crashing down like a trapdoor. This fault directly killed nobody, except for a driver bad instructed by road assistance personnel.	3
Figure 1.3	Failed support columns and collapsed upper deck of the Cypress Street Viaduct.	4
Figure 1.4	Detail of the bad anchorage of the rebar in Cypress Stree Viaduct.	4
Figure 1.5	State Route 1 collapsed in western Watsonville over Struve Slough after the 1989 Loma Prieta earthquake.	5
Figure 1.6	Northridge Earthquake, CA, January 17, 1994; Many roads, including bridges and elevated highways were damaged by the 6.7 magnitude earthquake. Approximately 114'000 residential and commercial structures were damaged and 72 deaths were attributed to the earthquake. Damage costs were estimated at 25 billion USD. FEMA News Photo, Author: Robert A. Eplett	5
Figure 1.7	Railway system in Italy, from OpenStreetMap Project.	6
Figure 1.8	The hazard map of Italy with 10% of probability of exceeding in 50 years.	9
Figure 2.1	The conceptual schema that starts from Shaking Scenario, computes business interruption and transportation system damages and, as final outcome, the earthquake risk.	15
Figure 2.2	The highway network in Los Angeles and Orange counties used in [8].	17
Figure 2.3	The methodology proposed by Kiremidjian et al in [21].	18
Figure 2.4	Conceptual schema for the estimation of indirect losses in the framework of Hazus.	25
Figure 2.5	Flowchart of RiskUe procedure for lifelines.	26
Figure 2.6	The workflow of REDARS for SRA on transportation networks	30
Figure 2.7	The data model for SRA in REDARS procedure	30
Figure 2.8	Excerpt from Hazus Technical manual [2] about the bridge classification.	32
Figure 2.9	Example of fragility curves as given in the Hazus manual[2]	34

List of Figures

- Figure 2.10 Generation of the transportation demand from node i to nodes j, k, m (on the left), and the corresponding T_{ij} entry on the OD matrix (on the right). 37
- Figure 2.11 The definition of the Topological model from the real network characteristics. Detail of the allowed and forbidden turns are inserted in a turn penalty file. 38
- Figure 2.12 A generic link cost function, where f is the flow on the link and c is the cost at the given flow f . As the link gets busy the cost increases due to mutual disturbance. 40
- Figure 2.13 The link cost function from B.P.R. as the value of capacity “ K ” increases, the cost of link is more stable. 41
- Figure 2.14 a) Determining the cost of each link at initialization iteration, b) Determining link cost function during the cycle 42
- Figure 2.15 43
- Figure 2.16 Monte Carlo method on the estimation of π with 1000 samples (on the left) the estimation is $\pi = 3,124$, while with 10'000 samples (on the right), the estimate is $\pi = 3,159$. Each time the simulation is run, due to its random number generation the result may slightly vary inside the confidence boundary. 45
- Figure 2.17 The test area is located on the north-east of Italy, it's a square of roughly 40 km x 40 km. 47
- Figure 3.1 The representation of aggregated hazard for different structural frequencies. From [12] and <http://zonesismiche.mi.ingv.it> 50
- Figure 3.2 A detail on the hazard for Veneto region computed on a 0.5" grid in ED50 datum 51
- Figure 3.3 A seismic scenario map representation from Sleijko and Rebez 2002[11]. 52
- Figure 3.4 Map of design ground acceleration (DGA) associated to an alarm in the Adria region. From Peresan et al. 2009 [28] 53
- Figure 3.5 Historical earthquakes from CPTI. 53
- Figure 3.6 a) Seismogenic zones using the ZS9 definition, inside the red box the testbed area. b) The comparison of ZS9 definite with DISS seismogenic zones. 54
- Figure 3.7 Recurrence relationship for seismogenic zones 905 and 906 the ones in the interest area. 55
- Figure 3.8 Plot of the chosen attenuation relationship (GMPE) from Sabetta and Pugliese 1996 [31]. 56
- Figure 3.9 The simulated epicenters plotted as red points on the map over the seismogenic zones. 57
- Figure 3.10 a) The proposed algorithm for the seismic scenario generation. b) A screenshot of the tool to generate seismic scenarios simulating a shakemap with epicenter in Montebelluna-Montereale, simulating maximum magnitude for the source: $M = 6.5$. 58
- Figure 3.11 In the figure is represented the hazard curve in red for a particular location, in this case Bridge # 1 location, blue the points represent all the accelerations from each seismic scenarios. 59

- Figure 3.12 For location Bridge #1 the hazard curve is represented in red, all scenarios are represented with gray dots, the chosen scenarios are represented with colored dot according to their cluster. 60
- Figure 3.13 The picture represents the mean value of each selected scenario for the locations corresponding to Bridge #1 and Bridge #31. The picture show a good accordance between the presented hazard curve and the selected scenario accelerations. 61
- Figure 3.14 The exposed risks. Red triangles are the bridges location, the blue squares the productive areas locations, the underling yellow areas are the seismogenic sources. 61
- Figure 3.15 The picture represents the conceptual schema of damage to productive system. The computes the state of damage using fragility curves, residual functionality is obtained using a model for the loss of functionality. The residual productivity is obtained. The module outputs can be used for different uses. 62
- Figure 3.16 A tilt up building during its construction. 63
- Figure 3.17 The fragility curve used to describe the seismic response of industrial buildings. 64
- Figure 3.18 Converge plot form Monte Carlo method of the definition of residual functionality. In the graph is represented the first earthquake scenario for business area #1. Iterations range from 10 to 100'000. 66
- Figure 3.19 Computed residual functionality with Monte Carlo method using 400 iterations. 67
- Figure 3.20 Risk curve in terms of business damage vs the probability of scenario. 67
- Figure 3.21 The first productive zone risk curve. The green line on the righthand side is the contribution of the zone to GRP, i.e. 22.4B EUR 68
- Figure 3.22 The risk curve of the residual GRP after the earthquake. 69
- Figure 3.23 a) The proposed recovery model in case of absence of external aids. b) The proposed recovery model with financial aids. 70
- Figure 3.24 The curves represent the recovery process in term of residual functionality vs. time. The black line represent the recovery process with no external financial aids, the red curve with external financial aids. 71
- Figure 3.25 The production during the recovery process expressed in terms of economic losses some representatives earthquake scenarios. 72
- Figure 3.26 Contribution to GRP of the productive area #1: Treviso in two hypotheses of financial aids, and without. The difference between the two set of bars is the positive contribution of financial aids. 73
- Figure 3.27 Cost benefit analysis. If the increase in GRP bar is higher than the aids cost bar, the operation is cost effective. 74
- Figure 3.28 Transportation module analysis schema. 76

List of Figures

- Figure 3.29 The partial Veneto transportation network topological model. The shaded area represents the analysis area where the earthquake scenarios are made and bridges damage are simulated. 77
- Figure 3.30 The figure represents the centroids in the transportation network in red diamonds. The yellow squares are the productive zones. The purple lines are the link of the transportation network. 78
- Figure 3.31 The figure shows the relation between the productive areas, as stars, and the centroids of the transportation model. The colors match the productive areas and the centroids. 78
- Figure 3.32 Risk in transportation network as delay due to damages to network. 79

ABSTRACT

Natural threats like earthquakes, hurricanes or tsunamis have shown serious impacts on communities. In the past, major earthquakes in the United States like Loma Prieta 1989, Northridge 1994, or recent events in Italy like L'Aquila 2009 or Emilia 2012 earthquake emphasized the importance of preparedness and awareness to reduce social impacts. Earthquakes impacted businesses and dramatically reduced the gross regional product. Seismic Hazard is traditionally assessed using Probabilistic Seismic Hazard Analysis (PSHA). PSHA well represents the hazard at a specific location, but it's unsatisfactory for spatially distributed systems. Scenario earthquakes overcome the problem representing the actual distribution of shaking over a spatially distributed system. The performance of distributed productive systems during the recovery process needs to be explored.

Scenario earthquakes have been used to assess the risk in bridge networks and the social losses in terms of gross regional product reduction. The proposed method for scenario earthquakes has been applied to a real case study: Treviso, a city in the North East of Italy. The proposed method for scenario earthquakes requires three models: one representation of the sources (Italian Seismogenic Zonation 9), one attenuation relationship (Sabetta and Pugliese 1996) and a model of the occurrence rate of magnitudes (Gutenberg Richter). A methodology has been proposed to reduce thousands of scenarios to a subset consistent with the hazard at each location. Earthquake scenarios, along with Mote Carlo method, have been used to simulate business damage. The response of business facilities to earthquake has been obtained from fragility curves for precast industrial building. Furthermore, from business damage the reduction of productivity has been simulated using economic data from the National statistical service and a proposed piecewise "loss of functionality model". To simulate the economic process in the time domain, an innovative businesses recovery function has been proposed.

The proposed method has been applied to generate scenarios earthquakes at the location of bridges and business areas. The proposed selection methodology has been applied to reduce 8000 scenarios to a subset of 60. Subsequently, these scenario earthquakes have been used to calculate three system performance parameters: the risk in transportation networks, the risk in terms of business damage and the losses of gross regional product. A novel model for business recovery process has been tested. The proposed model has been used to represent the business recovery process and simulate the effects of government aids allocated for reconstruction.

The proposed method has efficiently modeled the seismic hazard using scenario earthquakes. The scenario earthquakes presented have been used to assess possible consequences of earthquakes in seismic prone zones and to increase the preparedness. Scenario earthquakes have been used to simulate the effects to economy of the impacted area; a significant Gross Regional Product reduction has been shown, up to 77% with an earthquake with 0.0003 probability of occurrence. The results showed that limited funds available after the disaster can be distributed in a more efficient way.

ACKNOWLEDGMENTS

The authors gratefully acknowledge Fondazione Cassa di Risparmio di Padova e Rovigo for its financial support that made this work possible and the research to be carried on.

1 | INTRODUCTION

CONTENTS

1.1	Historical earthquakes	2
1.1.1	1989 Loma Prieta	2
1.1.2	1994 Northridge	3
1.1.3	Losses connected with earthquakes	6
1.2	State of the art	6
1.3	Objective and Scope	9
1.3.1	Known and Unknown	9
1.4	Organization of the Thesis	10

Natural hazard threaten life. Intense storms can damage farm and flood large areas, hurricanes proved to be very intense when dealing with complex modern cities, consider for a moment what the Katrina Atlantic hurricane did to the East coast in 2005. The hurricane disrupted electricity in the big city, but, other than coastal cities it destroyed several houses and facilities inland. It has been defined the deadliest and most destructive hurricane causing property damage for \$81 billion of 2005 USD. Last year, hurricane Sandy caused losses for \$50 billion of USD.



Figure 1.1: The Richter magnitude 7.5 Messina earthquake and related tsunami caused up to 200'000 casualties on December 28, 1908 in Sicily and Calabria[4].

On the other hand earthquakes proved to be even worse when dealing with losses, both in terms of life and monetary.

Earthquakes are known to cause injuries and death, they cause damage to road and bridges, general property damage, collapse or severe damage to buildings. After an earthquake the territory experiences diffuse fire, interruption of water supply, electrical outage, gas distribution disruption, sewage damage, transportation system disconnections. In addition to that, diseases can spread due to lack of hygienic supplies. When the epicenter is located offshore, a big displacement of seabed can produce a tsunami.

Government agencies along with the national protection agencies are involved in the process of supporting hit population and are required to rebuild infrastructure and housing and helping the economy to recover and restart.

Induced seismicity requires major attention. Let's think of large amount of water stored behind a dam, the earthquake could suddenly release it flooding and destroying large areas. The perforation of wells, coal mining and oil drilling are practices known to increase the consequences of an earthquake. As example, Sichuan earthquake was one of the most deadly earthquake of all times with 69'227 fatalities, the effect of the earthquake was increased by the resonant response of the water inside a dam over the underlying fault, this is a terrible example of induced seismicity.

The most noticeable effects of earthquakes are ground shaking and ground rupture. Along with that, landslides and avalanches are reported after an earthquake. The damage caused by shaking to both the electrical power and gas line frequently induces fire. The shaking effects in saturated granular soils can induce liquefaction and the consequent loss of bearing capacity.

In general terms, an earthquake may cause injuries and deaths, road and bridge damage, property damage of structures and content. Some earthquakes are followed by diseases that spreads after the quake.

As shown in table 1.1 when an earthquake hits a populated and developed area the property damage become consistent and, generally speaking, the direct losses in term of property damage are tens to hundreds of billions of USD. Magnitude isn't directly connected with the extent of damage, 1906 San Francisco earthquake of magnitude 7.8 caused 9.8 billions of actualized USD while 6.1 magnitude (almost 100 times smaller) 2012 Emilia earthquake caused 13.2 billions of USD of losses.

Rank	Name	Magnitude	Property damage USD
1	2011 Tohoku, Japan	9.0	122 billion
2	1995 Great Hanshin , Japan	6.9	100 billion
3	2008 Sichuan, China	8.0	75 billion
4	2010 Chile, Chile	8.8	15~30 billion
5	1994 Northridge, United States	6.7	20 billion
6	2012 Emilia, Italy	6.1	13.2 billion
7	2011 Christchurch, New Zealand	6.3	12 billion
8	1989 Loma Prieta, United States	7.0	11 billion
9	921 earthquake, Taiwan	7.6	10 billion
10	1906 San Francisco, United States	7.8	9.5 billion

Table 1.1: Property damage caused by earthquakes. Source:[1]

1.1 HISTORICAL EARTHQUAKES

The 9.03 M_w undersea Tohoku earthquake occurred in Japan in 2011, had a duration of 6 minutes and it's well remembered because of the tsunami wave that hit the coastal cities and induced a nuclear incident with radiation release. According to World Bank the total losses induced by that earthquake are of 235 billion USD. The World Bank economist, Vikram Nehru, states that after the Kobe 1995 earthquake Japan took one year to rebound its productivity back to 85% of normal level [20].

1.1.1 1989 Loma Prieta

In California the 1989 Loma Prieta earthquake was a major earthquake that struck San Francisco Bay area in the late afternoon. The earthquake lasted for 15 seconds with an intensity of 6.9 M_w . The quake killed 63 people in Northern California (57 by the jolt, the further 6 due to fatalities following the earthquake), and left 3'000-12'000 people homeless. The earthquake caused severe damage in some location in the San Francisco Bay Area, and it has been estimated that 11 billion USD was the total property damage.

Relief efforts were helped by private donation and by the relief package for California signed by former president George W. Bush.



Figure 1.2: The San Francisco-Oakland Bay bridge suffered relatively minor damage. A 76-by-60-foot (23m x 15m) section of the upper deck on the eastern cantilever side crashed onto the deck below. The quake caused the Oakland side of the bridge to shift 7in (18cm) to the east. The quake caused the bolts of one section to shear off, sending the 250-short-ton (230t) section of roadbed crashing down like a trapdoor. This fault directly killed nobody, except for a driver badly instructed by road assistance personnel.

On San Francisco–Oakland Bay bridge (Figure 1.2) one section collapsed and crashed onto the deck below.

The worst disaster of Loma Prieta earthquake was the collapse of the entire Cypress Street Viaduct (Figure 1.4) of 1880 in West Oakland: a failure of a 1.25 mile section that killed 42 people.

The Viaduct was built in late 1950s using reinforced concrete with non ductile design of sections and detailing. In 1977 a retrofitting was made, but did not fix the problem of possible buckling of the columns and didn't account the possible effects of the soil liquefaction. After the earthquake the complete rebuilding of the viaduct took 11 long years.

The BART¹ rail system was undamaged, but became soon congested as it was the quickest way to to San Francisco. In addition to BART, a disused transportation system revived: the Transbay Ferries service was re-activated during the closure of the Bay Bridge as alternative to the overcrowded BART.

The 1989 Loma Prieta showed the importance of the problem of transportation network failure under earthquake.

Along with this two major faults in bridges, other freeways experienced traffic problems, i.e. SR 480, I 280, U.S. Route 101, SR 17, SR 1. (Figure 1.5)

1.1.2 1994 Northridge

Later, in 1994 the Southern California "Northridge" earthquake hit the urban area of Los Angeles recording the strongest ground acceleration of 1.7g with a moment magnitude of 6.7M_w. The epicenter was in San Fernando Valley but the effects were felt in a radius of 85 miles(125km). The death

¹ Urban rail transportation system that serves the city of San Francisco and the Bay area



Figure 1.3: Failed support columns and collapsed upper deck of the Cypress Street Viaduct.



Figure 1.4: Detail of the bad anchorage of the rebar in Cypress Street Viaduct.

toll of Northridge earthquake is estimated between 60 and 75 casualties. 8'700 people were injured and 1'600 of them required hospitalization. The Northridge Fashion Center and California State University, Northridge also sustained very heavy damage with the most notably collapse of parking structures.

The earthquake gained worldwide media coverage because of a vast damage to freeway network that impacted the everyday life of millions of commuters. The most important damage was to I-10 Santa Monica Freeway that took three months to be repaired. Further north, the I-5 Golden State Freeway (Figure 1.6 , the collapsed bridge) and SR14 Antelope Valley freeway collapsed. The interchange was rebuilt one year later. It has been reported that the rail service was briefly interrupted.

The quake produced an unusually strong ground acceleration of 1.0g while damage was caused mainly by fire subsequent the earthquake and by landslides. Some estimates of the total damage range it as high as 25 billion USD.



Figure 1.5: State Route 1 collapsed in western Watsonville over Struve Slough after the 1989 Loma Prieta earthquake.



Figure 1.6: Northridge Earthquake, CA, January 17, 1994; Many roads, including bridges and elevated highways were damaged by the 6.7 magnitude earthquake. Approximately 114'000 residential and commercial structures were damaged and 72 deaths were attributed to the earthquake. Damage costs were estimated at 25 billion USD. FEMA News Photo, Author: Robert A. Eplett

Most of casualties and damages occurred in multi-story wooden buildings. In particular, buildings with an unstable first floor (such as the ones built on “pilotis”, the soft-floor) performed the worst. Numerous fires were also caused by broken gas lines from houses shifting off their foundations or unsecured water heaters tumbling. In the San Fernando Valley, several underground gas and water lines were severed, resulting in some streets experiencing simultaneous fires and floods. Damage to the system resulted in water pressure dropping to zero in some areas, predictably affecting fire-fighting operations. Five days after the earthquake it was estimated that between 40'000 and 60'000 customers were still without public water service. As typical in earthquakes, unreinforced masonry buildings and houses on steep slopes suffered more damage. This event was also connected with the unusual medical emergency: the spread of the Valley Fever disease.

1.1.3 Losses connected with earthquakes

It is evident that the earthquake induced risk must be assessed, estimated and evaluated in order to increase the preparedness, to retrofit unsafe structure and to increase the level of safety. Several elements contribute to this type of risk: casualties, direct economic losses of properties and indirect economic losses from the reduction of the productive capacity of industrial area.

On transportation side, the damage to network induces a bigger loss. According to ACI (Italian motor club) in Italy there are 3'983'502 trucks, that ship the 91% of the total 1'327 million of tons shipped every year (data from Istat: Italian National Statistical Institute). According to data from the minister of Transportation in Italy (published in 2004 CNIT report), there are 156 ports, 19'472 km of railroads and 837'493 km of public streets and 6'532 km of highways and 98 airports. In Italy in 2011 the Gross Domestic Product was of 2,19 trillions of USD.

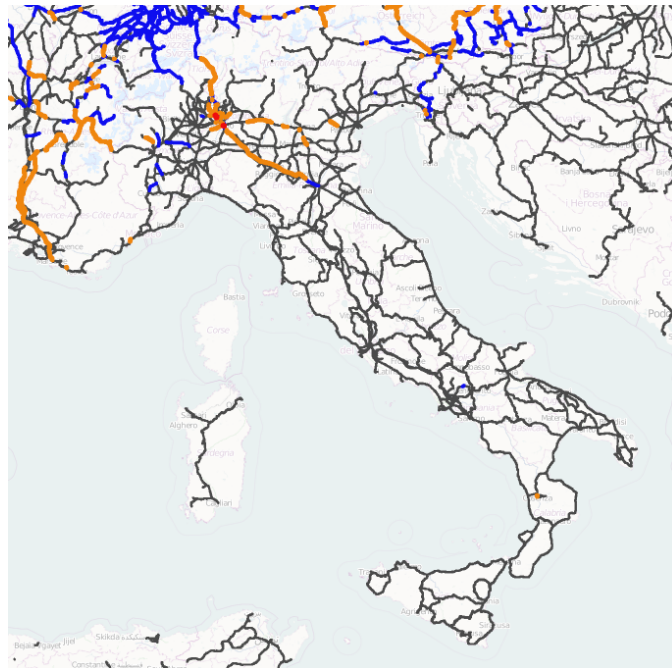


Figure 1.7: Railway system in Italy, from OpenStreetMap Project.

1.2 STATE OF THE ART

Earthquakes with epicenter close to urban areas, such as 1994 Northridge and 1995 Kobe earthquakes, have caused extensive physical damage to buildings and utility networks[8]. Damage to buildings resulted in significant direct losses (in terms of repair and replacement costs) and indirect losses (e.g. losses of decreased productivity). The performance of lifelines such as transportation, water, and electricity networks both immediately after the earthquake and after some time has effect on indirect economic losses. Among these lifelines, the transportation network is of critical importance since it provides the medium for transfer of personnel and materials required for recovery, repair and reconstruction. Moreover, recent

earthquakes have shown that transportation networks, in particular bridges, have high seismic vulnerability.

To be prepared for catastrophic events and reduce economic losses, it is peculiar to estimate the physical damage and economic losses from possible earthquakes with a good reliability. Since lifelines, like transportation networks, have a non linear behavior due to their intrinsic nature and the response to damage complex models are needed. Earthquake loss estimation involves many complexities and uncertainties related to earthquake occurrence, the effects of ground motion on buildings, and the resulting direct and indirect economic losses. The indirect economic losses depend not only on induced damage, but also on the post-earthquake recovery process and speed, which is affected, in turn, by limited capacity of the damaged network. The interaction among different economic sectors and geographic regions (mediated by the transportation network) makes it difficult to isolate regions or components of the system for analysis purposes. Due to these complexities, previous loss estimation studies have generally limited their scope and approach or confined themselves to a specific geographical scale.

When dealing with distributed systems and lifelines many factors affect the response of the system: the level of detail is limited by system size, by the big computational requirements involved in analysis, it has deal with the limited amount of available data. This section reviews some of the previous studies on regional loss estimation with a special regard to transportation networks. Some methodologies (e.g. ATC-13 or HAZUS) are comprehensive as they consider damage to buildings, bridges and utility network components and are not limited to building losses. Others concentrate on specific systems such as the transportation network (REDARS) or consider only selected loss components (HAZUS).

One of the earliest attempts of a comprehensive seismic loss estimation methodology is ATC-13, which has been developed in California. The ATC-13 methodology estimates earthquake damages and direct economic losses based on macroseismic intensity data and expert opinion. Moreover, ATC-13 concentrates on the estimation of damages and direct economic losses and does not deal with indirect losses or the effect of damage to transportation network but considers recovery time. ATC-13 also serves as the basis of more recent methodologies such as HAZUS, that is one of the most comprehensive regional loss estimation methodologies with the capability of application at different geographic scales. Rather detailed methods have been implemented to model ground motion, ground failures, and structural and nonstructural damages to buildings, the transportation network, and lifeline components. HAZUS also evaluates induced social and indirect economic losses. Indirect economic losses include changes in employment, loss in tax revenue, and production losses due to reduced demand. The only transportation related loss considered is the direct loss from damage to the transportation network. HAZUS lacks the capability to perform a transportation network analysis. Since transportation capacity constraints are not considered in the economic balancing process, indirect losses from commodity flow disruption, increased travel distances, and their evolution over time during the recovery phase are not evaluated. HAZUS is being increasingly used by the public sector in seismic risk analysis and policy decisions. For example, FEMA used HAZUS to evaluate the annualized losses for buildings in the US (FEMA- 366). The study used USGS seismic hazard maps and default parameters of HAZUS in calculating annualized losses.

In 1996 Basoz and Mander[27] made the first attempt to quantify the risk of a transportation network after an earthquake event for emergency planning purposes. Shinozuka in 2000 [32] looked at the performance of highway network in the Los Angeles area after the 1994 Northridge earthquake and proposed a probabilistic framework to predict the effect of bridge repairs after the event. In 2003 prof. Shinozuka and his team published another study for the same area. Using Monte Carlo simulation they estimate the damage of bridges and then run a simulation of the transportation network to evaluate consequences to the performance of the system. Cho et al. in 2001[9] developed a loss estimation methodology for the Los Angeles metropolitan region, where the earthquake impact on the transportation system and industrial sectors are modeled. Businesses in the affected region are assumed to interact through commodity flows on the urban transportation network. The reduced capacity of the transportation network along with the reduced transportation demand are considered. However, only recovery of the business firms is considered while recovery of the transportation network over time is modeled assuming damaged bridges closed for a period of one year. The use of models and data specific to southern California limits applicability beyond the Los Angeles region. Werner et al. in 2000[34] use a detailed transportation network model to estimate direct losses and indirect losses due to increased travel times, damage is estimated through fragility curves and uncertainty are explored through Monte Carlo simulation. Probability distributions of economic losses computed using seismic scenarios and by calculating the corresponding losses using Monte Carlo simulation. The recovery of transportation system is included for the transportation network, not considering damage to buildings environment and the associated changes in supply and demand in different economic sectors. Data requirements limit the scope of the approach to small regions. A. Kiremidjian [21] assessed the damage of the Bay Area transportation network bridges using four earthquakes scenarios and simulated the network performance using both fixed and variable post event trip demand. In the same study Authors address the problem of post event emergency response planning and present an example application to six hospitals located in the East Bay. Erdem Karaka in his PhD thesis examined, using anova techniques, the response of CSU region to earthquake events giving some details on how to model the problem[14]. In 2006 Moore et al.[25] explored the impact of electric power loss in the economy of Los Angeles and Orange County areas and on the transportation network. The Federal Emergency Management Agency developed Hazard U.S., written in short form as HAZUS, a software for risk mitigation and planning. The methodologies in[2]estimate the structural and the downtime losses to different systems after natural disasters; however, these methodologies do not have capabilities for transportation network post event analysis. Until recently, no software packages were available for the risk assessment of network systems. Absence of software packages means that researchers and practitioners need to develop their own models and assumptions. In an effort to overcome this lack of tools, the California Department of Transportation is developing software for Risk from Earthquake damage to Roadway Systems (REDARS). REDARS is a seismic risk analysis software package that estimates the structural and operational losses of transportation networks systems and is expected to enable California Department of Transportation (Caltrans) to improve its ability to plan for and respond to earthquake emergencies. Stergiou and Kiremidjian in 2006 proposed a framework for a probabilistic analysis of the problem

of calculation of risk in transportation network with a special attention to bridges and account the effects of shaking and liquefaction of soil[33].

1.3 OBJECTIVE AND SCOPE

The goal of the present thesis is to formulate a methodology to quantify the risk to transportation network and productive systems and explore their relations. In addition to the general practice that deals solely with direct structural losses, this work proposes an expandable framework that accounts for the operational loss caused by damage to network loss and by losses from reduced production. In addition to what has been done, the problem of the losses in Gross Domestic Product (GDP) due to damage to productive facilities is addressed. The present work addresses the problem of the transitory phase of the reconstruction process.

To test the applicability of the method, an analysis on the area of Treviso, in Veneto region on North-East Italy, has been done. The reduction of contribution from Treviso area to Gross Domestic Product(GDP) in terms of Gross Regional Product(GRP) is the result of the present analysis, along with the problem of relation to transportation network.

1.3.1 Known and Unknown

In Italy the Civil Protection agency required the production of the earthquake hazard maps (Figure 1.8). The assigned working group produced an aggregate hazard map [12] using the PSHA methodology proposed by Cornell in 1968 [10]. Further details will be given in section 3.2.1 .

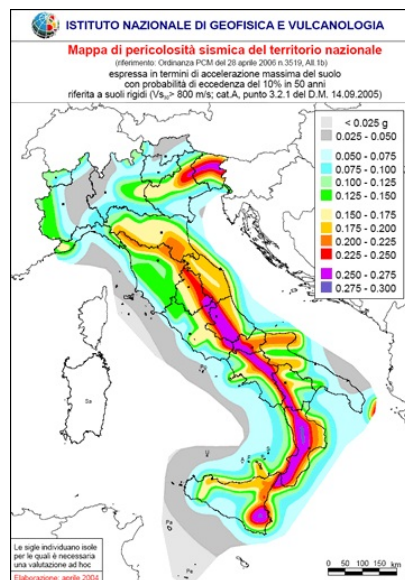


Figure 1.8: The hazard map of Italy with 10% of probability of exceeding in 50 years.

Some attempts have been made in past to analyze the effect of an earthquake to small transportation networks, but an approach to a regional transportation network with a fine detail (up to local streets) to observe the reduction of capacity in precise way has never been done before.

In Italy no seismic scenarios are publicly available, although hazard analysis are available for structural design purposes. To analyze the response of distributed systems, hazard consistent scenarios should be developed.

Risk analysis of complex areas is possible using the information from seismic scenarios together with information about the fragility of infrastructures and buildings.

Why it's important to conduct seismic risk scenarios analyses?

According to EERI[17], a scenario earthquake analysis can help in providing a common foundation for the analysis of the earthquake risk. It helps identifying the flaws of the system and enlightens its strengths. An earthquake scenario simulation helps in engaging and informing stakeholder and community decision makers. By simulating, it helps in examining the alternative futures. Lastly, it helps in testing and training people involved in the process and the broad audience.

What can be done to prevent damages from a catastrophic earthquake?

Traditional PSHA [10] is not enough to show the effect of earthquakes. From the physics of the system we know that waves travel from the ipocenter to buildings and lose some energy during their travel. PSHA is the best hazard analysis when dealing with a point system without spatial extension, but if the analysis is focused on a distributed system, scenario earthquakes are needed to account the spatial feature of the problem.

The present work addresses the lack of seismic scenarios to perform risk analysis in distributed systems. Here is presented a methodology to account the risk to transportation systems and business interruption of productive areas. The connection between the loss of regional product and the transportation system is shown. A novel model to represent the reconstruction process in time domain is presented. An estimate of the prioritization of the the government financial aids is given in the last part of the work with a benefit cost analysis.

The proposed procedure starts from acquiring data about the seismicity in the area of analysis. Data is processed to generate earthquake scenarios; to obtain the description of earthquake at each location of analysis. Using fragility curves the seismic performance of infrastructures is derived. Further models can relate the residual productivity of businesses and damage to transportation network. The two contribution are unified to obtain the seismic risk in terms of reduced revenue from businesses and increased travel cost in transportation network. The procedure can be used for optimization of budget, to perform benefit cost analysis, to assess the possible expenses in insurance market.

1.4 ORGANIZATION OF THE THESIS

The schema of the present work is organized as follows.

CHAPTER 1 Introduction of the problem. The chapter presents some background information about earthquakes, it presents the state of the art of the Seismic Risk Analysis and the scientific motivation of the work.

CHAPTER 2 covers the Basics of theory behind the problem. It states the problem in general terms, it deepens the problem of earthquake modeling, presents some previous work from which some models are drawn.

CHAPTER 3 deals with the materials and methods used in the present thesis starting from the general methodology, going through the problem of

development of a transportation network risk curve. Then it covers the availability of input data and describes the proposed algorithm to solve this problem. The chapter presents also the proposed models to account for the reduction of functionality of business areas, the reconstruction process and the model to account for the changes in both network and transportation demand after an earthquake. At the end of each module of the proposed methodology the results are summarized and some insights about the findings are presented.

CHAPTER 4 present the results of the work, explores possible applications of the proposed procedure and expresses some possible future works.

2 | BACKGROUND

CONTENTS

2.1	Statement of the problem	15
2.1.1	Seismic risk analysis for distributed systems	16
2.1.2	Seismic risk assessment for transportation network: Kiremidjian et al. approach	18
2.2	Earthquake modeling	19
2.2.1	Deterministic Seismic Hazard Analysis	20
2.2.2	Probabilistic Seismic Hazard Analysis	20
2.2.3	Earthquake source characterization	21
2.2.4	Spatial uncertainty	21
2.2.5	Size uncertainty	21
2.2.6	Gutenberg-Richter Recurrence Law	21
2.2.7	Characteristic earthquake recurrence law	22
2.2.8	Ground Motion Predictive relationships	23
2.2.9	Temporal uncertainty	23
2.3	Indirect losses	24
2.4	RiskUe projects	25
2.4.1	Procedure to define the risk in lifeline systems	26
2.4.2	Transportation system	28
2.4.3	Bridges vulnerability	28
2.5	Redars	29
2.6	Models	29
2.6.1	Bridges damage	29
2.6.2	Businesses damage	34
2.6.3	Residual functionality	34
2.6.4	Damage to transportation network	35
2.6.5	Post earthquake transportation demand	36
2.7	Transportation modeling	37
2.7.1	Supply model	38
2.7.2	Demand model	38
2.7.3	Equilibrium models	39
2.7.4	Topological model	39
2.7.5	Transportation network	39
2.7.6	Incidence matrix: links-paths	40
2.7.7	Link cost functions: B.P.R.	40
2.7.8	Frank and Wolfe algorithm	41
2.8	Monte Carlo method	44
2.8.1	General notes on the method	44
2.9	Testbed	47

Transportation is a derived demand. From its definition, transportation demand is an implicit demand to provide a service, to transform, buy or ship a good. The level of service of a network, after a seismic event, is given by the equilibrium between the demand and the supply.

The equilibrium equation account two terms; the supply is affected by the earthquake because it reduces the level of service of the network and the connectivity of the network; while on the other hand, the demand decreases (or in specific cases, it can increase due the effect of demand surge). The behavior of a transportation network is strictly related to the response of

its components this implies that damage of network component affects the performance of the whole network.

Determining the seismic risk is key step in the planning of the management of extreme event response. Seismic risk analysis is a tool that helps to obtain data and information about the risk itself and provides an estimation of the economy of the process.

The proposed methodology gives information about the performance of complex systems after an earthquake, this methodology can be expanded to be multi-perils and account different sources of hazard, e.g. floods, hurricanes, storms, etc.

The output of this procedure can be of interest for different stakeholders, different levels of the public administration can be interested; owners or manager of transportation network can use the procedure for planning purposes and national protection agencies can use this informations for rescue and preparedness.

With the outcomes of the proposed procedure it's possible to:

- determine the economic risk of an insurance company portfolio;
- improve the quality of insured risk by identifying its weakness;
- help the political decision makers to be aware when budgeting retrofitting policies;
- define the retrofitting priority of existing infrastructures;
- help the planning process of extension of a network to increase its redundancy to seismic action;
- to plan the transportation policies in post-event;
- and others that will be explained in the text.

The proposed procedure can be run off-line pre-event for economical analysis, or performed in real time for a quick estimation of the the most probable losses of an asset.

To analyze the problem there are four main steps:

1. Estimate the hazard of the region of study;
2. Analyze the fragility of the components of the system;
3. Define the residual functionality of components of the system;
4. Account the losses in terms of direct losses of properties, indirect losses due to increased travel time and losses of productivity due to damage to productive infrastructures.

The proposed methodology is multi-disciplinary because different expertise are required to understand the problem from specific point of view, earth scientists, engineers, data modelers, urban planners, economists. The procedure is composed in several moduli to understand the complexity of the problem, each one of the to model a specific component of the problem; each module can be improved, updated, implemented without affecting the functionality of the rest of the procedure. Since the big number of elements involved in the analysis a big amount of data is generated. Some specific output are chosen to represent a specific feature of the problem, anyway thanks to its modular design, the procedure can show data in different shapes according to the role of the user.

To summarize, the procedure can be used to:

- In finance by insurers, lenders, building stock managers, investment funds on properties, etc. to calculate the risk as economic exposure of their portfolio.
- In public agencies for planning before the earthquake:
 - define the strengths and the weakness of the system,
 - give an estimation of the effect of different policies in the system,
 - to plan the future expansion,
- for civil protection finalities, after the quake to:
 - evaluate the possible expenditures for the insurance and re-insurance market,
 - give a quick estimation of damage to property and infrastructure
 - serve as a tool to plan the emergency response both from the humanitarian and economic view

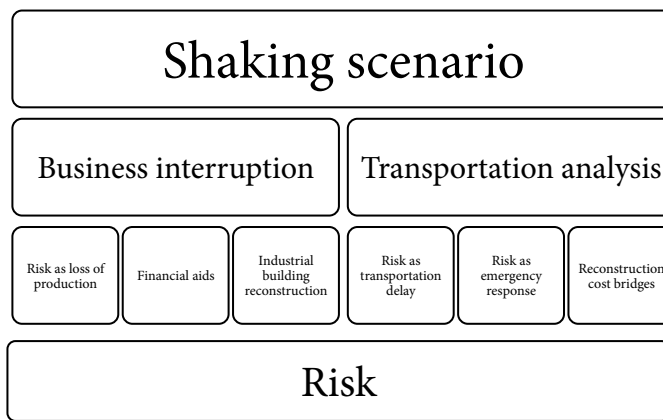


Figure 2.1: The conceptual schema that starts from Shaking Scenario, computes business interruption and transportation system damages and, as final outcome, the earthquake risk.

2.1 STATEMENT OF THE PROBLEM

As past earthquakes have shown, earthquake induced losses can be categorized in two types: direct and indirect losses. In the same way seismic risk assessment needs to account these two categories: *Direct losses* are the economical loss due to collapse or damage of infrastructure or building, *Indirect losses* are related to the purpose that the particular infrastructure or building serves, for a bridge the indirect loss refers to increase in travel time in the transportation that the specific bridges belongs or the inaccessibility of a location; in case of industrial building the indirect cost is the loss of profit connected with the scope that serves the building. In the later case, a building can have moderate damage but be assessed as unsafe for occupants; in this case people cannot work inside due to security issues and the production is stopped. Two examples of indirect losses have been shown.

According to Jelienek and Krasumann [19], risk in abstract terms is the product of hazard, vulnerability and exposure as in equation (1). This definition can be applied to different type of hazard (i.e. earthquake as in

the present work, floods, hurricanes, structural reliability); the relation has a general meaning and applicability to different risk analyses.

$$R = H \times V \times E \quad (1)$$

where:

- R is Risk
- H is a description of Hazard
- V is a measure of the vulnerability due to the specified Hazard level, in general terms $V(H)$
- E is the economic value of exposed goods, defined as Exposure, in general terms can be $E(V, H)$

2.1.1 Seismic risk analysis for distributed systems

In 2000 Chang, Shinozuka and Moore [8] published a foundation paper for Seismic Risk Analysis (shortened in "SRA") for spatially distributed systems. The paper addresses the problem of performing seismic risk analysis on distributed systems and specifically addresses problems that arise from the spatial feature of the problem. First, the spread in space of a set of infrastructures is the key characteristic that invalidates the efficacy of PSHA [10] or DSHA. That type of analysis has been conceived for a point infrastructure, for this reason the paper proposes an extension of PSHA to spatially distributed systems. Authors underline that the correlation between different location is the key to perform SRA for distributed systems. As first step they develop a set of deterministic earthquake scenarios and then assign the probability of occurrence of each scenario from geological characteristics of faults. They prove that these scenarios are hazard consistent with the hazard maps derived from USGS. The set of earthquake scenarios has been made using EPEDAT by Eguchi et al. [13]. Using the acceleration of scenarios and fragility curves they build damaged networks where a transportation analysis is run.

According to FEMA the benefit of a mitigation measure is considered cost-effective if the expected benefit exceeds costs, the problem is expressed in equation (2).

$$B_t = \int_h [L_0(h, x) - L_R(h, z)] \cdot p(h, x) \quad (2)$$

where:

- B_t total Benefit from mitigation intervention
- x a specific site where the analysis is done
- h a measure of earthquake hazard, such as PGA
- $L_0(h, x)$ loss at site x , given a specific hazard level h , without mitigation
- $L_R(h, x)$ loss at site x , given a specific hazard level h , with mitigation
- $p(h, x)$ annual probability of an earthquake that produces a specified hazard level at site x

Equation (2) needs a modification to be extended to the context of spatially distributed systems risk analysis.

The probabilistic hazard is discretized to indicate individual scenario earthquakes and the loss is measured for the entire system, rather than at a particular site. The expected annual benefit for mitigation of equation (2) can be rewritten as:

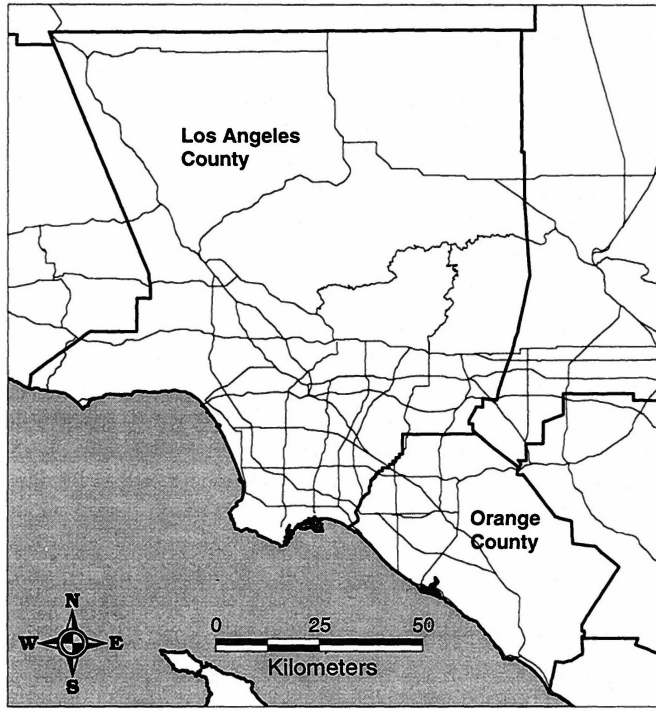


Figure 2.2: The highway network in Los Angeles and Orange counties used in [8].

$$B_t = \sum_{i=1}^N (L(S_0|Q_i) - L(S_R|Q_i)) \cdot p_i \quad (3)$$

where:

- B_t total Benefit from mitigation intervention
- N total number of possible earthquakes
- L loss of functionality
- S_0 system performance without mitigation
- S_R system performance with mitigation
- Q_i i -th possible earthquake
- p_i annual probability of i -th possible earthquake

Authors suggest that a smaller subset of scenario earthquakes may be used to reduce computation times to a reasonable extent but retaining the same accuracy to fully represent the risk curve choosing only some hazard consistent scenarios.

The paper presents also a model to relate the damage index of bridges to the link damage index, with this model it's possible to build earthquake degraded networks.

$$D_l = \sqrt{\sum_{g=1}^{G_l} \delta_{gl}^2} \quad (4)$$

where:

- D_l link damage index on link l
- G_l total number of bridges on link l
- δ_{gl} bridge damage index, bridge g on link l

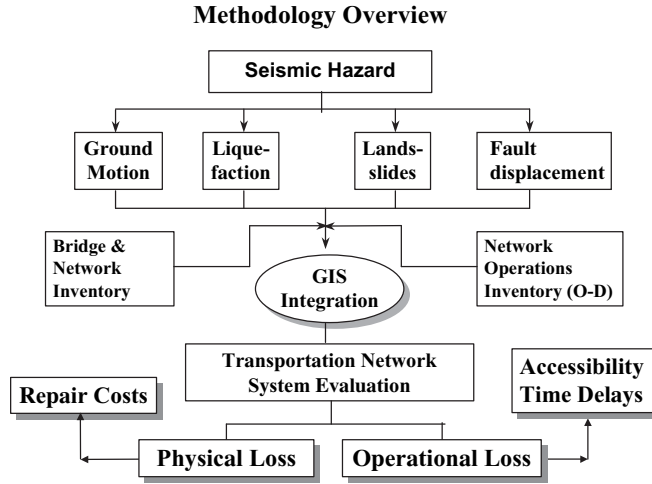


Figure 2.3: The methodology proposed by Kiremidjian et al in [21].

2.1.2 Seismic risk assessment for transportation network: Kiremidjian et al. approach

In 2007 Kiremidjian et al. published a work on seismic risk assessment in transportation network systems[21]. The authors present a work on estimation of losses due to earthquake to transportation systems accounting the integrated effect of ground shaking, liquefaction and landslides at network component level and system level. The risk from earthquakes to transportation systems is evaluated in terms of direct loss from damage to bridges and travel delays in the transportation network. The damage and loss to bridges from ground shaking from ground displacement, from liquefaction and from landslides are computed for a 7.0 scenario earthquake. The authors present the transportation network damage analysis using a fixed demand (i.e. the pre-earthquake demand) and a variable (post-event degraded) demand. Their findings show that travel times remain relatively unchanged or decrease with variable demand assumption. The method they propose is tested on San Francisco bay area.

The proposed formal approach by Kiremidjian et al. (shown in figure 2.3) is summarized by equation (5) .

For a given earthquake event Q_i the total losses $E[\text{Loss}]$, i.e. the sum of direct and increase of network travel time are:

$$E[\text{Loss} = Q_i] = \int_0^1 l(D|Q_i) \cdot f_D(d|Q - i) dd + \int_0^1 l(t|Q_i) \cdot f_D(d|Q - i) dd \quad (5)$$

where:

- $l(D|Q_i)$ Cost of repair of components
- $f_D(d|Q - i)$ Probability density of Damage D due to an event Q_i
- $l(t|Q_i)$ Cost associated with time delays

For a specific set of earthquakes each one of them with a specific occurrence rate ν_i the risk becomes:

$$E[\text{Loss} = Q_i] = \sum_{\text{allevents}} E[\text{Loss}|Q_i] \cdot \nu_i = \sum_{\text{allevents}} \nu_i \int_0^1 l(D|Q_i) \cdot f_D(d|Q-i) dd + \int_0^1 l(t|Q_i) \cdot f_D(d|Q-i) dd \quad (6)$$

At this point integral in equation (6) is split into three parts to account for shaking, liquefaction and landslide. The analysis follows with the application to San Francisco Bay area using one scenario earthquake.

Authors estimate the repair cost as in equation (7), where the repair cost is a function of the damage.

$$l(D|Q_i) = \text{Repair Cost} = \text{Repair Cost Ratio} \cdot \text{Area} \cdot \text{Cost} \quad (7)$$

In the application to Bay Area in San Francisco, where is susceptible of liquefaction. In this case losses induced by liquefaction dominate the risk as shown in table 2.1 .

Ground shaking only	Shaking + liquefaction	Shaking + landslides
494'046 USD	1'392'593	571'497

Table 2.1: The losses in Bay area application divided according to cause in application by Kiremidjian et al. 2007 [21].

2.2 EARTHQUAKE MODELING

The performance of a social system subject to earthquake has a complex response due to its intrinsic complex nature. The system can be observed from several point of views. From the structural engineering point of view the damage to structure as buildings or bridges can be interesting and enough for the purpose. Others can study the performance of utilities, their related disruptions and effects to society as discomfort. Moreover, others can observe the performance of the transportation system and the flow redistribution. From the economic point of view an interesting topic can be the loss of productivity of the region stroke by the earthquake. In this study two different point of view have been merged, the transportation performance has been simulated with the residual productivity of the region stroke by the earthquake, the relation between the two systems has been investigated and a model to account the connection between the two systems has been proposed. The present problem has been divided into four parts.

The first part deals with construction of hazard consistent seismic scenarios, that are needed for seismic risk analysis.

The second part explores the effect of the seismic action to industrial facilities and proposes several models to relate the seismic action as input to the residual production in monetary terms.

The third part of the work deals with the consequences to the transportation system. Given the seismic scenario, total network performance is represented as a consequence of the transportation demand assigned to the damaged network.

The forth, and last, part deals with the reduction of transportation demand and the assignment of this varied demand to a damaged transportation network that concludes the work with the computation of seismic risk.

(Adapted from Kramer 1996 [22].)

2.2.1 Deterministic Seismic Hazard Analysis

At the beginning of earthquake engineering the prevalent type of analysis was the deterministic, due to its simplicity in calculation and results.

A Deterministic Seismic Hazard Analysis (DSHA) involves the development of a particular seismic scenario upon which a ground motion hazard evaluation is based. A typical DSHA can be described as a four-step process (as in Jayaram 2010 [18]) consisting of:

- Identification and characterization of all earthquakes sources capable of producing significant ground motion at the site. Source characterization includes the definition of each source's geometry (the source zone) and earthquake potential.
- Selection of a source-to-site distance parameter for each zone. In most cases the shortest source to site distance is used.
- Selection of the controlling earthquake (i.e. the earthquake that is expected to produce the strongest level of shaking), generally, expressed in terms of some ground motion parameter, at the site. The selection is made easy by comparing the levels of shaking produced by earthquakes (from step 1) assumed to occur at the distances identified in step 2. The controlling earthquake is described in terms of size and distance from the site.
- The hazard at the site is formally defined, usually, in terms of the ground motion produced at the site by the controlling earthquake. Its characteristics are usually described by one or more ground motion parameters obtained from predictive relationships. Peak acceleration, peak velocity, and response spectrum ordinates are commonly used to characterize the seismic hazard.

Concluding, DSHA is the best tool to obtain the worst case scenario for design of structures.

2.2.2 Probabilistic Seismic Hazard Analysis

The use of probabilistic concepts allowed to account uncertainties in the size, location, and rate of recurrence of earthquakes and the variation of ground motion characteristics with earthquake size and location.

Probabilistic Seismic Hazard Analysis (PSHA) provided a framework in which these uncertainties can be identified, quantified, and combined in a rational manner to provide a more complete picture of the seismic hazard.

Cornell in 1968 described the methodology to perform PSHA [10].

The PSHA can also be described as a procedure in four steps (according to Reiter 1990 [29]), where each step has some degree of similarity to the steps of the DSHA procedure.

1. The first step is identification and characterization of earthquake sources, with the probability distribution of potential rupture locations within the source. These distributions are combined with the source geometry to obtain the corresponding probability distribution of source-to-site distance.

2. Next, the seismicity or temporal distribution of earthquake recurrence must be characterized. A recurrence relationship, which specifies the average rate at which an earthquake of some size will be exceeded, is used to characterize the seismicity of each source zone.
3. The ground motion produced at the site by earthquakes of any possible size occurring at any possible point in each source zone is determined with the use of predictive relationships (GMPE). The uncertainty inherent in the predictive relationship is also considered in PSHA.
4. Finally, the uncertainties in earthquake location, earthquake size and ground motion parameter prediction are combined to obtain the probability that the ground motion parameter will be exceeded on a particular time period (e.g. 10% of exceeding probability in 50 years, i.e. a Return Time of 475 years).

2.2.3 Earthquake source characterization

Characterization of an earthquake source requires consideration of the spatial characteristics of the source and the distribution of earthquakes within that source, of the distribution of earthquake size for each source, and of the distribution of earthquakes with time. Each of these spatial characteristics involves some degree of uncertainty.

2.2.4 Spatial uncertainty

For the purposes of seismic hazard analysis, the source zones may be similar to or somewhat different than the actual source, depending on the relative geometry of the source and site of interest and on the quality of the information about the sources. For example, a relatively short fault from a site can be modeled as a point since the distance can be assumed constant. Earthquakes are assumed to be uniformly distributed within a particular source zone (i.e. earthquakes are considered equally like to occur at any location). The attenuation relationship needs a source to site distance, that has its own uncertainty, the uncertainty in source to site distance can be described by a probability density function.

2.2.5 Size uncertainty

All source zones have a maximum earthquake magnitude potential that cannot be exceeded. In general, the source zone will produce earthquakes of different size up to the maximum earthquake, with smaller earthquakes occurring more frequently than larger ones. The strain energy may be released a-seismically or in form of earthquakes; assuming that all strain energy is released by earthquakes of magnitude from 5.5 to 9.0 and that the average fault displacement is one half the maximum surface displacement the size of earthquake can be defined by a mechanical model.

2.2.6 Gutenberg-Richter Recurrence Law

Gutenberg and Richter gathered data for Southern California earthquakes over a period of many years and organized the data according to the number

of earthquakes that exceeded different magnitudes during that time period. They divided the number of exceedance of each magnitude by the length of the time period to define a mean annual rate of exceeding λ_m of an earthquake of magnitude m . As would be expected, the mean annual rate of small earthquakes is greater than that of large earthquakes. The reciprocal of the annual rate of exceeding for a particular magnitude is commonly referred to as the return period of earthquakes exceeding that magnitude. When the logarithm of the annual rate of exceeding of southern California earthquakes was plotted against earthquake magnitude a linear relationship was observed as shown in equation (8).

$$\log \lambda_m = a - b \cdot m \quad (8)$$

Where λ_m is the mean annual rate of earthquakes of magnitude m , and 10^a is the mean yearly number of earthquakes of magnitude greater than or equal 0, and b describes the relative likelihood of large and small earthquakes. As the b value increases, the number of larger magnitude earthquakes decreases compared to those of smaller magnitude.

The a and b parameters are generally obtained by regression on a database of seismicity for the zone of interest.

Unless the zone is particularly active, the database is likely to be relatively sparse. Since the use of both instrumental and historical events is usually required, the database may contain both magnitude and intensity data, necessitating the conversion of one measure of size to the other. In some areas, the record of seismicity may be distorted by the presence of dependent events such as after-shocks and fore-shocks. Although such events can cause significant damage, PSHA is intended to evaluate the hazard from discrete, independent release of seismic energy. Therefore, dependent events must be removed from the seismicity database and their effects accounted in separate analyses.

Completeness of the database must also be considered.

Fitting a straight line such as that implied by the Gutenberg-Richter law through recurrence data in which the mean rate of exceeding of small earthquakes is underestimated will tend to flatten the line.

Seismogenic sources have a limit in their earthquake potential, this means that the GR relationship should be limited by an upper bound like m_{max} .

The standard GR relationship can be trimmed in order to account the maximum event and to exclude events with a lower intensity:

m_0 will be the lower magnitude accounted while m_{max} is the maximum expectable event, equation (8) is re-arranged as (9). The shape of the model is curved on logarithmic plot, while the previous expression was linear.

$$\lambda_m = v \cdot \frac{\exp(-\beta(m - m_0)) - \exp(-\beta(m_{max} - m_0))}{1 - \exp(-\beta(m_{max} - m_0))} \quad (9)$$

with the constraint $m_0 \leq m \leq m_{max}$ and $\beta = 2.303 \cdot b$.

2.2.7 Characteristic earthquake recurrence law

The Gutenberg Richter law was developed for a set of regional seismicity data that may include many different seismic sources. Since PSHA are usually conducted for a specific site rather than large regions, the earthquake generating characteristics of individual faults is important.

Paleoseismic studies indicate that individual points on faults and faults segments move by approximately the same distance in each earthquake. This has been interpreted to suggest that individual faults repeatedly generate earthquake of similar (within about one-half magnitude unit) size, known as characteristic earthquakes at, or near, their maximum magnitude.

Alternatively, the apparently repetitive nature of fault movement at individual points may be controlled by localized geological constraints and, consequently, not reflect earthquake magnitude very accurately. Resolution of these alternative interpretations awaits further paleoseismic research.

By dating characteristic earthquakes, their historical rate of occurrence can be estimated. Geologic evidence indicates the characteristic earthquakes occur more frequently than would be implied by extrapolation of the GR law from high exceeding rates (low magnitudes) to low exceeding rates (high magnitudes). The result is a more complex recurrence law that is governed by seismicity data at low magnitudes and geological data at high magnitudes.

2.2.8 Ground Motion Predictive relationships

The predictive relationships are nearly always obtained empirically from least square regression on a particular set of strong motion data. Since then, some amount of scattering is always present in data. This scatter results from randomness in the mechanism of rupture and from variability and heterogeneity of the source, travel path, and site condition.

Scatter in data can be quantified by confidence limits or by standard deviation of the predicted parameter. Reflecting the form of the most common predictive relationships, the standard deviation of the natural logarithm of the predicted parameter is usually computed. This considerable uncertainty must be accounted in computation of the seismic hazards.

The probability that a particular ground motion parameter Y exceeds a certain value, y^* , for an earthquake of given magnitude, m , occurring at a given distance, r , in probabilistic terms is given by (10)

$$P[Y > y^* | m, r] = 1 - F_Y(y^*) \quad (10)$$

where $F_Y(y)$ is the value of CDF of Y at m and r .

2.2.9 Temporal uncertainty

To calculate the probabilities of various hazards occurring in a given time period, the distribution of earthquake occurrence with respect to time must be considered. Earthquakes have long been assumed to occur randomly with time, and in fact, examination of available seismicity record has revealed little evidence of temporal patterns in earthquake recurrence. The assumption of random occurrence allows the use of simple probability models, but it's inconsistent with the implications of elastic rebound theory.

The temporal occurrence of earthquakes is most commonly described by a Poissonian process. The Poisson model provides a simple framework for evaluating probabilities of events that follows a Poisson process, one that yields values of a random variable describing the number of occurrences of a particular event during a given time interval or in a specified spatial region. Since PSHAs deals with temporal uncertainty the spatial application of the Poisson model will not be considered further.

Poisson processes possess the following properties:

1. The number of occurrences in one time interval are independent of the number that occur in any other time interval.
2. The probability of occurrence during a very short time interval is proportional to the length of the time interval.
3. The probability of more than one occurrence during a very short time interval is negligible.

These properties indicate that the events of a Poisson process occur randomly, with "no memory" of the time, size, or location of any precedent event. For a Poisson process, the probability of a random variable N , repeating the number of occurrences of a particular event during a given time interval is given by:

$$P[N = n] = \frac{\mu^n e^{-\mu}}{n!} \quad (11)$$

where μ is the average number of occurrences of the event in that time interval. The time between events in a Poisson process can be shown to be exponentially distributed. To characterize the temporal interval distribution of earthquake recurrence for PSHA purposes, the Poisson probability is usually expressed as (12) .

$$P[N = n] = \frac{(\lambda t)^n e^{-\lambda t}}{n!} \quad (12)$$

where λ is the average rate of occurrence of the event and t is the time period of interest. Note that the probability of occurrence of at least one event in a period of time t is given by (13) .

$$P[N \geq 1] = P[N = 1] + P[N = 2] + \dots + P[N = \infty] = 1 - P[N = 0] = 1 - e^{-\lambda \cdot t} \quad (13)$$

When the event of interest is the exceeding of a particular earthquake magnitude, the Poisson model can be combined with a suitable recurrence law to predict the probability of at least one exceeding in a period of t years by the expression (14) .

$$P[N \geq 1] = 1 - e^{-\lambda_m \cdot t} \quad (14)$$

2.3 INDIRECT LOSSES

The problem of business damage is complex due to the very inter-related nature of economic processes. Business damage contributes to the definition of risk because it's the main component of indirect losses along with the increase in travel time in transportation networks. The main theory behind economic loss modeling is the equilibrium between supply and demand. Direct damage to properties and pre-event economic conditions (unemployment rate, import-export balance, the shape of the economic system) are the main feature of the problem. The possible funding by state in form aids after seismic event can condition the process. As past earthquakes revealed the magnitude of indirect losses is usually 10 to 100 times the direct loss.

It is well known that an earthquake can cause effects also on un-affected economic sectors due to business relation causing the effect known as “ripple effect”. All businesses are known to be both *forward linked* and *backward linked*. The forward link represents the businesses need to sell their product, the demand can come from the affected region or outside. The backward link expresses the fact that each business needs raw material or semi-worked goods to produce its products. The best model to account this effect would be a micro-economics model that simulates the relation between businesses or sectors of activity. It’s interesting to note that, if previous agreements are made, the failure in supply of product could imply to pay a penalty. Some industries in the supply chain for the automotive market were declared failed due to the payment very high penalties that was unsustainable.

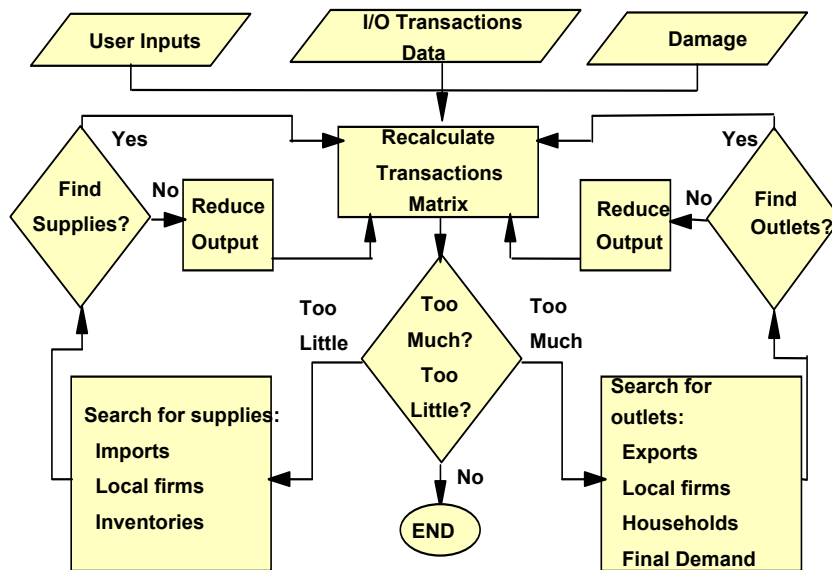


Figure 2.4: Conceptual schema for the estimation of indirect losses in the framework of Hazus.

2.4 RISKUE PROJECTS

In Europe a project on “assessment of risk in European cities” has been founded by European Commission during the FP6, this project is: “An advanced approach to earthquake risk scenarios with applications to different European towns” [26]. The main objective of the project was to estimate the risk of European towns, to increase the awareness of population on risk management procedures and to increase awareness of political managers in risk reduction. The idea was to simulate earthquake scenarios to get data about damages, casualties, economical impacts, direct and indirect costs to give city managers tools to improve their ability to manage extreme case scenarios when dealing with risks. A main work package of the project was about the definition of seismic hazard in European towns; the outcome of this scenario was a group of maps to represent earthquake scenarios.

This project developed some seismic hazard maps using the deterministic and the probabilistic approach, it then presented a comparison of the results of the two procedures. The main scope of this work package was the

definition of quantitative description of the scenarios using homogeneous parameters to describe the seismic hazard.

The WP6 of the project dealt with lifelines. It particularly it studied the functionality of water supply, of waste management, energy, telecommunication and transportation system. These system play a key role in the emergency management and in community functionality, they help to save human lives and prevent more damage to properties.

Usually the spatial characteristic of the lifelines goes behind the urban boundaries, with a specific discrepancy between demand and supply (consider the water supply system, water is produced in a location and then used miles away.) These systems are made up of networks of connected point and line infrastructures in a strong relation between them. These systems are interconnected, and their relations are hard to understand and forecast.

For each of these lifelines some common traits can be defined to describe their performances:

- compile an inventory of elements at risk;
- define seismic hazard and shaking scenarios;
- elaborate fragility models;
- compute recovery models;

2.4.1 Procedure to define the risk in lifeline systems

The procedure proposed in RiskUe project can be explained as shown in figure 2.5 .

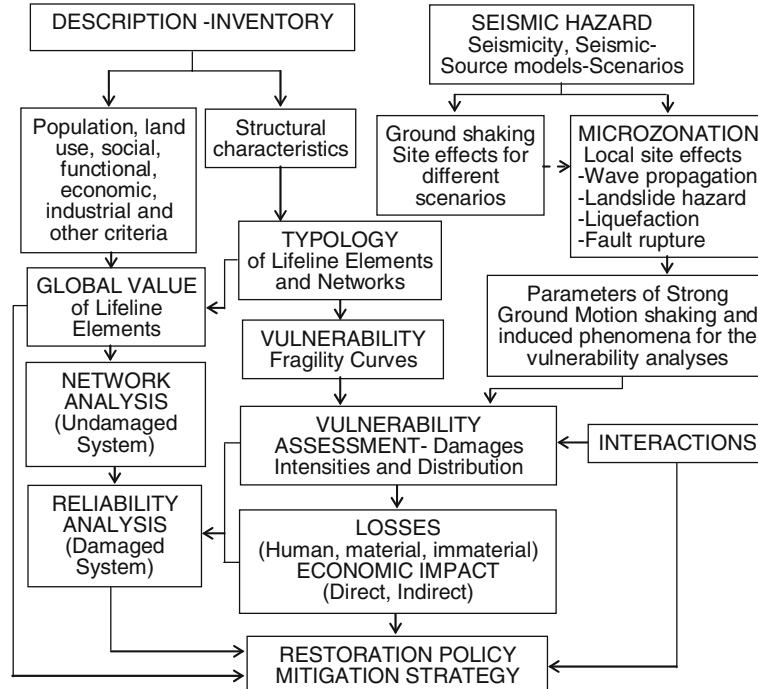


Figure 2.5: Flowchart of RiskUe procedure for lifelines.

According to [26] lifelines present the following characteristics:

- spatial distribution in a very large area, where supply and demand are not located in the same area;
- the structure is made up of different nodes and links connected together with multiple critical elements;
- each network has a specific group of characteristics that make their description complex;
- some network have a specific redundancy that lowers the vulnerability, like the interconnection between power lines and every re-routing according to the geometry;
- most networks are inter-dependent, due to this feature special attention is required in the evaluation of risk.

Lifelines are particularly exposed to earthquake, principal damages to this type of infrastructure are due to ground shaking, liquefaction, slope instability and permanent ground deformation.

In accordance to Hazus [2], RiskUe states that the most common description of performance after earthquake of lifelines is made by the use of fragility curves, and particularly five damage states are defined:

1. No damage
2. Slight
3. Moderate
4. Extensive
5. Complete

In addition to these performance level other information are needed to describe the residual level of service. The first parameter to account is the definition of the residual degree of functionality; i.e. complete functionality that mens no damage or cosmetic damage; damage factor and its replace or repair cost expressed as a percentage from 0% to 100%.

The consequences can be assessed also in terms of injuries to people, damage to non structural components or direct economic losses related to replace or repair of the component. The indirect losses can arise from the loss of productivity and loss of profit, or can be related to the sensation of fear, uncertainty or other psychological reasons. The losses due to environmental damage, pollution and etc. are even harder to estimate.

The main requirement of this procedure is the ability to judge the performance of a damaged component in relation to the level of seismic action that he experienced. Usually this relation is described by mean of a probabilistic relationship that relates the residual functionality to shaking intensity, and the several other models that accounts the relation between the residual functionality and the economic losses. Typically the relation between the intensity measure of the action and the state of damage is given by the mean of probabilistic fragility curves; these are log-normal curves where descriptive parameters like mean and dispersion are computed from regression of historical data.

Along with the fragility curves, in order to describe the recovery process, the functional recovery curves are defined. To account for the recovery transitory, some specific times need to be defined. The first time is the "normal"

condition. This is how the component or the system behave during normal times. The second time is the “recovery” time; during recovery time the system has been stroke by the earthquake but activities are recovering, housing is recovering. This is a transition time between the pre-earthquake conditions and complete restoration after the quake. On more specific time is the so-called “day zero”. Day zero is the immediate post earthquake; one can find still the ruins on the streets, rescue team trying to help people and emergency restoration of services.

2.4.2 Transportation system

Among other lifelines the transportation system is one of the most critical because it allows to rescue people in need, to ship good, to satisfy the basic need of transportation for various reasons, both work-related or for leisure.

The transportation system usually is made up of:

- roads;
- bridges;
- tunnels.

Other structural construction can be accounted:

- slopes;
- river banks;
- retaining walls;
- accessory buildings (warehouse, toll booth, etc.).

Past experiences showed that damages to transportation systems has a severe impact on the local economy, to the recovery process and on recovery operations.

Based on historical data infrastructures can be ranked according to their vulnerability level with respect to ground shaking. The most vulnerable are bridges, followed by river banks or retaining walls and lastly tunnels. In urban areas the main cause to road un-availability is the presence of debris from the collapse of buildings.

2.4.3 Bridges vulnerability

As previously mentioned, bridges are the most vulnerable elements in transportation systems, usually their redundancy is none. The damage to a bridge implies a long detour and an increase in total transportation time.

RiskUe procedure is derived from Hazus, and describes bridges according to the following set of parameters:

- material;
- structural schema;
- type of piles;
- type of bearings;
- slab continuity;

- code of design;
- span number;
- skewness angle;
- span length;
- pile height;
- number of expansion joints;
- type of foundation system.

Given the information from historical earthquakes typical bridge damages can be:

- damage to approaching slabs;
- collapse of the slab due to unseating or excessive displacements;
- damage to piles due to excessive bending moment or shear demand;
- damage to foundation due to high shear demand.

The procedure to account the vulnerability of bridges follows as shown in 2.6.1 .

2.5 REDARS

In California several studies have been made to assess the transportation network post-earthquake functionality. A tool for California has been developed by Werner et al. [34], the tool is called REDARS 2. The technical manual present a possible definition of the problem of definition of a seismic risk analysis on transportation systems. In figure 2.6 the conceptual model of the software is described. A following schema about a possible workflow to define the recovery is shown in figure 2.7

2.6 MODELS

2.6.1 Bridges damage

The damage of bridges in transportation network is modeled using fragility curves as described in Hazus methodology [2]. The transportation module accounts the possible damage to three key elements of transportation infrastructures: road, bridges and tunnels. For each component of the transportation system the relation between damage index DI and earthquake intensity IM is given by the mean of fragility curves:

$$DI = f(IM) \quad (15)$$

where:

DI is damage index

IM is a certain intensity measure of earthquake(PGA,Sa,PGD,PGV).

BACKGROUND

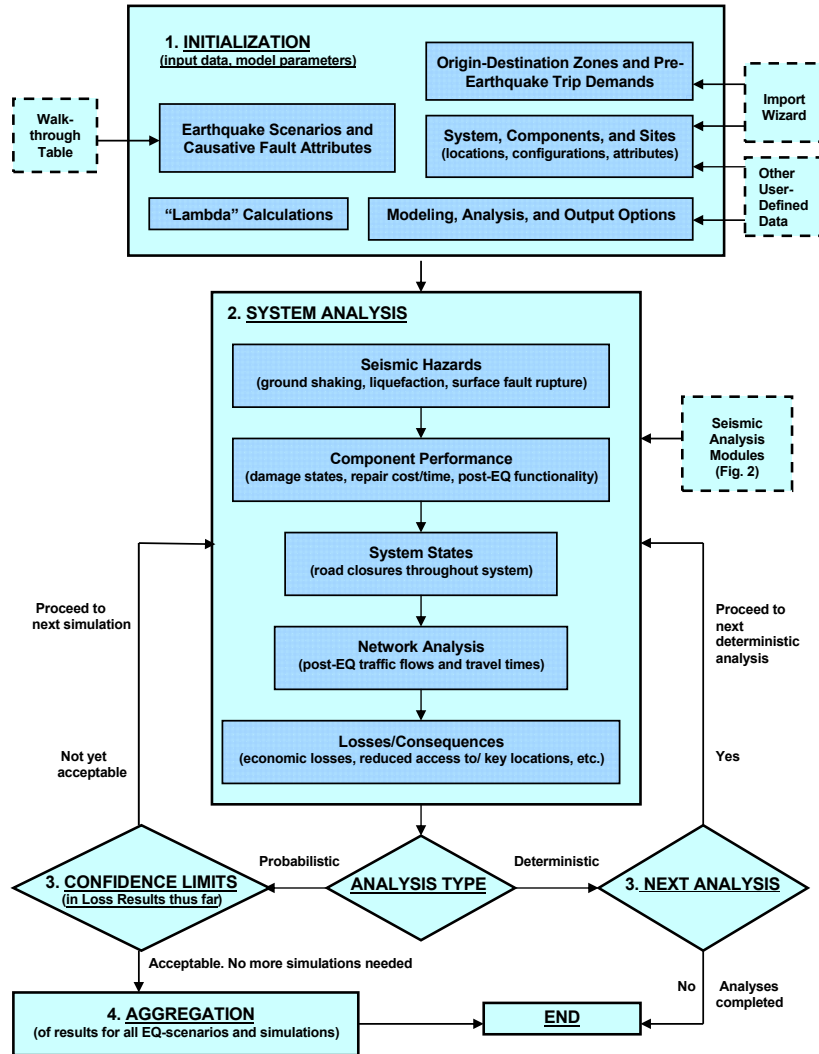


Figure 2.6: The workflow of REDARS for SRA on transportation networks

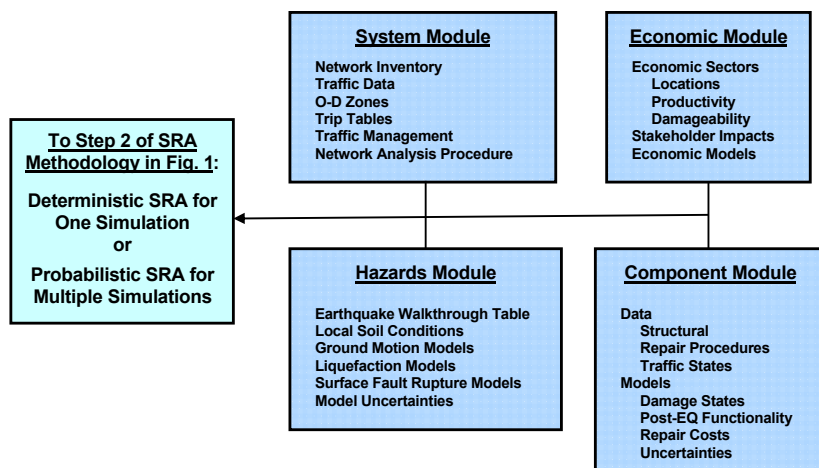


Figure 2.7: The data model for SRA in REDARS procedure

The fragility curves for bridges are defined by a set of parameters that account for the geographical position, the typology, the mechanical characteristics. Data about damage is inferred from the NBI (National Bridge Inventory) using the following parameters:

- seismic design of the bridge;
- number of spans: one span or multiple spans;
- material: concrete, steel, others;
- type of piles: mono-columns, multi-columns, abutments;
- type of bearing and seismic isolation;
- if the static scheme is continuous or simply supported.

The functional form for fragility curve is a cumulate log-normal distribution:

$$P[ds|PGA] = \Phi \left[\frac{1}{\beta_{ds}} \ln \left(\frac{PGA}{PGA_{d,ds}} \right) \right] \quad (16)$$

Where:

- β is the standard deviation of the natural logarithm of PGA of damage state, ds
- Φ is the standard cumulative log-normal distribution function

The table in figure 2.8 allows to classify bridges according to Hazus methodology.

Hazus procedure suggest a five steps procedure to evaluate bridge fragility:

STEP 1 As first step gather all data about position, bridge class, span number, skewness angle, span length, bridge width.

STEP 2 Evaluate quake intensity at bridge location, in temrs of PGA, spectral accelerations ($S_a[0.3s]$ e $S_a[1.0s]$), PGD.

STEP 3 Determine updating parameters

$$\begin{cases} K_{skew} = \sqrt{\sin(90 - \alpha)} \\ K_{shape} = 2.5 \times \frac{S_a(1.0s)}{S_a(0.3s)} \\ K_{3D} = 1 + A/(N - B) \end{cases} \quad (17)$$

STEP 4 Update the base fragility parameters according to the following rule:

$$\begin{cases} \text{New Median}_{slight} = \text{Old Median} \times \text{Factor}_{slight} \\ \text{New Median}_{moderate} = \text{Old Median} \times K_{skew} \times K_{3D} \\ \text{New Median}_{extensive} = \text{Old Median} \times K_{skew} \times K_{3D} \\ \text{New Median}_{complete} = \text{Old Median} \times K_{skew} \times K_{3D} \end{cases} \quad (18)$$

where: $\text{Factor}_{slight} = 1$ if $I_{shape} = 0$ else $\min(1, K_{shape})$

STEP 5 Using the updated mean values along with dispersion $\beta = 0.6$ evaluate each damage level probabilities according to quake level.

BACKGROUND

CLASS	NBI Class	State	Year Built	# Spans	Length of Max. Span (meter)	Length less than 20 m	K _{SD} (See note below)	I _{shape} (See note below)	Design	Description
HWB1	All	Non-CA	< 1990		> 150	N/A	EQ1	0	Conventional	Major Bridge - Length > 150m
HWB1	All	CA	< 1975		> 150	N/A	EQ1	0	Conventional	Major Bridge - Length > 150m
HWB2	All	Non-CA	>= 1990		> 150	N/A	EQ1	0	Seismic	Major Bridge - Length > 150m
HWB2	All	CA	>= 1975		> 150	N/A	EQ1	0	Seismic	Major Bridge - Length > 150m
HWB3	All	Non-CA	< 1990	1		N/A	EQ1	1	Conventional	Single Span
HWB3	All	CA	< 1975	1		N/A	EQ1	1	Conventional	Single Span
HWB4	All	Non-CA	>= 1990	1		N/A	EQ1	1	Seismic	Single Span
HWB4	All	CA	>= 1975	1		N/A	EQ1	1	Seismic	Single Span
HWB5	101-106	Non-CA	< 1990			N/A	EQ1	0	Conventional	Multi-Col. Bent, Simple Support - Concrete
HWB6	101-106	CA	< 1975			N/A	EQ1	0	Conventional	Multi-Col. Bent, Simple Support - Concrete
HWB7	101-106	Non-CA	>= 1990			N/A	EQ1	0	Seismic	Multi-Col. Bent, Simple Support - Concrete
HWB7	101-106	CA	>= 1975			N/A	EQ1	0	Seismic	Multi-Col. Bent, Simple Support - Concrete
HWB8	205-206	CA	< 1975			N/A	EQ2	0	Conventional	Single Col., Box Girder - Continuous Concrete
HWB9	205-206	CA	>= 1975			N/A	EQ3	0	Seismic	Single Col., Box Girder - Continuous Concrete
HWB10	201-206	Non-CA	< 1990			N/A	EQ2	1	Conventional	Continuous Concrete
HWB10	201-206	CA	< 1975			N/A	EQ2	1	Conventional	Continuous Concrete
HWB11	201-206	Non-CA	>= 1990			N/A	EQ3	1	Seismic	Continuous Concrete
HWB11	201-206	CA	>= 1975			N/A	EQ3	1	Seismic	Continuous Concrete
HWB12	301-306	Non-CA	< 1990			No	EQ4	0	Conventional	Multi-Col. Bent, Simple Support - Steel
HWB13	301-306	CA	< 1975			No	EQ4	0	Conventional	Multi-Col. Bent, Simple Support - Steel
HWB14	301-306	Non-CA	>= 1990			N/A	EQ1	0	Seismic	Multi-Col. Bent, Simple Support - Steel
HWB14	301-306	CA	>= 1975			N/A	EQ1	0	Seismic	Multi-Col. Bent, Simple Support - Steel
HWB15	402-410	Non-CA	< 1990			No	EQ5	1	Conventional	Continuous Steel
HWB15	402-410	CA	< 1975			No	EQ5	1	Conventional	Continuous Steel
HWB16	402-410	Non-CA	>= 1990			N/A	EQ3	1	Seismic	Continuous Steel
HWB16	402-410	CA	>= 1975			N/A	EQ3	1	Seismic	Continuous Steel

CLASS	NBI Class	State	Year Built	# Spans	Length of Max. Span (meter)	Length less than 20 m	K _{SD} (notes below)	I _{shape} (notes below)	Design	Description
HWB17	501-506	Non-CA	< 1990			N/A	EQ1	0	Conventional	Multi-Col. Bent, Simple Support - Prestressed Concrete
HWB18	501-506	CA	< 1975			N/A	EQ1	0	Conventional	Multi-Col. Bent, Simple Support - Prestressed Concrete
HWB19	501-506	Non-CA	>= 1990			N/A	EQ1	0	Seismic	Multi-Col. Bent, Simple Support - Prestressed Concrete
HWB19	501-506	CA	>= 1975			N/A	EQ1	0	Seismic	Multi-Col. Bent, Simple Support - Prestressed Concrete
HWB20	605-606	CA	< 1975			N/A	EQ2	0	Conventional	Single Col., Box Girder - Prestressed Continuous Concrete
HWB21	605-606	CA	>= 1975			N/A	EQ3	0	Seismic	Single Col., Box Girder - Prestressed Continuous Concrete
HWB22	601-607	Non-CA	< 1990			N/A	EQ2	1	Conventional	Continuous Concrete
HWB22	601-607	CA	< 1975			N/A	EQ2	1	Conventional	Continuous Concrete
HWB23	601-607	Non-CA	>= 1990			N/A	EQ3	1	Seismic	Continuous Concrete
HWB23	601-607	CA	>= 1975			N/A	EQ3	1	Seismic	Continuous Concrete
HWB24	301-306	Non-CA	< 1990			Yes	EQ6	0	Conventional	Multi-Col. Bent, Simple Support - Steel
HWB25	301-306	CA	< 1975			Yes	EQ6	0	Conventional	Multi-Col. Bent, Simple Support - Steel
HWB26	402-410	Non-CA	< 1990			Yes	EQ7	1	Conventional	Continuous Steel
HWB27	402-410	CA	< 1975			Yes	EQ7	1	Conventional	Continuous Steel
HWB28										All other bridges that are not classified

Figure 2.8: Excerpt from Hazus Technical manual [2] about the bridge classification.

Class	Sa(1.0s) for ground shaking				PGD [in] ground failure			
	Slight	Moderate	Extensive	Complete	Slight	Moderate	Extensive	Complete
HWB1	0.40	0.50	0.70	0.90	3.90	3.90	3.90	13.80
HWB2	0.60	0.90	1.10	1.70	3.90	3.90	3.90	13.80
HWB3	0.80	1.00	1.20	1.70	3.90	3.90	3.90	13.80
HWB4	0.80	1.00	1.20	1.70	3.90	3.90	3.90	13.80
HWB5	0.25	0.35	0.45	0.70	3.90	3.90	3.90	13.80
HWB6	0.30	0.50	0.60	0.90	3.90	3.90	3.90	13.80
HWB7	0.50	0.80	1.10	1.70	3.90	3.90	3.90	13.80
HWB8	0.35	0.45	0.55	0.80	3.90	3.90	3.90	13.80
HWB9	0.60	0.90	1.30	1.60	3.90	3.90	3.90	13.80
HWB10	0.60	0.90	1.10	1.50	3.90	3.90	3.90	13.80
HWB11	0.90	0.90	1.10	1.50	3.90	3.90	3.90	13.80
HWB12	0.25	0.35	0.45	0.70	3.90	3.90	3.90	13.80
HWB13	0.30	0.50	0.60	0.90	3.90	3.90	3.90	13.80
HWB14	0.50	0.80	1.10	1.70	3.90	3.90	3.90	13.80
HWB15	0.75	0.75	0.75	1.10	3.90	3.90	3.90	13.80
HWB16	0.90	0.90	1.10	1.50	3.90	3.90	3.90	13.80
HWB17	0.25	0.35	0.45	0.70	3.90	3.90	3.90	13.80
HWB18	0.30	0.50	0.60	0.90	3.90	3.90	3.90	13.80
HWB19	0.50	0.80	1.10	1.70	3.90	3.90	3.90	13.80
HWB20	0.35	0.45	0.55	0.80	3.90	3.90	3.90	13.80
HWB21	0.60	0.90	1.30	1.60	3.90	3.90	3.90	13.80
HWB22	0.60	0.90	1.10	1.50	3.90	3.90	3.90	13.80
HWB23	0.90	0.90	1.10	1.50	3.90	3.90	3.90	13.80
HWB24	0.25	0.35	0.45	0.70	3.90	3.90	3.90	13.80
HWB25	0.30	0.50	0.60	0.90	3.90	3.90	3.90	13.80
HWB26	0.75	0.75	0.75	1.10	3.90	3.90	3.90	13.80
HWB27	0.75	0.75	0.75	1.10	3.90	3.90	3.90	13.80
HWB28	0.80	1.00	1.20	1.70	3.90	3.90	3.90	13.80

Table 2.2: Mean values for each bridge class according to Hazus fragility estimation procedure [2]

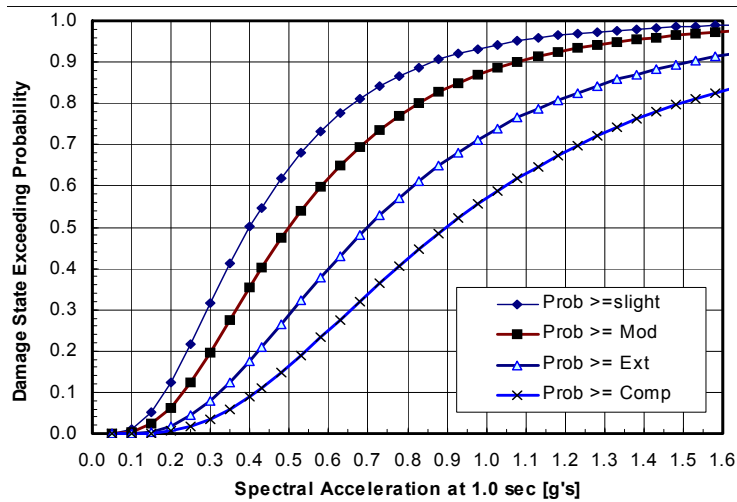


Figure 2.9: Example of fragility curves as given in the Hazus manual[2]

2.6.2 Businesses damage

To be consistent with the model adopted for bridges, damage to business is computed following the same approach, i.e. the fragility curves express damage as a function of the seismic action.

Fragility curves for industrial buildings are derived from the Hazus procedure. Fragility curves will be further sampled to obtain the probability of each one of the four damage states according to level of earthquake.

For the specific problem is assumed that the fragility of the most common building of the stock represents the fragility of the entire stock. This assumption is necessary because there's not enough data to particularize fragility curves for each and every business.

In north-east Italy, productive buildings are generally made of pre-cast concrete, while other areas are built using steel or wooden frames. For the specific application concrete pre-cast, tilt up building have been assumed for the description of the fragility of productive areas.

2.6.3 Residual functionality

Sensibly, residual functionality of a productive building is strongly bonded to the damage state of the building where the production is made.

Given that, in present work authors decided to adopt a step model. It has been noted that productive plants with no damage, maintain the production as if no-earthquake occurred. If the damage is slight, some minor repairs are needed and the reduction of productivity is very low, ranging from 10% to 30%. If the damage is moderate, the work needed to restore the buildings is harder and lowers more the production, almost it cuts in half the residual productivity of the area. If the area suffered a stronger stroke, only few building are in condition to allow the production; this can be accounted with a reduction around 80%. If the buildings are collapsed the production is no longer possible; the proposed model assumes that residual functionality is null. A description of the residual functionality model is given at page 66 with figure 3.6 .

2.6.4 Damage to transportation network

The problem of network damage is quite complex since it deals with modeling of the reduction of supply in problem of transportation equilibrium.

It's necessary to build damaged networks, where each link supported or overpassed by a bridge express a reduction in its functionality due to its damage state.

The solution of this problem has been realized using two matrices to represent the belonging of a bridge to a specific link. Matrix $A_{L \rightarrow B}$ express the correspondence of Links to Bridges, while the transpose of the matrix represents the correspondence of Bridges to Links: $A_{L \rightarrow B}^T = A_{B \rightarrow L}$. The correspondence expressed by this matrix is: one-to-many, since each link can have multiple bridges; from this follows that A is non-invertible, i.e. $A \neq A^{-1}$.

To the extent that the network description in present model is very fine and local roads are modeled, it's important to note that if a bridge collapse over a road that road is not transit able. To account this effect two incidence matrices are given; the first express the incidence of bridges that belong to a specific road:

$$A_{L \rightarrow B}^{\text{belong}} \quad (19)$$

while a different matrix account the bridges that overpass other links.

$$A_{L \rightarrow B}^{\text{overpass}} \quad (20)$$

In the present problem $A_{L \rightarrow B}^{\text{overpass}}$ is much sparser than $A_{L \rightarrow B}^{\text{belong}}$.

The following model has been adapted from Shinozuka et al. 2000[32] and Chang et al. 2000[8] as described in paragraph 2.1.1. The description of the link damage is provided by a vector defined LDI, that is Link Damage Index, as:

$$LDI_l = \sqrt{\frac{\sum_{p=1}^{n_{\text{BRIDGES}}} \alpha_{l,p} BDI_p^2}{\|n_{\text{BRIDGES}}\|}} \quad (21)$$

where:

LDI is Link Damage Index, an index vector that stores, for each iteration, the damage of specific link

p is the summation index over the total number of bridges that have a relation with Link l , from 1 to n_{BRIDGES}

$\alpha_{l,p}$ is the entry of incidence matrix to relate link l to bridge p

BDI_p is the p -th bridge on link l .

It should be noted that it's necessary to normalize the summation of the BDI over each link because the number of bridges that are related to each link can vary greatly and induce errors in definition of LDI.

The composition of LDI_l follows the rule:

$$LDI_{l,s} = \begin{cases} \text{if } LDI_{\text{overp},s}^2 \geq LDI_{\text{collapse}}^2 \rightarrow \sqrt{LDI_{\text{bel},s}^2 + LDI_{\text{overp},s}^2} \\ \text{if } LDI_{\text{overp},s}^2 < LDI_{\text{collapse}}^2 \rightarrow \sqrt{LDI_{\text{bel},s}^2} \end{cases} \quad \forall \text{ link} \quad (22)$$

The conversion from literal damage of bridges is made as:

while the link damage index is converted as follows.

Description	BDI
No damage	0,00
Minor	0,10
Moderate	0,30
Extensive	0,75
Collapse	1,00

Table 2.3: Bridge Damage Index BDI

Once the bridge damage has been obtained to build a damaged network it's essential to define a model to reduce the level of service of each network link.

From definition of link damage index the damaged network will be altered as:

Link functionality reduction	
No damage	100
Minor damage	100
Moderate damage	50
Major damage	1
Collapse	1

Table 2.4: Link functionality reduction model

The presented functionality reduction is translated into reduction of network level of service as:

100% FUNCTIONALITY The level of service of the link is identical of its state pre-earthquake, no reductions will be applied.

50% FUNCTIONALITY The chosen reduction, after a discussion with network managers, has modeled as:

1. Reduction of free-flow speed to a limited value of 30 km/h (18.6 mph)
2. Reduction of free flow time according to new speed limit
3. Freight truck detour, due to lowered level of reliability of bridges.

1% FUNCTIONALITY This state is a complete loss of functionality, the link is closed and traffic needs to detour. The closure of the link is obtained via the penalty method, so the free flow time is such high that no vehicles choose that route.

2.6.5 Post earthquake transportation demand

An earthquake changes also the level of transportation demand. Past cases have shown different alternative circumstances, a demand reduction (like in Loma Prieta 1989) or a demand increase due to increased demand of goods (as happened in Kobe 1995 earthquake). In the present application we assume that, since the productive system has a decrease of production itself, the demand should follow in the same way. This hypothesis can be removed using an economical model to simulate the equilibrium between

different sectors of industry and to simulate the demands of materials of reconstruction.

The idea is to simulate the relation with a damaged network and a demand that varies due to earthquake damage to activity system. As previously expressed, in present work we don't represent damage to residential system.

Starting from the observation that freight demand is strongly related to production, its demand level is directly related to post-earthquake demand; on the other hand, car demand is influenced by business damage only for the component of the demand that is directly related to business activities.

To simulate the previous observation we adopt the hypotheses that transportation demand from centroid i to centroid j has a linear freight demand reduction with business residual functionality, while light vehicles (cars) demand is affect by 50% of business reduction. Further details on transportation modeling will be given in paragraph 3.7 .

2.7 TRANSPORTATION MODELING

For the transportation simulation it ha been modeled a deterministic user equilibrium analysis; using a fixed and a variable post-earthquake demand.

In general terms the transportation problem can be divided into four main phases: Generation \rightarrow Distribution \rightarrow Modal definition \rightarrow Assignment of transportation demand.

The *Generation* phase is modeled from socio-economic variables, data about the productive system and gives, as output, the generation of zone out-bound transportation demand.

The *Distribution* phase determines the attractive potential of each zone, and determines the in-bound of transportation demand.

The output of the two phases of *Generation* and *Distribution* is the Origin-Destination Matrix, shortened in OD matrix.

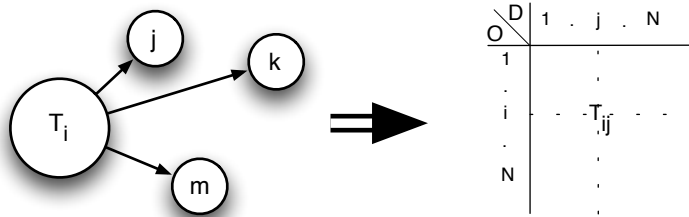


Figure 2.10: Generation of the transportation demand from node i to nodes j, k, m (on the left), and the corresponding T_{ij} entry on the OD matrix(on the right).

During the *Modal definiton* phase the transportation demand, according to socio-economic variable, level of service, cost functions and etc is assigned to different modes available for the connection. This accounts for the possible modal shift, like in the Loma Prieta earthquake in 1989 when commuters shifted from car to BART system.

The last component of the analysis is *Assignment of transportation* demand to the chosen network to obtain the flows in the network links.

In analogy with economy, the transportation model can be classified according to the three categories: *Demand, Supply, Equilibrium*.

2.7.1 Supply model

The *Topological model* describes the model of the transportation network by mean of a graph model. The *Functional model* describes the characteristics of the network that complete the topological model: length of network arches, number of lanes, free-flow speed, damage state, etc.

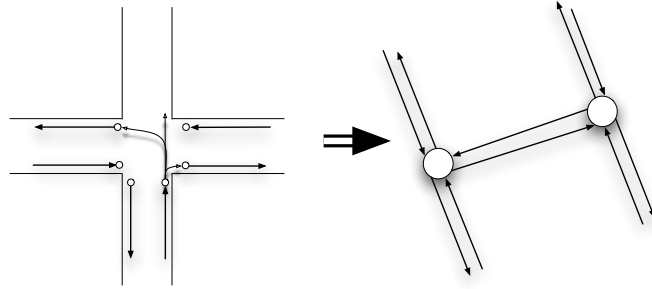


Figure 2.11: The definition of the Topological model from the real network characteristics. Detail of the allowed and forbidden turns are inserted in a turn penalty file.

The performance functions describe the response of one component to demand. The level of service is modeled as follows:

$$\vec{L\bar{S}} = \vec{f}(\vec{u}, \vec{c}) \quad (23)$$

where:

$\vec{L\bar{S}}$: This model explains the performance of the network according to usage, it's a vector of performance functions, one per each link.

\vec{f} : general performance function.

\vec{u} : vector with the usage level.

\vec{c} : network link characteristics.

2.7.2 Demand model

This set of models represent the demand of transportation in the network. There are 6 characteristics modeled: the motivation, the origin, the destination, the frequency, the mode of transportation, the times of the trip.

$$\vec{D} = \vec{g}(\vec{S\bar{E}}, \vec{A}, \vec{L\bar{S}}) \quad (24)$$

where:

\vec{D} : Demand vector as described in 2.7 .

Eg: T_{ijm} Trips from i to j with mode m.

$\vec{S\bar{E}}$: Socio-Economic characteristic of users.

\vec{A} : relation with the activity system in the territory.

$\vec{L\bar{S}}$: Level of service of network elements.

2.7.3 Equilibrium models

Equilibrium models describe the interaction between the demand and the supply. These models compute the number of trips assigned to network and allows to calculate the flow in the arches in terms of vehicle per hour (for private transportation) $\left[\frac{\text{veic}}{\text{h}}\right]$, passenger per hour (on public transportation) $\left[\frac{\text{pass}}{\text{h}}\right]$, tons of goods per hour $\left[\frac{\text{t}}{\text{h}}\right]$ for goods delivery problems.

The equilibrium problem is, in general terms, the fixed-point schema:

$$\vec{D} = \vec{g}[\vec{S\vec{E}}, \vec{A}, \vec{f}(\vec{u}, \vec{c})] = \vec{h}(\vec{S\vec{E}}, \vec{A}, \vec{u}, \vec{c}) \quad (25)$$

The *Network loading model* allows to compute the flows in network \vec{u} given the trips demand $\vec{U} = \vec{w}(\vec{D})$.

$$\vec{u} = \vec{w}[\vec{h}(\vec{S\vec{E}}, \vec{A}, \vec{u}, \vec{c})] = \vec{q}(\vec{S\vec{E}}, \vec{A}, \vec{u}, \vec{c}) \quad (26)$$

The final goal of the problem is to find the \vec{u} that allows:

$$\vec{u} = \vec{z}(\vec{u}) \quad (27)$$

2.7.4 Topological model

The transportation network is schematized as a direct graph such as:

$$G = (N, L) \text{ con } L \subseteq N \times N \quad (28)$$

where N is the total of nodes of which the graph is made up, L are the couples of nodes that belong to N: the links.

$$n_N = |N|$$

$$n_L = |L|$$

Usually the graphs are oriented that means that the link $(i, j) \neq (j, i)$

2.7.5 Transportation network

The network is usually represented as a very connected oriented graph in which each link has its own cost function.

$$T = (N, L, FC) \quad \text{con } L \subseteq N \times N \quad (29)$$

$$|N| = n_N$$

$$|L| = n_L$$

$$|FC| = n_L$$

One more definition is needed. On the transportation network some nodes have a special destination, they are the Origin or the destination nodes. From these nodes the trips start and to these nodes the trips arrive. These nodes are called "*centroids*".

$$N_c \subset N$$

Inside the set of links in the transportation network there's one more subset of paths. The paths are all the possible connections in one network that allow to connect Origin to Destination.

$$P_{OD} \subset P \quad \text{con } P = \text{all network paths} \quad (30)$$

BACKGROUND

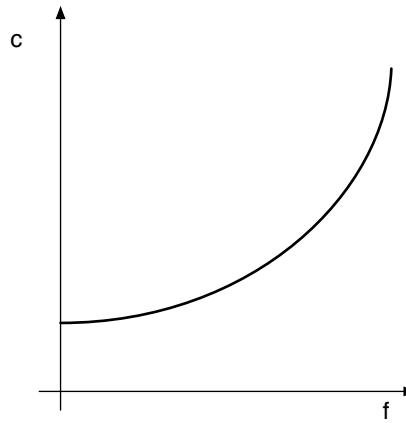


Figure 2.12: A generic link cost function, where f is the flow on the link and c is the cost at the given flow f . As the link gets busy the cost increases due to mutual disturbance.

$$|P_{OD}| = n_p$$

2.7.6 Incidence matrix: links-paths

This is a binary matrix where the value is 1 if the link is on the path from O to D otherwise is zero. This matrix is very sparse and usually is built using shortest path algorithms like Dijkstra.

Let $l = 1, \dots, n_L$ be the links and $k = 1, \dots, n_p$ the paths.

$$A \text{ with elements } a_{lk} \begin{cases} 1 & \text{if } l \in k \\ 0 & \text{otherwise} \end{cases} \quad (31)$$

The matrix is rectangular with size: $A_{(n_L \times n_p)}$

2.7.7 Link cost functions: B.P.R.

The most common function for Deterministic User Equilibrium problem solved with the Frank and Wolfe algorithm is one developed by B.P.R. based on observation of flows. The general functional form is:

$$t = t_0 \cdot \left[1 + \alpha \left(\frac{f}{K} \right)^\beta \right] \quad (32)$$

Where:

$t_0 = \frac{1}{V_0}$ Is the free flow time.

f Is the flow on the link.

K is link capacity.

Based on the first calibration of the B.P.R. in 1964 the parameters where $\alpha = 0.15$ $\beta = 4$ with K defined as $K_{practical}$. Nowadays the parameters are calibrated each time using data from surveys.

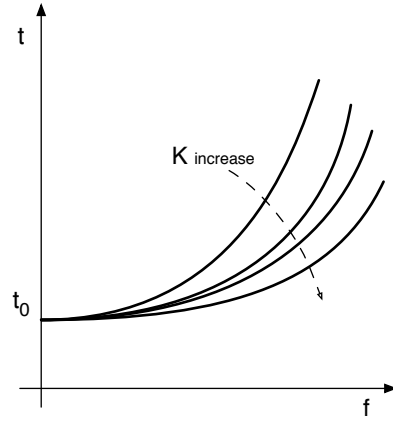


Figure 2.13: The link cost function from B.P.R. as the value of capacity “K” increases, the cost of link is more stable.

2.7.8 Frank and Wolfe algorithm

In 1956 Frank and Wolfe published a minimizing algorithm that has been efficiently used to solve the problem of assignment transportation demand to a network [15].

The analytical solution of the problem is unfeasible due to the dimension of the variables, but the problem can be solved using a series of successive approximations:

$$\vec{f}^1, \dots, \vec{f}^{k-1}, \vec{f}^k, \vec{f}^{k+1}, \dots$$

$$\lim_{k \rightarrow \infty} \vec{f}^k = \vec{f}^*$$

and

$$\forall \epsilon > 0, \exists n \text{ that } \|\vec{f}^n - \vec{f}^*\| \leq \epsilon$$

The algorithm can be summarized into a 5 steps procedure as described:

STEP 0) INITIALIZATION The algorithm is started using an assignation of type All or Nothing as starting vector.

$$\vec{f}^1 \text{ AoN with } c_l^0 = c_l(0) \quad \forall l$$

(Shown on fig. 2.14 a)

STEP 1) UPDATE LINK COST Using the last available approximation of flows in the network each link cost is updated.

$$\vec{f}^k \text{ with } c_l^k = c_l(f_{lk}) \quad \forall l$$

(Shown on fig. 2.14 b)

STEP 2) DETERMINE DESCENT DIRECTION VECTOR In the second step a linear approximation of the objective function is given and the effort is to minimize it. This approximation is a hyperplane tangent to the objective function at the point \vec{f}^k .

$$\min_{\vec{g}} \left[z(\vec{f}^k) + \vec{\nabla} z(\vec{f}^k) \cdot (\vec{g} - \vec{f}^k) \right] \quad (33)$$

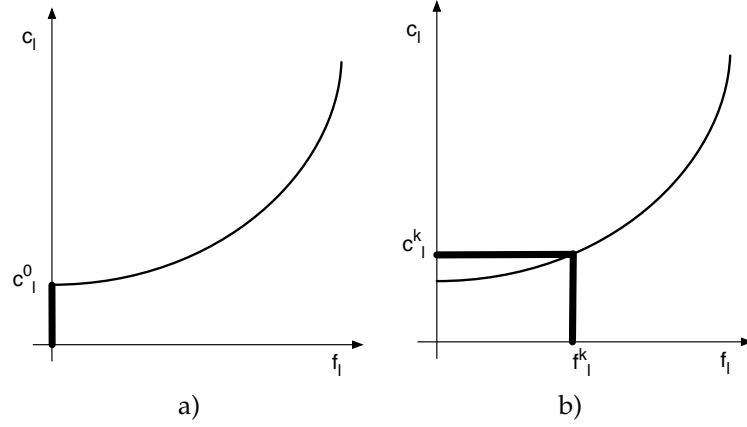


Figure 2.14: a) Determining the cost of each link at initialization iteration, b) Determining link cost function during the cycle

with the constraints in terms of vector \vec{g} :

$$\begin{cases} \vec{T} = B \vec{G} \\ \vec{G} \geq \vec{0} \\ \vec{g} = A \vec{G} \end{cases}$$

To minimize the function the constant terms are cancelled from equation (33) :

$$\min_{\vec{g}} \vec{\nabla} z(\vec{f}^k) \cdot \vec{g} \quad (34)$$

Our objective function is the total network cost:

$$z(f) = \sum_{l=0}^{n_l} \int_0^{f_l} c_l(x) dx \quad (35)$$

using the last expression the linear problem (Eq. (34)) simplifies in:

$$\sum_{l=1}^{n_l} \frac{\partial z(\vec{f}^k)}{\partial f_l}(\vec{f}^k) \cdot g_l = \sum_{l=1}^{n_l} c_l(f_l) \cdot g_l \quad (36)$$

This optimization problem can be solved using the simplex method.

STEP 3) DETERMINE LENGTH ALONG DESCENT DIRECTION Along the direction of descent, a section is made with the hyperplane defined by the descent direction vector and the vector \vec{d}^k ; we find the optimum parameter that minimizes the objective function. Using a convex combination of vectors f^k and g^k we compute d^k . At this point the direction and length of research direction are defined:

$$(1 - \lambda) \vec{f}^k + \lambda \vec{g}^k \quad 0 \leq \lambda \leq 1 \quad (37)$$

Using a convex combination of f^k and g^k the objective function is:

$$\min_{\lambda} z \left[(1 - \lambda) \vec{f}^k + \lambda \vec{g}^k \right] = \sum_{l=1}^{n_l} \int_0^{(1-\lambda) f_l^k + \lambda g_l^k} c_l(x) dx \quad (38)$$

The solution of the problem in equation (38) can be obtained using the bisection method. it usually converges in 10 iterations.

$$\left. \frac{dz}{d\lambda} \right|_k = \sum_{l=1}^{n_L} \left\{ c_l \left[(1-\lambda) f_l^k + \lambda g_l^k \right] \cdot (g_l^k - f_l^k) \right\} \quad (39)$$

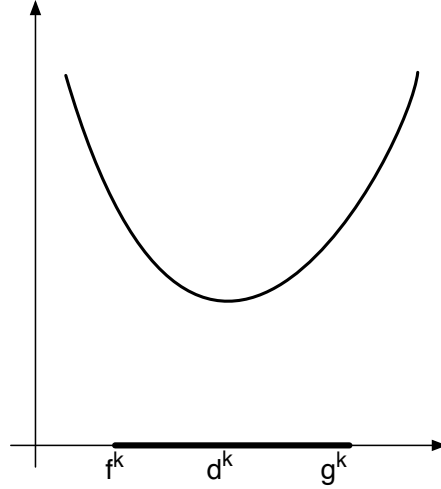


Figure 2.15: Minimization procedure for optimal d^k

STEP 4) SOLUTION UPDATE Using λ_k and g_k from the previous step we update the solution:

$$\bar{f}^{k+1} = \lambda_k \bar{g}^k + (1 - \lambda_k) \bar{f}^k \quad (40)$$

λ_k decrease at each step and tends to zero.

STEP 5) CONVERGENCE TEST At each step of the cycle evaluate if the criteria is met and exit.

$$MC_k \stackrel{?}{\leq} \epsilon \text{ If TRUE exit else goto Step 1.}$$

The following are possible measures of the convergence of the problem:

1.

$$MC_k = \frac{z(f^k) - z(f_{k-1})}{z(f_k)} \times 100 \quad (41)$$

2.

$$MC_k = \frac{LBI^k}{z(f_k)} \quad (42)$$

3.

$$MC_k = D(f_k, f_{k-1}) \quad (43)$$

D is a distance between two following approximates of the true solution. One can use, as example, the max norm:

$$MC_k = \max_{l: f_l^k > 0} \frac{|f_l^{k+1} - f_l^k|}{f_l^k}$$

Frank and Wolfe algorithm to solve deterministic user equilibrium problem has the following advantages:

- The algorithm computes directly flow of each link.
- The descent direction is computed using a AoN assignment algorithm which is very efficient.

2.8 MONTE CARLO METHOD

During the analysis business damage levels and bridges damage levels are needed to assess the probability of each state according to the scenario earthquake and to proceed with the calculation of earthquake risk. The determination of the damage level could be made using an analytical approach, but on a practical basis this is unfeasible. Monte Carlo Method is a possible solution technique that helps in determining the bridge or the business damage state according to the earthquake level.

2.8.1 General notes on the method

In general terms Monte Carlo methods are a broad class of computational algorithms that rely on random sampling to obtain numerical results. The method was invented in 1940s by Stanislaw Ulam, while he was working on nuclear weapon projects at the Los Alamos National Laboratory. It was named, by Nicholas Metropolis to Monte Carlo Casino[24]. The main idea of Monte Carlo Method is to estimate the mean value of the response of a complex system using a subset of the space of the solution. The subspace is determined sampling the original space a sufficient number of time to get an “accurate enough” estimation of the mean value and dispersion of the chosen variable.

A classic example of the method is the estimation of the π value using the sampling technique.

In this bi-dimensional problem, the application of the method is to extract a number n of casual samples of the coordinates of a point inside a square of unitary length. Then count the number of times when the random point, of coordinates (x, y) , falls inside the circle $\sqrt{x^2 + y^2} \leq 1$ of the total number of samples.

$$\bar{x} = \frac{\sum_{i=0}^n (\lambda_{i, inside})}{n} \quad (44)$$

$\lambda_{i, inside}$ is a boolean vector variable that counts the number of times that the random point is sampled inside the circle. The method has a good rate of convergency, in figure 2.16 there’s a representation of the convergence of the method using $n = 1000$ samples and $n = 10'000$ samples.

The method was firstly introduced in the 18th century, then applied by Enrico Fermi to determine the physical properties of the neutron and lastly formalized during the Manhattan project by von Neumann and Ulam

In a stochastic model θ is the required variable.

Running the simulation, the *random variable* X_1 is sampled such that θ is the *expected value* of X_1 .

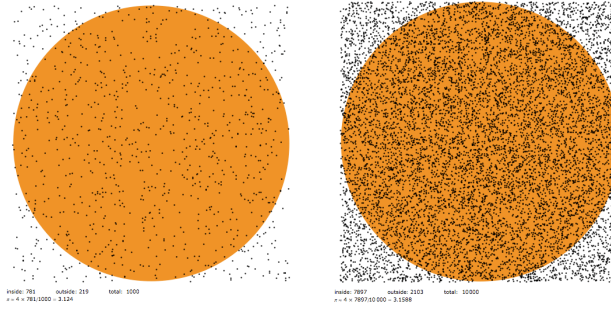


Figure 2.16: Monte Carlo method on the estimation of π with 1000 samples (on the left) the estimation is $\pi = 3,124$, while with 10'000 samples (on the right), the estimate is $\pi = 3,159$. Each time the simulation is run, due to its random number generation the result may slightly vary inside the confidence boundary.

On the second iteration, a new sampled variable is given X_2 with *expected value* of θ . We can perform the sampling k times, getting X_k samples with $E[X_k] = \theta$.

A good estimator of θ can be the mean of k samples, that is:

$$X = \frac{\sum_{i=1}^k X_i}{k} \quad (45)$$

since it is $E[X] = \theta$.

In order to determine the optimal number of samples k we should make some considerations.

Take as hypothesis that n independent random variable have the same distribution, X_1, \dots, X_n Given σ^2 as the variance of X_i and θ the expected value:

$$\begin{cases} E[X_i] = \theta \\ \text{Var}(X_i) = \sigma^2 \end{cases} \quad (46)$$

The sampling mean is:

$$X = \frac{\sum_{i=1}^n X_i}{n} \quad (47)$$

while the expected value of the sampling mean is:

$$E[X] = \frac{\sum_{i=1}^n E[X_i]}{n} = \theta \quad (48)$$

Given that fact, X is a non-biased estimator of θ . Its variance is:

$$\text{Var}(X) = E[(X - \theta)^2] = \text{Var}\left(\frac{\sum_{i=1}^n X_i}{n}\right) = \frac{\sum_{i=1}^n \text{Var}(X_i)}{n} = \frac{\sigma^2}{n} \quad (49)$$

Follows that X is a random variable with mean value θ and variance σ^2/n , so X is a good estimator of θ when σ^2/n is small enough. Given a specific value of σ^2/n the number of n iteration to reach convergence can be derived.

We can impose that the expected value of the estimator belongs to a specific confidence interval. To prove this affirmation one can use the central limit theorem.

Let $X_1, X_2, \dots, X_n, \dots$ be a serie of random variables with mean value μ and σ^2 a finite value, it follows

$$\lim_{n \rightarrow \infty} P\left(\frac{X_1, X_2, \dots, X_n, \text{dots} - n\mu}{\sigma\sqrt{n}}\right) = \Phi(x) \quad (50)$$

Where $\Phi(x)$ is the probability density function of normal standard variable:

$$\Phi(x) = \frac{1}{2\sqrt{2\pi}} \int_{-\infty}^x e^{-\frac{y^2}{2}} dy \quad (51)$$

if $n \gg 1$ the central limit theorem assert that:

$$Z = \frac{(X - \theta)}{\frac{\sigma}{\sqrt{n}}} \quad (52)$$

has the standard normal distribution ($Z \sim N(0, 1)$). That is a mean convergence of the mean value of the population.

Now we prove the fact that variance is an estimator of the convergence.

Let $z\alpha$ with $0 < \alpha < 1$ and let α be such that $P(Z > z\alpha) = \alpha$ according to the central limit theorem, for an n big enough

$$P \left\{ X - z\left(\frac{\alpha}{2}\right)\frac{\sigma}{\sqrt{n}} < \theta < X + z\left(\frac{\alpha}{2}\right)\frac{\sigma}{\sqrt{n}} \right\} = 1 - \alpha \quad (53)$$

The equation (53) can be re-written in probabilistic terms, so the probability that the mean is inside the following interval is:

$$\left(X - z\left(\frac{\alpha}{2}\right)\frac{\sigma}{\sqrt{n}}, X + z\left(\frac{\alpha}{2}\right)\frac{\sigma}{\sqrt{n}} \right) \quad (54)$$

needs to be equal to $1 - \alpha$.

Given $1 - \alpha$ and given the value of σ one can assess the value of n . At this point we need to determine the value the variance $\sigma^2 = E[(X - \theta)^2]$.

The sampling variance is:

$$S^2 = \sum_{i=1}^n \frac{(X_i - X)^2}{(n-1)} \quad (55)$$

The expected value of the population variance is S^2 and $E[S^2] = \sigma^2$, it's true that:

$$\sum_{i=1}^n (X_i - X)^2 = \sum_{i=1}^n (X_i^2 - nX^2) \quad (56)$$

from this follows:

$$(n-1)E[S^2] = E \left[\sum_{i=1}^n X_i^2 \right] - n[X^2] = n \cdot E[X_i^2] - n[X^2] \quad (57)$$

In general terms, for a random variable, one have: $E[Y^2] = \text{Var}(Y) + (E[Y])^2$ and follows:

$$E[X_i^2] = \text{Var}(X_i) + E[X_i]^2 = \sigma^2 + \theta^2 \quad (58)$$

and for the second part of equation:

$$E[X^2] = \text{Var}(X) + E[X]^2 = \frac{\sigma^2}{n} + \theta^2 \quad (59)$$

given that, equation (57) can be re-arranged as:

$$(n-1)E[S^2] = n\sigma^2 + n\theta^2 - \sigma^2 - n\theta^2 = (n-1)\sigma^2 \quad (60)$$

Now, make as hypothesis that w have n independent random variables X_1, X_2, \dots, X_n with the same probability distribution as F ; now we need to estimate the value of $\theta(F)$, the value of PDF of F

Let $g(X_1, X_2, \dots, X_n)$ be the estimator of $\theta(F)$.
An estimation of the mean quadratic error is:

$$\text{MSE}(F) = E_F[(g(X_1, X_2, \dots, X_n) - \theta(F))^2] \quad (61)$$

In the last equation the sub-script F means that the mean value is computed with respect to F distribution, that is still unknown. To estimate the value the bootstrap technique can be used using $F_e(x)$ as an empirical tentative distribution:

$$F_e(x) = \frac{(\# \text{ of } i : X_i \leq x)}{n} \quad (62)$$

Follows the big number theory, for a n big enough with probability = 1, if $F_e(x) \rightarrow F(x)$ an approximate value of MSE using the bootstrap technique is:

$$\text{EQM}(F) = E_{F_e}[(g(X_1, X_2, \dots, X_n) - \theta(F_e))^2] \quad (63)$$

The number of iteration, according to [8] can be as low as $n = 10$ for the purpose of the work.

Further details on the convergence of Monte Carlo method for the specific problem of businesses interruption will be given in paragraph 3.4.3 .

2.9 TESTBED

The area chosen as testbed for the proposed procedure needs to be an area with moderate to high seismicity, with a good industrial system, with a complete transportation system (ranging from small municipal roads, to highways).

Treviso has a contribution to GRP of about 20 billions of EUR, according to Italian hazard maps it has a moderate seismicity and the transportation system has local street as well as highway like A27 Venezia–Belluno. The system of Treviso has been described with 41 bridges, 4 business areas, 11'000 links, 630 OD nodes, 64'500 registered local businesses.

Given its characteristics, Treviso has been chosen because it satisfies the above criteria (in figure 2.17 location of Treviso).

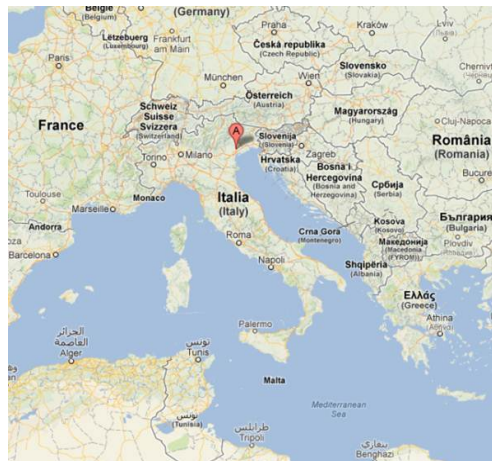


Figure 2.17: The test area is located on the north-east of Italy, it's a square of roughly 40 km x 40 km.

3

MATERIALS, METHOD AND RESULTS

CONTENTS

3.1	Earthquake scenarios	49
3.1.1	Previous study: Sleijko and Rebez 2002	51
3.1.2	Previous study: Peresan et al. 2009	52
3.1.3	Proposed methodology	52
3.2	Input data	53
3.2.1	Seismogenic sources	53
3.2.2	Recurrence law	54
3.2.3	Attenuation relationships	55
3.3	Earthquake scenario generation	56
3.3.1	Filtering scenarios	58
3.4	Loss of productivity	61
3.4.1	Fragility curves	63
3.4.2	Residual functionality	65
3.4.3	Computing Business damage scenario	66
3.4.4	Indirect economic losses	68
3.5	Time domain analysis	69
3.5.1	Recovery model	70
3.6	Cost benefit analysis	72
3.7	Relation Businesses–transportation system	74
3.7.1	Hypotheses	75
3.8	General loss model	76
3.9	Notes on parallelization	77

Before analyzing earthquake losses on distributed systems it's needed to compute some hazard consistent scenario earthquakes.

The first part of the works deals with the generation and filtering of simulated earthquake scenarios in terms of distribution of accelerations.

In the second part, possible earthquake losses scenarios are computed by mean of simulation using models to relate accelerations to damages. The simulation includes the direct losses in terms of bridges and buildings damage and indirect losses due to reduced production in factory plants and indirect losses in transportation systems due to reduced network functionality. In the presented work, importance sampling techniques with Monte Carlo method are used to derive statistical data. The distribution of possible earthquake is sampled with higher density in low probability of occurrence and high consequences areas of the curve.

3.1 EARTHQUAKE SCENARIOS

In Italy there are no publicly available scenario earthquakes, though they're needed to perform seismic risk risk analysis, particularly in distributed systems. INGV developed information about seismic hazard, several hazard maps are made publicly available[12]. The INGV working group produced 9 hazard maps with different probability of occurrence and are referenced

according to the correspondent Return Time: 30 years, 50y, 72y, 101y, 140y, 201y, 475y, 975y, 2475y.

The hazard scenarios developed by INGV have been plotted in hazard maps and printed in tabular data made available through the institutional website <http://zonesismiche.mi.ingv.it>. In figure 1.8 on page 9 is given the 475 years map. The INGV project defined the hazard maps for each structural frequency as shown on picture 3.1. The hazard calculation have a spatial resolution of 0.2" on datum ED50.

The hazard analysis are documented in technical manual that gives some insights on background data and preliminary works to compute the hazard. The project improved former seismogenic zoning of the italian territory to the version named ZS9. Also the historical catalogue of past earthquake has been updated from previous version including new earthquakes, new magnitude definitions and timeframe extension to include newer earthquakes not present in the former CPI2 catalogue. The attenuation relationships, GMPEs, have been revised to account for the new european definition of a_{max} and to account the focal mechanisms according to Bommer 2003. Two different completeness sets of data in earthquake catalogue have been defined.

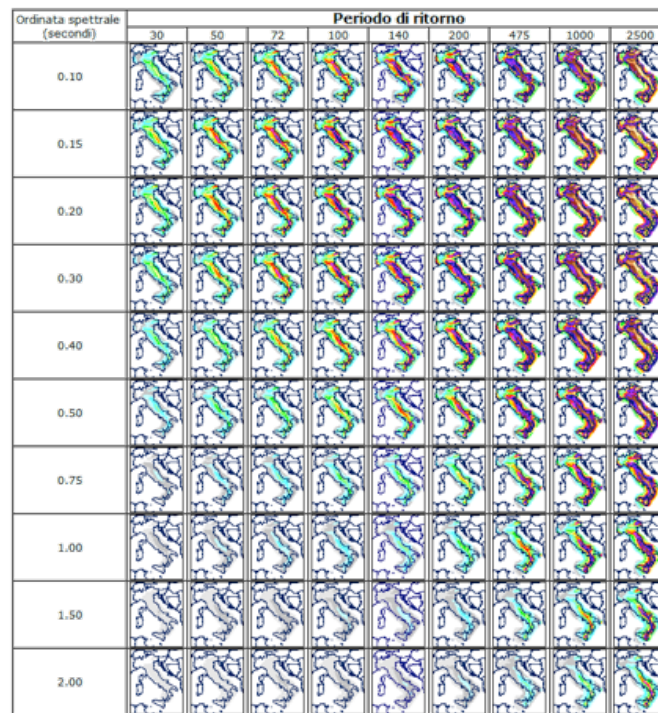


Figure 3.1: The representation of aggregated hazard for different structural frequencies. From [12] and <http://zonesismiche.mi.ingv.it>

To compute earthquake hazard, the working group decided to adopt the classic Cornell 1968 approach, because widely used in past italian projects and in Europe.

The unavoidable background uncertainties of the methodology are addressed using a logical tree approach. The seismogenic zoning dealt with the definition of fault location, epicentral distance, fault depth, faulting mechanism, a particular attention was given to the definition of the zones to allow, in a prospective work, to use regionalized attenuation relationships.

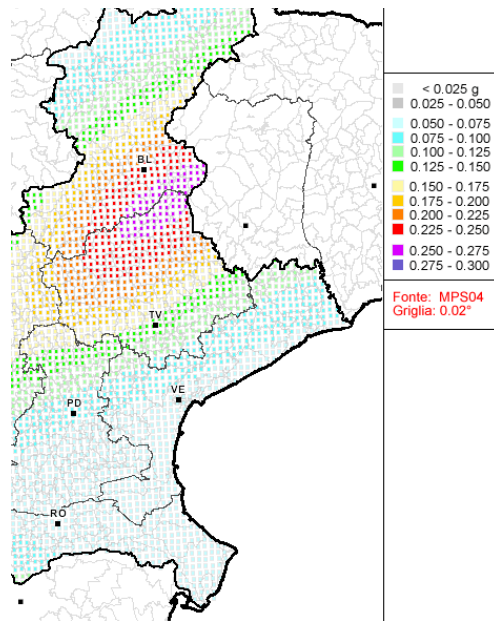


Figure 3.2: A detail on the hazard fo Veneto region computed on a 0.5" grid in ED50 datum

The project used the relation by Ambraseys of 1996[3] and the italian revision by Sabetta and Pugliese 1996[31] adopting the correction by Bomer 2003 for the faulting mechanism and implementing a correction factor for near epicenter increase of earthquake response.

The completeness intervals that characterize the historical earthquake database are defined as "CO-04.2" if the completeness is historical, while the completeness "CO-04.4" refers to statistical completeness using the Albarello 2001 methodology.

The maximum expected value of magnitude for each seismogenic zone M_{max} is stored in each seismogenic zone following definition: M_{max1} is the "observed" maximum seismicity, that refers to historical series, while, the M_{max2} is the safe estimation of the possible maximum magnitude.

The seismicity in time scale has been defined using the activity rate definition or the Gutenberg Richter (GR) b definition. The parameter b for GR occurrence relationship has been defined using the historical series for each seismic zone. On the other hand, the parameter a of GR relationship has been assumed to be the occurrence of the M_{wmin} earthquake. This guarantees the consistency of energy estimation among different zones.

The probability distribution of a_{max} have been calculated using the code SEISRISK III by USGS. The uncertainties have been weighted using a logical tree approach for the 10% probability in 50 years reference time, i.e. 475years of return time. Given the hazard calculation for Italy, one more step is needed to get earthquake scenarios that are suitable for seismic risk assessment on distributed systems.

3.1.1 Previous study: Sleijko and Rebez 2002

In 2002 Sleijko and Rebez published a paper on "Probabilistic seismic hazard assessment and deterministic ground shaking scenarios for Vittorio Veneto (N.E. Italy)"[11]. In this work the authors present some deterministic ground

shaking scenarios for the design and the extreme earthquakes; they show two scenarios: the most probable and the extreme one.

In figure 3.3 there's a scenario representation using the software Seisrisk III by USGS, using the seismogenic zones of 2002 from GNDT and three different attenuation relationship:

- Ambraseis(1996)
- Sabetta and Pugliese(1996)
- Chiaruttini and Siro(1981)

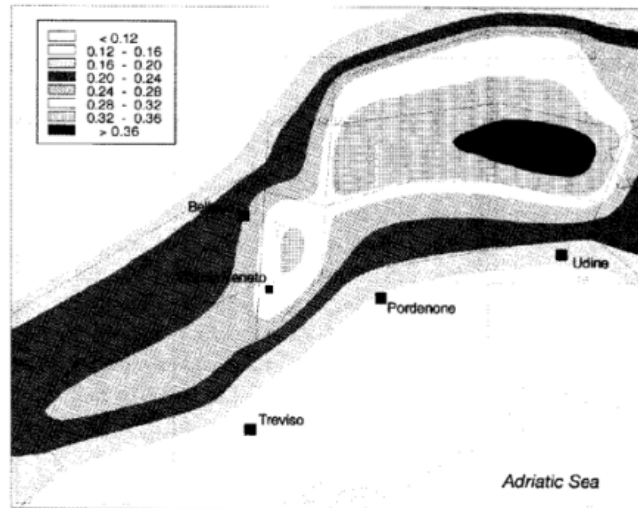


Figure 3.3: A seismic scenario map representation from Sleijko and Rebez 2002[11].

3.1.2 Previous study: Peresan et al. 2009

In 2009 Peresan et al. published a work on “Neo deterministic seismic hazard scenarios for North Eastern Italy” [28]. In this work the authors presented a novel approach, defined neo-deterministic for the simulation of earthquake scenarios associated with the alarm on the Adria region. Using prediction algorithms like CN, MS8 and PULSYN software by Gusev (2008) the authors get ahead classical statistical approaches using historical earthquakes, and run f.e. simulation from seismic nodes to get the scenario earthquakes. Seismic nodes are the classic seismogenic sources but also the nodes that arise from geological structural analysis. According to the paper, if no historical data is available classical statistic approaches can under-estimate the actual hazard because of lack of data.

3.1.3 Proposed methodology

Since there are no available de-aggregated seismic scenarios to perform SRA on distributed systems a broader area needs to be covered with sufficient detail for the purpose of simulation of earthquake consequences.

To compute the seismic losses scenarios the distribution of acceleration is needed in the study area.

The proposed methodology require 6 steps:

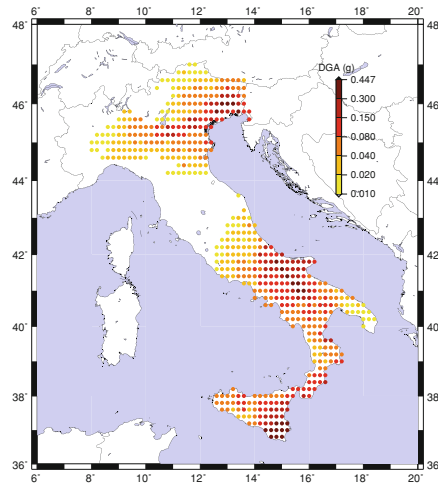


Figure 3.4: Map of design ground acceleration (DGA) associated to an alarm in the Adria region. From Peresan et al. 2009 [28]

1. Retrieve data for seismogenic sources;
2. Adapt and import data on seismogenic sources;
3. Compute the distribution of the chosen intensity parameter at the required locations using an attenuation relationship, GMPE;
4. Generate a set of possible epicenters;
5. Create the scenario using the desired intensity measure;
6. Filter scenarios to reproduce the hazard of the area.

3.2 INPUT DATA

3.2.1 Seismogenic sources

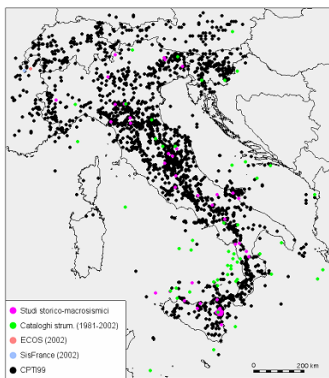


Figure 3.5: Historical earthquakes from CPTI.

There are two definition of seismogenic areas available: the DISS catalogue and the catalogue from INGV project ZS9. DISS catalogue has been composed by INGV Working group and it's updated to version 3.1.1. The ZS9 catalogue has been developed during the seismic hazard project funded by Civil Protection Agency.

Both options have been analyzed and the ZS9 has been used in the present application because of the completeness of data to perform probabilistic analysis.

"Zone Sismiche ZS9"

The ZS9 seismogenic sources definition has been derived from the parametric catalogue of historical earthquakes up to 2002.

This catalogue stores all the known earthquakes from year 217BC to year 2002 AD. In figure 3.5 is presented a plot on the map of all epicenters of historical earthquake contained in the catalogue. The working group classified the Italian territory in six macro-zones following the tectonic and geologic homogeneity, accounting for the different rupture mechanism as described in (Montone et al.,2003). In figure 3.6 a) there's a representation of the seismogenic zones from the ZS9 catalogue, fig. Figure 3.6 b) represents the comparison of zones from ZS9 and DISS version 2.0. ZS9 zones are wider than the DISS counterpart; ZS9 generally fully include DISS zones.

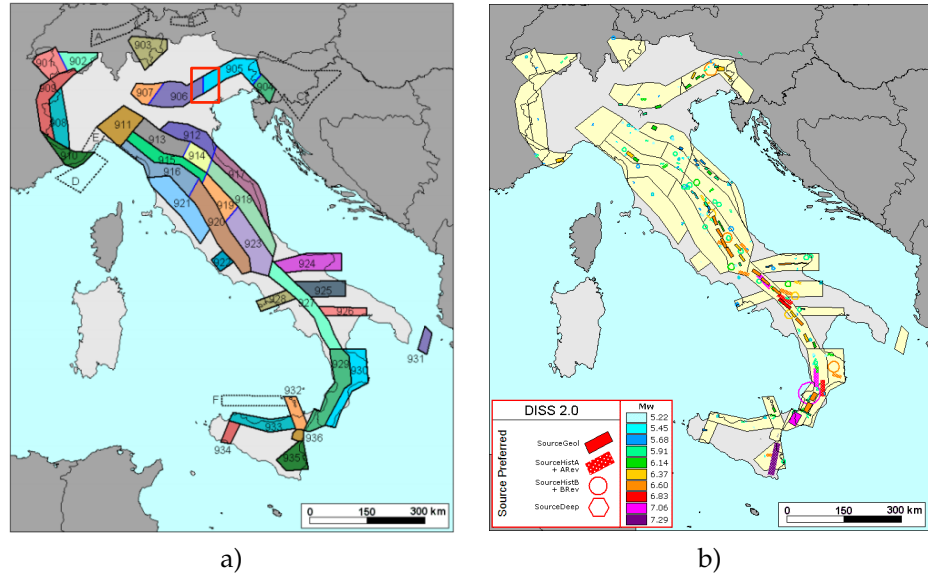


Figure 3.6: a) Seismogenic zones using the ZS9 definition, inside the red box the testbed area. b) The comparison of ZS9 definite with DISS seismogenic zones.

3.2.2 Recurrence law

During the INGV research projects for each seismogenic zone “a” and “b” parameters for Gutenberg-Richter relationship were derived. The functional form of the equation is:

$$\log \lambda_m = a - b \cdot m \quad (64)$$

where:

- λ_m mean annual rate of occurrence of EQs with magnitude m .
- 10^a mean yearly number of earthquakes; the a value is determined with a rate of $M_{w_{min}} = 4.8M_w$ to be consistent with the energy content of the samples from the historical earthquakes database.
- b relative likelihood of large and small earthquakes.

Since earthquakes energy follows an exponential distribution with magnitude, magnitude linear space is converted into a logarithmic space and is linearly sampled from 4.8 to the maximum magnitude for each source. In table 3.1 for each source are given the estimation of b , a and the maximum estimated magnitude are computed from data of INGV project. Figure 3.7 shows the recurrence relationships of two zones one interest for the current application. The mean value of earthquake of a certain magnitude λ_M is important because it defines the probability of each seismic scenario.

ZS Name	ZS9	b Co-04.2	b Co-04.4	MwMax GR	a (Co.04.2)	a (Co.04.4)
Ts–Monte Nevoso	904	-1.12	-1.32	6.14	4.52	5.29
Friuli–Veneto W	905	-1.06	-1.12	6.60	4.66	4.91
Garda–Veronese	906	-1.14	-1.70	6.60	4.51	7.06
Bergamasco	907	-1.71	-1.48	6.14	6.81	5.88

Table 3.1: Seismogenic zones recurrence rate parameters

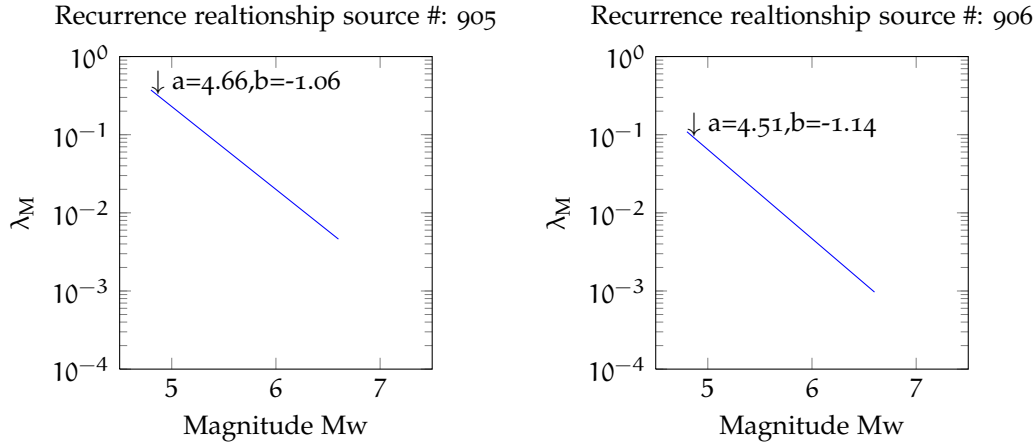


Figure 3.7: Recurrence relationship for seismogenic zones 905 and 906 the ones in the interest area.

3.2.3 Attenuation relationships

Attenuation relationship, also called ground motion prediction equations (GMPE) are a model to relate input parameters (p.e. the distance from epicenter/ipocenter, the magnitude of the earthquake, the soil type and others) can predict the value of an intensity measure of the seismic action (PGA, PGD, Sa, etc). In literature several attenuation relationships are available for the Italian earthquakes. In the present work we present the three more interesting for the sake of this study.

The classical Ambraseys 1996 [3] is the most diffused, but this equation has been calibrated using data from all Europe, so this could be not accurate enough. Another option, one of the most recent, is Bindi et al. 2011[5], the functional form is rather similar to Ambraseys; but in 1996 the first GMPE for Italy appeared, by Sabetta and Pugliese[31]. In this case the functional form is identical to Ambraseys but has been calibrated on Italian earthquakes, it has been widely used and tested.

In the present study *Sabetta and Pugliese* attenuation relationship has been chosen.

Sabetta and Pugliese 1996

The Sabetta and Pugliese attenuation relationship published in 1996 has the following functional form:

$$\log_{10}(Y) = a + b \cdot M + c \cdot \log_{10}(R^2 + h^2)^{1/2} + e_1 \cdot S_1 + e_2 \cdot S_2 \pm \sigma \quad (65)$$

where:

- Y Response parameter as (PGA[g], PGV[cm/s], PV)
- M Magnitude of the earthquake as $[M_w]$
- R epicentral distance in [km]
- $S_{1,2}$ dummy variable used to account the soil type
- σ standard deviation of logarithm of Y

The parameters for Sabetta and Pugliese 1996 are derived from table 3.2 . In figure 3.8 the plot of the GMPE Sabetta and Pugliese 1996 for the magnitude range of interests and calibrated distance.

Const. Term	Magnitude	Distance	Site 1	Site 2		
a	b	c	$e1$	$e2$	h	σ
-1.845	0.363	-1	0.195	0	5.0	0.190

Table 3.2: Coefficients to be used in Sabetta and Pugliese 1996 for PGA for horizontal component and epicentral distance.

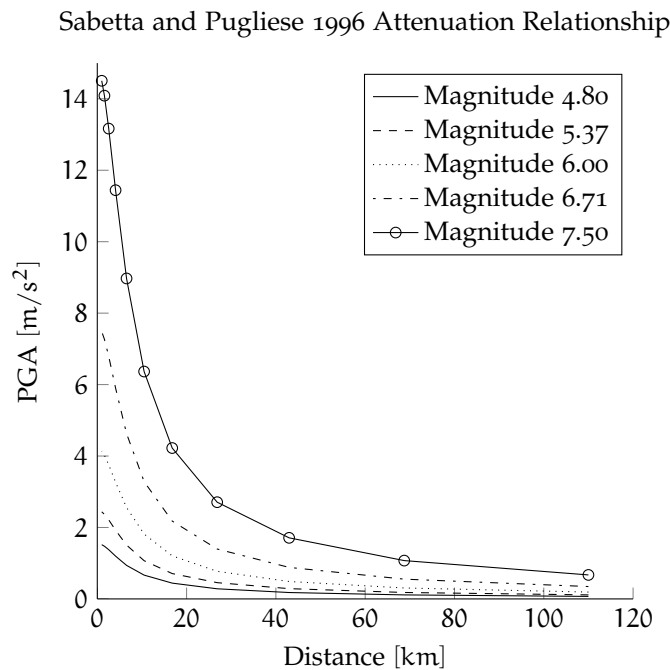


Figure 3.8: Plot of the chosen attenuation relationship(GMPE) from Sabetta and Pugliese 1996 [31].

3.3 EARTHQUAKE SCENARIO GENERATION

This paragraph details the procedure to generate seismic scenarios.

The procedure starts acquiring some data about the seismogenic zones, about the bridges and businesses that are under analysis. In figure 3.14 red points represent the bridges in transportation network; in blue the centroids of the productive areas. The procedure, if data is available, can be extended to finer level of detail modeling each business instead of business areas, giving a finer representation of the risk, especially for insurance industry

purposes. This allows to get a better estimation of risk in terms of direct and indirect losses related to each entry in portfolio.

The algorithm randomly samples points inside seismogenic areas with a pre-defined number of possible epicenter. The sampling is uniform inside each area. In the present application for each seismogenic zone 500 epicenters are simulated, in figure 3.9 the epicenters generated for each seismogenic source.

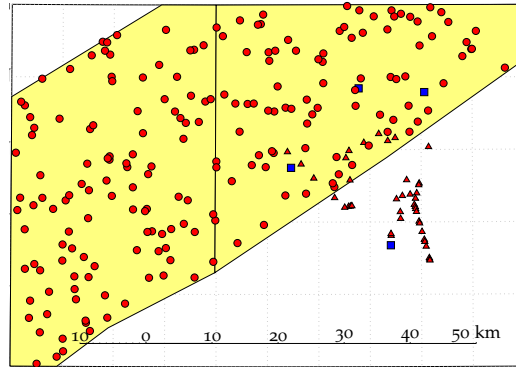


Figure 3.9: The simulated epicenters plotted as red points on the map over the seismogenic zones.

For each epicenter, the distance of each locations (i.e. bridges and productive areas) is computed and stored into a vector. The distances that are bigger 120 km (the interval of definition of the GMPE) are deleted, because beyond the range of applicability. The space of possible magnitudes is transformed in an exponential space in order to be uniformly sampled. The samples of magnitudes used in the current application are: [4.80 5.37 6.00 6.72 7.50].

A consistent number scenario earthquakes is generated. The total number of scenarios is filtered according to the procedure shown on paragraph 3.3.1 to get an accurate representation of hazard with a smaller number of scenarios. Since following transportation analyses nested in Monte Carlo method are time-consuming the number of scenarios needs to be reduced.

The proposed algorithm has been coded using Matlab environment[23]. In the following lines the pseudo-code of the proposed algorithm is presented:

Listing 3.1: The pseudo code for scenario generation algorithm

```

Foreach source
  Random generate n epicenters
  Foreach epicenter
    Foreach magnitude
      Foreach location (Bridge, Business)
        Compute PGA @locations
        Discard if too low
      End
    End
  End
End
End
End

```

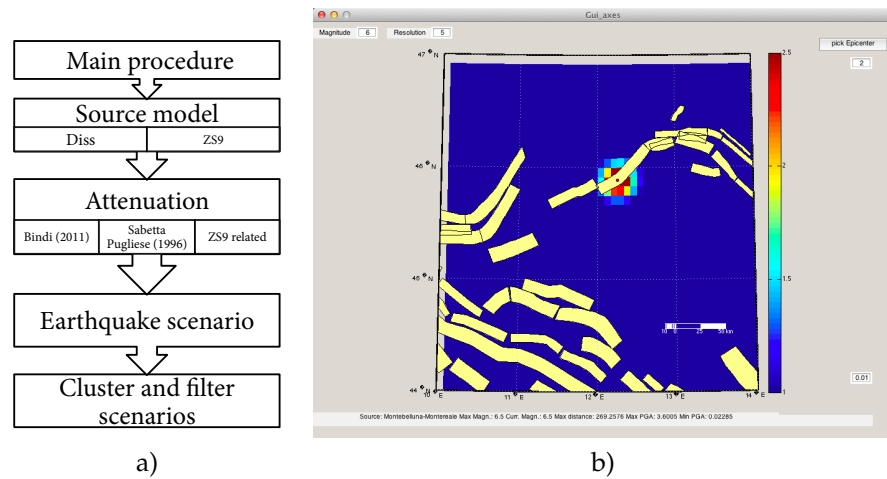



Figure 3.10: a) The proposed algorithm for the seismic scenario generation. b) A screenshot of the tool to generate seismic scenarios simulating a shakemap with epicenter in Montebelluna-Montereale, simulating maximum magnitude for the source: $M = 6.5$.

3.3.1 Filtering scenarios

To be accurate enough, the simulation of earthquake scenarios produces a big number of simulations. Since the following Monte Carlo method has a nested Frank and Wolfe algorithm on a very detailed network (that is very time consuming by its nature), a selection of the computed scenarios is needed.

The idea is to choose a fixed number of scenarios, to reduce the computational workload of the subsequent phases. The remaining scenarios need to be consistent for hazard description. The conceptual scheme of the proposed procedure is shown in figure 3.10 a).

The proposed selection procedure computes the distance of each scenario as the distance of each scenario acceleration from each specific hazard curve. For each analyzed location the hazard curve from the INGV [12] is derived. Earthquake scenarios are clustered according to their probability of occurrence, that follows from the occurrence relationship.

For each location, the distance from the hazard curve of the specific location and the simulated scenario acceleration is computed and stored into a matrix.

The distance matrix represents in its rows the vector of the distance from hazard curve for each bridge, in its columns the distance for each scenario. The distance is then computed as the Euclidean norm of the columns of matrix D . For each cluster only the first 5 scenarios are chosen, i.e. the closest 5 scenarios for each cluster; in figure 3.12 a representation of the selection process. From table 3.3 in the present simulation: from the 8'000 scenarios (in figure 3.9 are represented the generated epicenters), 6 magnitudes \cdot 2 sources \cdot 5 selected scenarios = 60 have been selected.

The scenario selected with the presented procedure are in good accordance with the hazard for the same location derived from previous works as can be noted from the following figure 3.13 where the scenarios accelerations are plotted over the hazard curves for two different locations for sake of comparison.

Variable	#
Sources	2
Epicenter \forall source	2
Magnitude classes	8

Table 3.3: Variables to be permuted to obtain all possible combinations of scenarios

$$SCN_{sel(i)} \# (\sqrt{HAZ_{loc}^2 - SCN_{loc,Pr_i}^2}) < n \forall Pr_i \forall locations \quad (66)$$

where:

- $SCN_{del(i)}$ The i -th selected scenarios
- HAZ_{loc} Hazard at location loc
- SCN_{loc,Pr_i} Scenario acceleration at location SCN_{loc,Pr_i} for earthquake scenario
- n number of scenarios to be selected per each cluster
- Pr_i Probability of i -th clusters, derived from (64)
- locations all the locations included in the analysis.

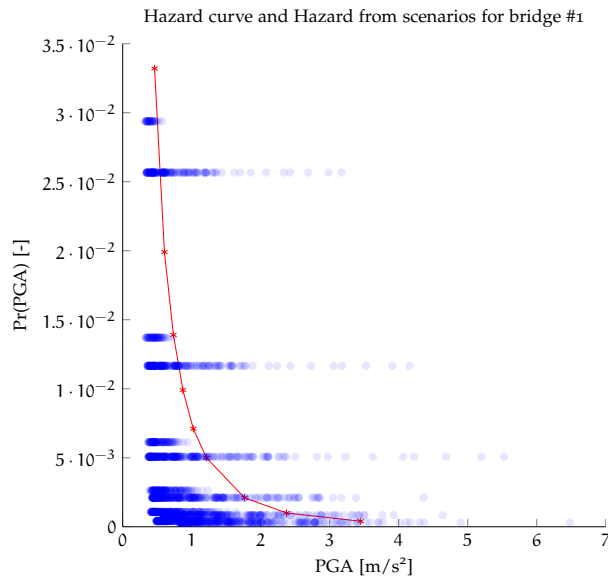


Figure 3.11: In the figure is represented the hazard curve in red for a particular location, in this case Bridge # 1 location, blue the points represent all the accelerations from each seismic scenarios.

In figure 3.11, for a specific location (in this case the location corresponding to bridge #1) in red is presented the hazard curve derived from hazard maps of the INGV project; blue circles represent the acceleration simulated using the proposed procedure. Data is scattered because of two reasons. The first: the location of the epicenters can be close or far from the location inspected, this produces the scattering in the horizontal direction of blue points. The other noticeable difference is that some series are more scattered, while other series are less scattered along horizontal axis. This follows directly from the definition of seismogenic areas. Zone 906, the western one, doesn't intersect any location; because of the distance the distance

of each epicenter to locations is less variable, and this reduces the scattering. Earthquakes simulated from source 905, that intersect locations, are more scattered because there are more possible configuration of the epicenters that can be very close and very far from the location. The last observation is that the scattering increase with intensity of the earthquake (intensity can be derived from the probability of the earthquake because is directly related to magnitude).

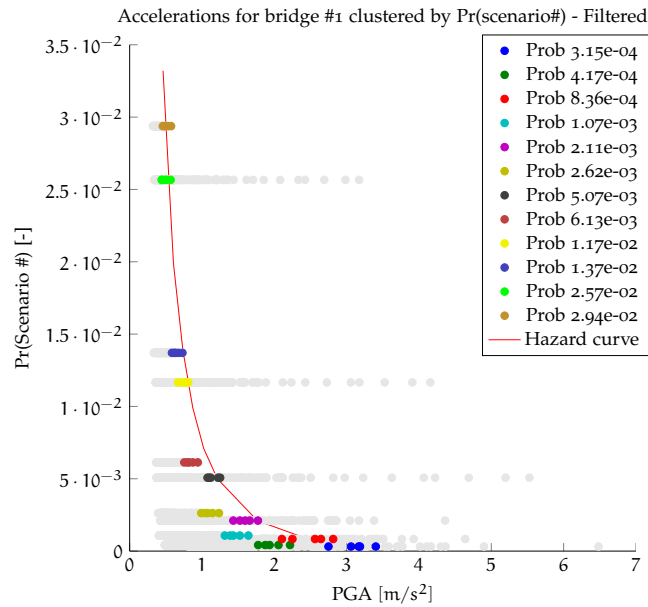


Figure 3.12: For location Bridge #1 the hazard curve is represented in red, all scenarios are represented with gray dots, the chosen scenarios are represented with colored dot according to their cluster.

In figure 3.12 , for a specific location (for sake of comparison with previous observations, location bridge#1 is chosen) the hazard curve is represented as a red line, while scenarios are represented as colored dots. Under each colored series there are gray dots that correspond to un-selected scenarios. As expected, selected scenarios, are the closest to hazard curve. Some scenarios are closer while other are little more far because this is a specific location, while the selection method is, actually, reducing the “global error” of difference of all scenarios at each an every location, instead of the “local error” that can be seen looking at the figure that depicts only one location at time.

Since the accordance is made to minimize the global error that could be done when reducing the number of scenarios that represent that hazard, from figure 3.13 a) can be seen that the mean acceleration, computed as the mean of the acceleration of all scenarios that belong to one cluster, is fitting properly the hazard curve also for different locations. In figure 3.13 is presented the fitting of two locations, that are far away in space. Following the proposed methodology, for each location the specific hazard curve is plotted and the respective selected scenario accelerations are plotted.

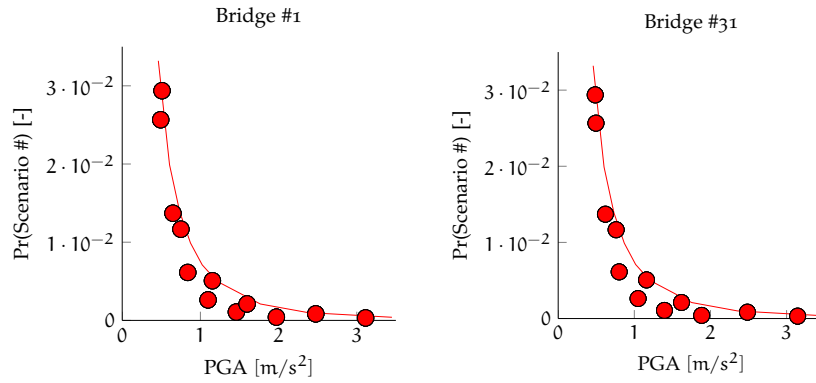


Figure 3.13: The picture represents the mean value of each selected scenario for the locations corresponding to Bridge #1 and Bridge #31. The picture show a good accordance between the presented hazard curve and the selected scenario accelerations.

3.4 LOSS OF PRODUCTIVITY

The main topic of analysis in the present work, and the most innovative approach to the problem of the loss of production is based on the definition of residual productive capacity after an earthquake.

To approach the problem some assumption have been made. The first hypothesis is that residual productivity of a business is directly related to the damage of its buildings. This hypothesis can be improved taking into account that the building isn't the only responsible for production, but the human workforce plays a key role along with the residual functionality of plants, machineries and availability of materials.

Should be noted that if the business is big enough to have different production sites, activities could be relocated in plants un-affected by the earthquake. The proposed model doesn't account that at the present stage of development. In figure 3.14 the productive zones analyzed are shown in blue squares.

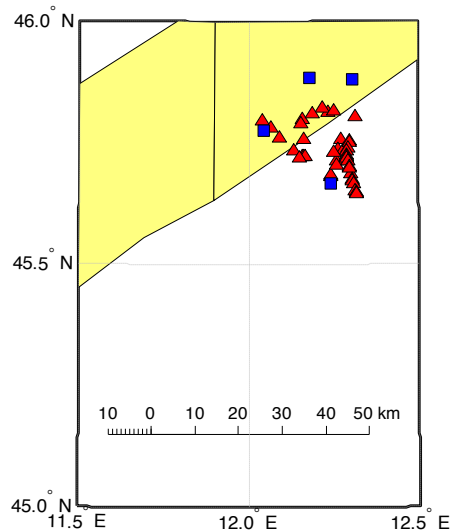


Figure 3.14: The exposed risks. Red triangles are the bridges location, the blue squares the productive areas locations, the underlying yellow areas are the seismogenic sources.

The second hypothesis is connected with the economical description of the problem. It is assumed that each industrial facility has no relation with other business. To remove this hypothesis an economical model should be developed to account possible damages to supply chain and model the so-

called “inter-ripple” effect, i.e. the supply of materials can be shortened or the buyer can experience damage itself and reduce its demand.

Derived loss of functionality can be derived from the shortage in supply of basic services, e.g. electrical power or water. The present model accounts the relation to transportation system.

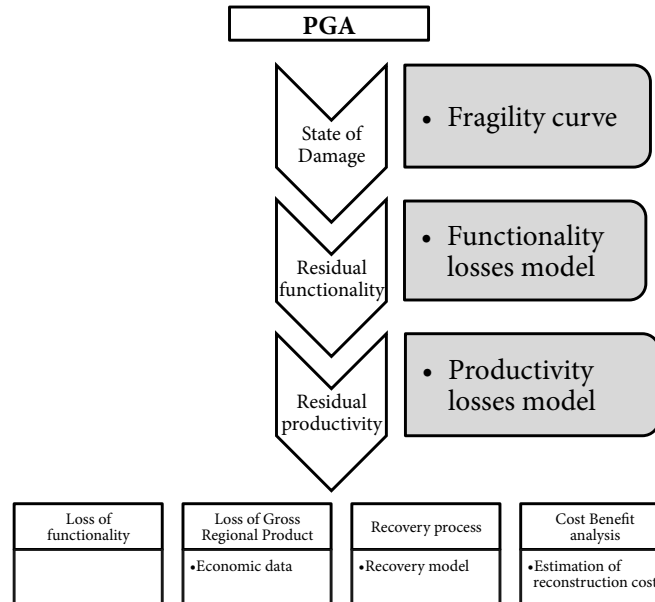


Figure 3.15: The picture represents the conceptual schema of damage to productive system. The computes the state of damage using fragility curves, residual functionality is obtained using a model for the loss of functionality. The residual productivity is obtained. The module outputs can be used for different uses.

The conceptual schema for the assessment of loss of productivity and loss of GRP is presented in figure 3.15 . This module of analysis accepts as input a measure of the intensity of the earthquake at each productive location. The module compute damage state using the provided fragility curves. Then, residual functionality is accounted using a model for the loss of functionality. Further, residual productivity is obtained from the model that relates the residual functionality of the building to the ability to produce revenue. At the end of run the module outputs can be used for many uses. The loss of functionality of a building or a productive area can be assessed.

Using economic data the model can predict the loss of gross regional product. It can be used for a subsequent analysis of the recovery process adding a recovery description module. Economic data can be used for the estimation of the reconstruction cost and to perform a Benefit-Cost analysis if dealing with government aids.

The estimation of direct and indirect losses can be useful for portfolio management in insurance market. Results can also be used to explore new areas of business for emerging catastrophe insurance market.

In formal terms the model is:

$$BD = f(PR, RR, FR, E) \tag{67}$$

where:

- BD is Business Damage of a productive area of any size (from small business to aggregated macro-productive area)
 PR is the residual productivity after earthquake
 RF is Residual Functionality
 F is the fragility of building
 E the earthquake, i.e. the input.

The economic data to perform the analysis has been retrieved from the Data Warehouse of Istat (*Italian statistical institute*.) Four districts have been considered to perform the economic analysis: Conegliano, Montebelluna, Pieve di Soligo and Treviso. In table 3.4 are given the details of the number of businesses per each productive district and the relative contribution to the Gross Regional Product (GRP). Since GRP data is provided of each productive district, for the purpose of the present work it has been considered that each business has a unitary contribution to the GRP and the rate of contribution to GRP is directly the rate of business of the district when related to the total of businesses in the region.

ID	District	Businesses	Rate	GRP (EUR)
152	Conegliano	16'572	3.73%	11'604'009'825.61
153	Montebelluna	11'913	2.68%	8'341'694'970.59
154	Pieve di Soligo	4'124	0.93%	2'887'698'317.69
155	Treviso	32'017	7.20%	22'418'874'160.43
	Sum	64'626	19.22%	59'835'013'735.12
	Regional total	444'578	100.00%	311'301'441'000.00

Table 3.4: Productive system data representation. In *italic* data from Istat. Other data is computed from the previous.

3.4.1 Fragility curves

As stated in the second chapter, the description of fragility in this application to define residual functionality of productive plants, is founded on the description of the fragility of industrial areas.

In this application we assume that the fragility of each productive area is represented by the fragility of the most command industrial building, in this application, of the area of Treviso, a tilt-up wall pre-cast concrete building has been assumed. Another assumption is made, since the earthquake scenario has no directionality, the response of the structural system is a-directional.



Figure 3.16: A tilt up building during its construction.

The fragility of the industrial building is described using the fragility curves from Hazus.[2]

These type of building has a wood or a metal deck roof diaphragm. Usually, walls are thin, while the roofs are relatively light. They are designed

using older or non-seismic codes, that gives a poor seismic performance because the buildings have inadequate or no-connections. The typical height of tilt-up buildings is one or two stories. Walls can have numerous openings to give the access through doors, to allow room for windowing, etc.

The functional form of the fragility curve of industrial buildings is:

$$P[ds|PGA] = \Phi \left[\frac{1}{\beta_{ds}} \ln \left(\frac{PGA}{\overline{PGA}_{d,ds}} \right) \right] \quad (68)$$

Where:

- β_{ds} is the standard deviation of the natural logarithm of PGA of damage state, ds, assumed as 0.64
- Φ is the standard cumulative log-normal distribution function
- $\overline{PGA}_{d,ds}$ is the PGA that denotes the mean value of each damage state given in table 3.5 .

The hypothesis of the fragility curve derived from Hazus are:

BUILDING CODE the building is assumed to be designed according to the building code for a moderate seismicity zone.

MEASURE OF INTENSITY to be consistent with the previous module the intensity measure chosen is PGA

METHOD The method for building fragility curves is "Equivalent PGA"

BUILDING TYPE According to the source the type of building is "PC1"

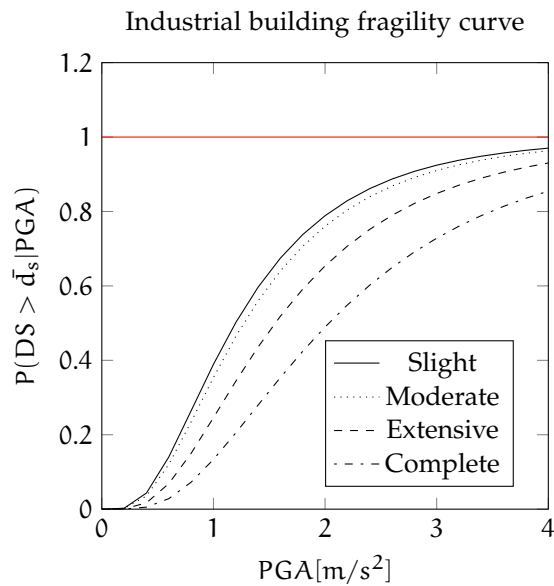


Figure 3.17: The fragility curve used to describe the seismic response of industrial buildings.

The four damage states in figure 3.17 correspond to:

SLIGHT Hairline cracks of the walls, minor concrete spalling;

MODERATE Wall surface exhibits diagonal cracks; Some welded panel connections may have been broken;

EXTENSIVE Through-the-wall diagonal cracks; Extensive spalling.

COMPLETE Structure is collapsed or in imminent danger of collapse; 15% of buildings with complete damage are expected to be collapsed.

Damage state	Mean value
"Slight"	0.18
"Moderate"	0.24
"Extensive"	0.44
"Complete"	0.71

Table 3.5: The residual functionality model.

The fragility of industrial buildings could also be represented using a f.e. simulation of the non linear response of the industrial building, starting from a plastic SDOF structural model to a detailed and complex non linear model to account the weak connection of the building. Several studies have been published in this field; the only counter effect of this choice is the increase of computational time because of high demanding resource f.e. analyses.

In present work the earthquake direction is not accounted because of the novel approach to the problem. Future works can apply the concept of directionality to the simulation of earthquake scenarios implementing a complex f.e. simulation of the soil behavior after the release of energy by the quake. So, a future work can use this data to improve the response of buildings accounting the directionality of the response of the structural system in 3 directions.

3.4.2 Residual functionality

At this stage, damage state DS are available, but a model is needed to obtain the residual functionality RF of industrial facility.

$$RF = f(DS) \quad (69)$$

To relate the damage state to residual functionality has been proposed a step model. The model express the fact that an undamaged business has no productivity reductions, if there's a slight damage the loss of productivity is 20% because some minor repairs are needed. If the damage state is moderate, the loss of productivity is of 60%. When the damage state is extensive, the residual productivity is about 20%, considering that some parts of the production plant can still be sound, while other are unavailable. If the building is collapsed no production is possible, the residual functionality is 0. Following previous observation the calibration parameters for the Residual Functionality model adopted are: $\alpha = 0.80$, $\beta = 0.40$ and $\gamma = 0.20$.

The proposed model can be calibrated with historical data, if available. The model is discrete, but can be easily converted into a continuous model, if there's enough data for a proper calibration. Data could be retrieved from historical earthquakes in areas with homogeneous characteristics.

A parametric study can be done to assess the influence of proposed tentative parameters calibration.

Damage state	RF
1 "No damage"	1.0
2 "Slight"	α
3 "Moderate"	β
4 "Extensive"	γ
5 "Collapse"	0.0

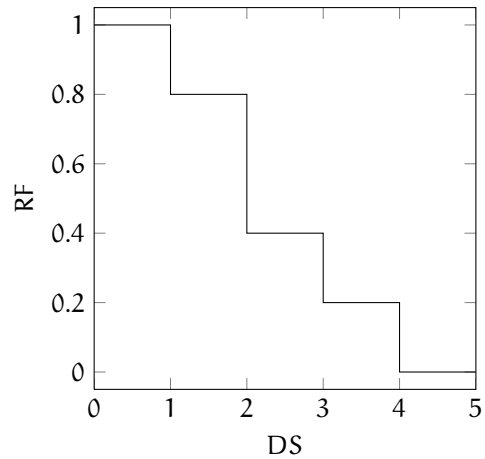


Table 3.6: Residual functionality model. The residual functionality model has been applied using: $\alpha = 0.80$, $\beta = 0.40$ and $\gamma = 0.20$

3.4.3 Computing Business damage scenario

As seen in paragraph 3.4.1 fragility curves are described in probabilistic form, to compute the damage scenario they need to be randomly sampled in correspondence of accelerations coming from the earthquake simulation module, cfr. figure 3.17 . We decided to adopt the Monte Carlo method to sample the fragility curves of each industrial facility and obtain the corresponding mean value of Damage State DS.

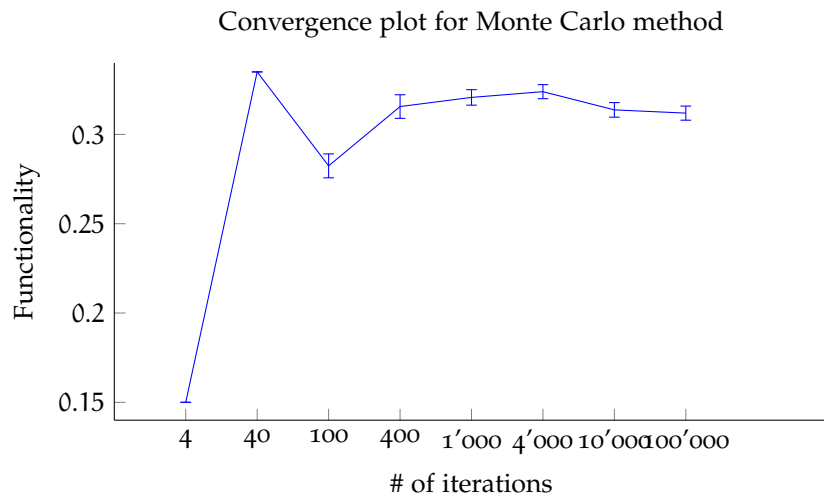


Figure 3.18: Converge plot form Monte Carlo method of the definition of residual functionality. In the graph is represented the first earthquake scenario for business area #1. Iterations range from 10 to 100'000.

An explorative convergence study on Monte Carlo method for the specific problem has been performed using one seismic scenario. The resulting convergence plot is presented in figure 3.18 . According to the convergence plot, residual functionality settles to the value of $RF = 0.32$ with 400 iterations, while the error bar, that accounts for dispersion is almost stable. With a very small number of iterations, i.e. 4 and 40, the method isn't able to represent the variability of the problem. With 100 iterations the solution is

oscillatory, but finally with 400 iteration is reasonably stable with comparison to computational time.

The application of Monte Carlo method is presented in figure 3.19 as a box plot of the error bars vs each computed scenario. The variability expressed in the application is related to the scatter in the input scenario accelerations, due to spatial variability caught by the model.

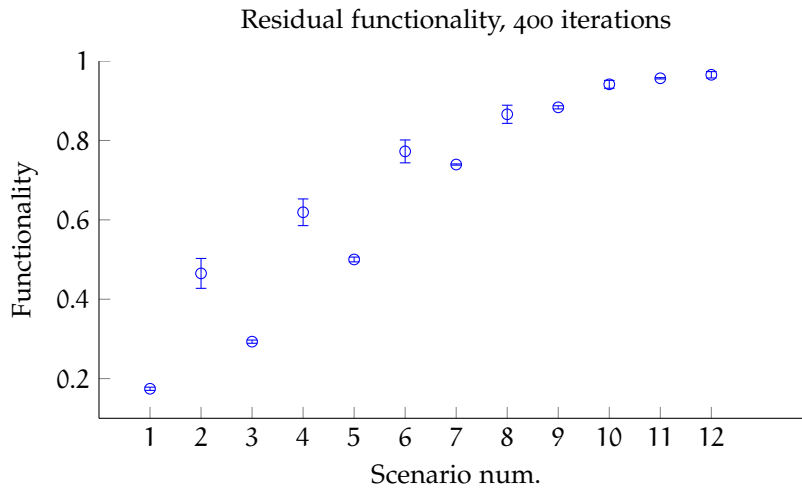


Figure 3.19: Computed residual functionality with Monte Carlo method using 400 iterations.

The risk has been computed in terms of reduction of functionality. Risk, as business damage, is defined as $1 - RF$. In figure 3.20 the risk curve of the the Industrial area #1 is presented. As expected more rare events induce higher damage: an event with probability $3.0 \cdot 10^{-2}$ causes a business damage almost negligible, while the rarer event with $3.0 \cdot 10^{-4}$ probability, that means higher earthquake magnitude, implies a damage bigger than 0.8.

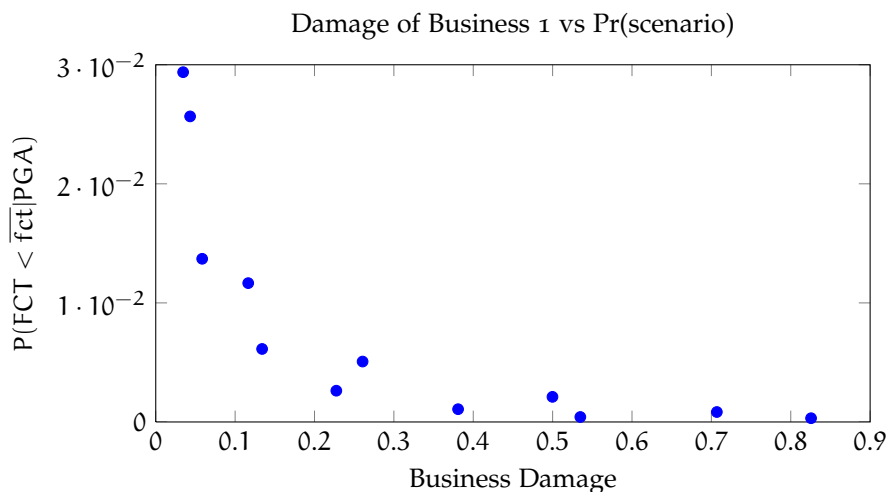


Figure 3.20: Risk curve in terms of business damage vs the probability of scenario.

3.4.4 Indirect economic losses

It's interesting to compute how the earthquake affects the economic capacity of the affected region. This is done relating the residual productive capacity to the gross regional product. The residual gross product is the product of the residual functionality times the un-affected gross regional product.

$$\text{Loss} = \text{RF} \times \text{GRP}_0 \tag{70}$$

where:

- Loss Economic indirect losses from current scenario due to diminished production;
- RF Residual Functionality of industrial zone due to earthquake damage;
- GRP₀ Reference Gross Regional Product contribution before earthquake.

Using equation (70) from the residual functionality the indirect economic loss is computed. In figure 3.21 the "Indirect losses" due to earthquake damage to industrial facilities are plotted. According to simulation, the earthquake with an occurrence probability of $3.0 \cdot 10^{-4}$ in the productive area #1 reduces the GRP contribution to 3.76B EUR. While earthquake with higher annual probability of occurrence, i.e. $3.0 \cdot 10^{-2}$, leave practically unaffected the productivity with a loss of 3%. In figure 3.22 the risk curve for the entire analyzed region is presented. The curve is made using an interpolation of data from the scenario analyses using 400 Monte Carlo iterations.

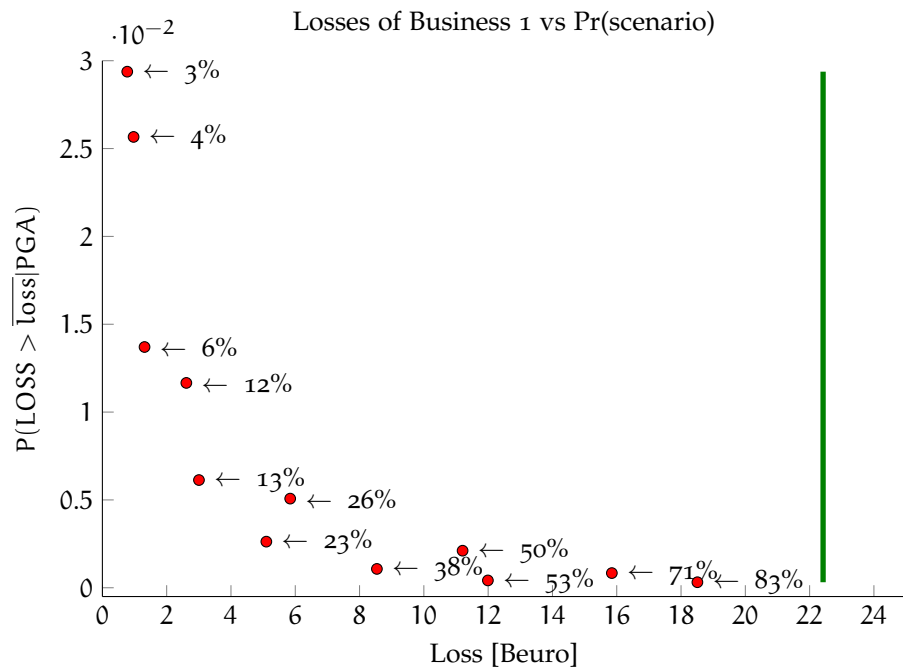


Figure 3.21: The first productive zone risk curve. The green line on the righthand side is the contribution of the zone to GRP, i.e. 22.4B EUR

The same analysis of residual productivity is done on the 4 productive zones. The reduced productivity is generated with the same method, i.e. the residual functionality of each zone is the linear responsible for GRP reduction, given its contribution as in table 3.4 . Figure 3.22 presents the risk

curve of the region obtained as a cubic regression on the plane of logarithm of probabilities (y-axis) and economic losses (x-axis).

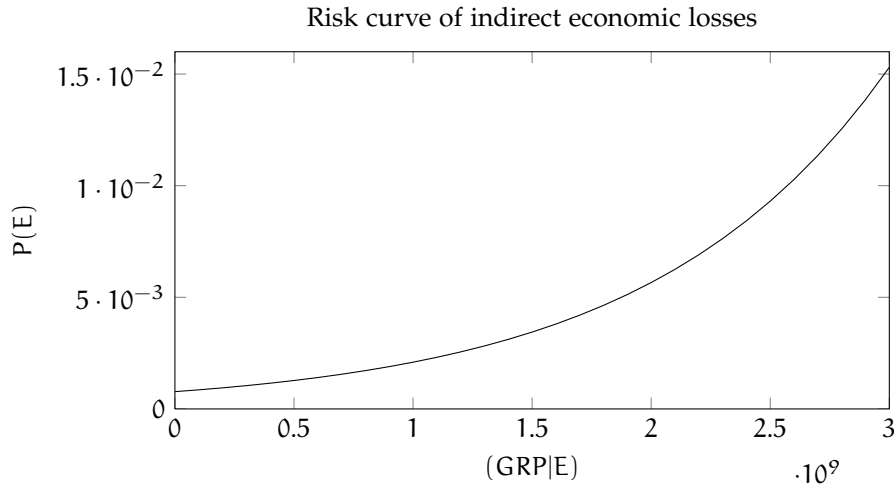


Figure 3.22: The risk curve of the residual GRP after the earthquake.

3.5 TIME DOMAIN ANALYSIS

The post earthquake scenarios exhibits many societal changes. The state government and the civil protection agencies immediately start to help the hit population, while lifeline managers start their emergency procedures to recover as soon as possible all the facilities. Engineers start their work to assess the structural health of buildings and infrastructures.

In the immediate post event, the structure of society changes to adapt itself to a new urban configuration. After the first shock, people are moved in temporary shelters until their houses are assessed for structural safety. If reconstruction in the same area is not feasible, new settlement areas are identified and residential building are constructed.

The same happens to buildings that are used for production. According to the size of the activity some parts of production can be dislocated in different areas of the plant or relocated in different plants; while other activities, that are not strong enough to support the treat may go out of business.

In general terms the reconstruction process is a key feature of the new arrangement of the area. Reconstruction is a pricey and very time consuming operation.

The challenge of the work is to simulate this recovery transitory when the building stock goes back to pre-earthquake situation or moves to a different configuration. Here we try to simulate the process from the engineering point of view by looking at the macro-economical effects of this process.

The simulation is a challenging task because several elements need to be accounted. The economic system is complex, each business is related to others in a multi connected network. Forward link connection can be damaged, this is a supply damage. On the other hand, the consume link can experience damage, this is a backward damage.

Other effects are financial, one should account the borrowing cost of capitals needed for reconstruction or economic aids from government agencies.

A very delicate relationship is between the businesses and the transportation system. It can happen that a demand surge because of the reconstruction process completely changes the behavior.

To simulate this complex process some hypotheses are assumed:

- The external financial aids impact the reconstruction process reducing the reconstruction time.
- In the present work, as a first step to explore the connection with the transportation system connection we will assume some hypothesis shown in further paragraph 3.7 .
- Since the change in time of demand is hard to simulate, it has been assumed that future profits account for the grout of money de-valuation, i.e. the annual borrow cost is assumed to be 0%.

The model assumes that at the beginning it takes more time for industrial facilities to recover from an earthquake. On the long run, i.e. several years after the earthquake, all business recover to 100% of pre-earthquake functionality.

The model could be improved using a micro-economy model to account all the relation between businesses both inside the study area and outside.

In figure 3.23 there is a plot of the proposed model for recovery, in case of absence of external aids (a) and if external financial aids are given (b).

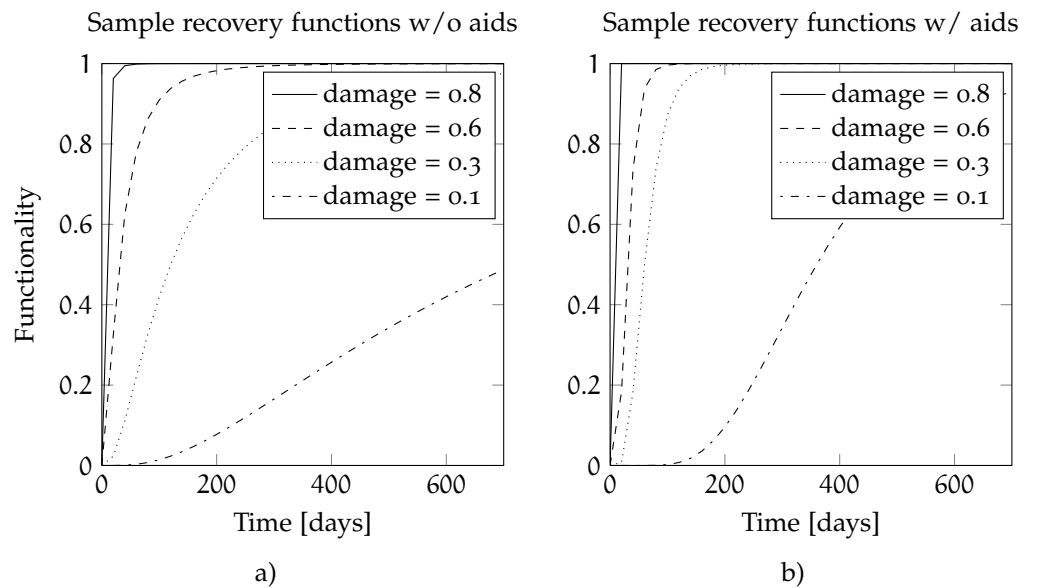


Figure 3.23: a) The proposed recovery model in case of absence of external aids.
 b) The proposed recovery model with financial aids.

3.5.1 Recovery model

The recovery model should account the residual functionality after earthquake, the possible external financial aid from government agencies, and the relation with different societal systems.

Observing past catastrophes it can be seen that, in the immediate post-event, it takes some times to restart the business.

One more observation, entrepreneurs that are waiting for financial aids, usually, delay the reconstruction process when the aids are available, instead of financing the process borrowing capitals from banks.

The proposed model follows a cumulative lognormal distribution with a fixed value for dispersion of 0.9 and a mean value according to table 3.7 :

$$R_{Fr} = \frac{1}{2} \operatorname{erfc} \left[-\frac{\ln t - \mu}{\sigma\sqrt{2}} \right] \quad (71)$$

where:

- R_{Fr} residual functionality recovery
- t is the time starting from day 0 (earthquake)
- erfc complementary error function
- μ and σ as in table 3.7 .

Residual functionality	Mean (w/o aids)	Mean (w/ aids)	Std. deviation
0.8 < RF < 1.0	4	4	0.9
0.4 < RF < 0.8	30	30	0.9
0.2 < RF < 0.4	120	60	0.9
0.0 < RF < 0.2	360 * 2	360	0.9

Table 3.7: Chosen parameters for simulation of the reconstruction process.

The simulation in time domain has been run starting from the earthquake scenarios. In figure 3.24 the recovery process is represented. The intersection between the line without aids(in black) and the line with aids(in red) represent the break-even point in time domain for the worthiness of financial aids. The same analysis can be done considering the economic process as in figure 3.25 .

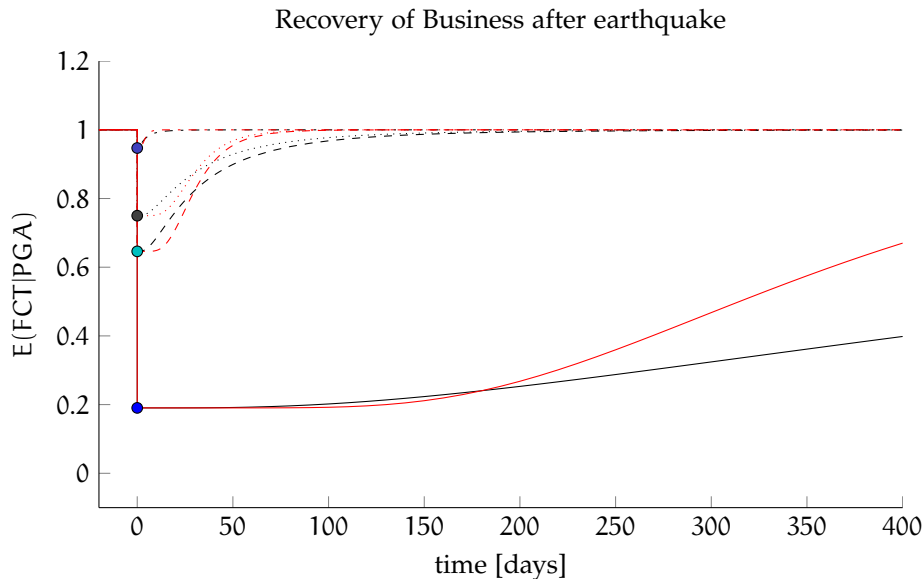


Figure 3.24: The curves represent the recovery process in term of residual functionality vs. time. The black line represent the recovery process with no external financial aids, the red curve with external financial aids.

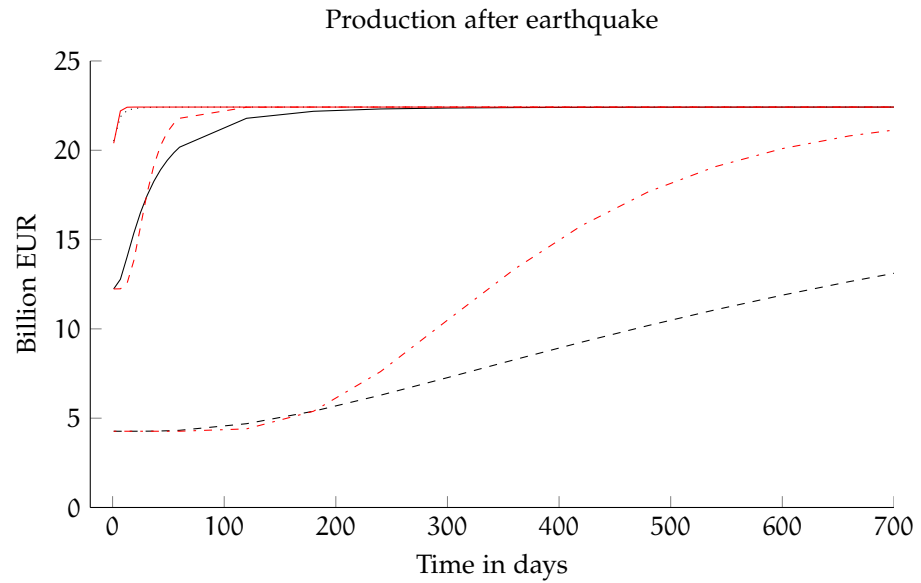


Figure 3.25: The production during the recovery process expressed in terms of economic losses some representatives earthquake scenarios.

3.6 COST BENEFIT ANALYSIS

The integral of curve in figure 3.25 is the Gross Regional Product. The difference with baseline is the indirect loss due to earthquake.

$$GRP_{eq} = \int_{t_0}^{t_{end}} RP dt \tag{72}$$

$$Losses = GRP_{ref} - GRP_{eq} \tag{73}$$

where:

- GRP Gross Regional Product, with subscript “ref” it refers to baseline, with subscript “eq” it refers to post-earthquake conditions.
- t_0 is day-zero the day of earthquake
- t_{end} day when the economy goes back to “normal” condition
- RP is the residual productivity
- Losses are the indirect losses due to earthquake.

Given the assumption in table 3.8 , an estimation of the reconstruction cost from with follows the amount of state aids as of the form:

$$Aids = Surf \times \#Buildgs \times RecCost \times (1 - RF) \tag{74}$$

where:

- Aids Total amount of predicted government aids
- Surf mean surface per building
- #Buildgs number of building in analysis zone
- RecCost unitary reconstruction cost
- $(1 - RF)$ Damage entity as complement to 1 of Residual functionality.

An application of proposed procedure follows showing the results of the analysis for the zone # 1: Treviso.

Parameter	Value
Square footage per building	1000 m ² /building
Number of building	# of businesses
Reconstruction cost	150EUR/m ²

Table 3.8: default

In zone #1 Treviso there are 20'826 industrial buildings. Figure 3.26 presents the contribution of the productive zone #1 to GRP under different scenario earthquakes. The difference between the black and white sets of bars is the increase in production when financial aids are given.

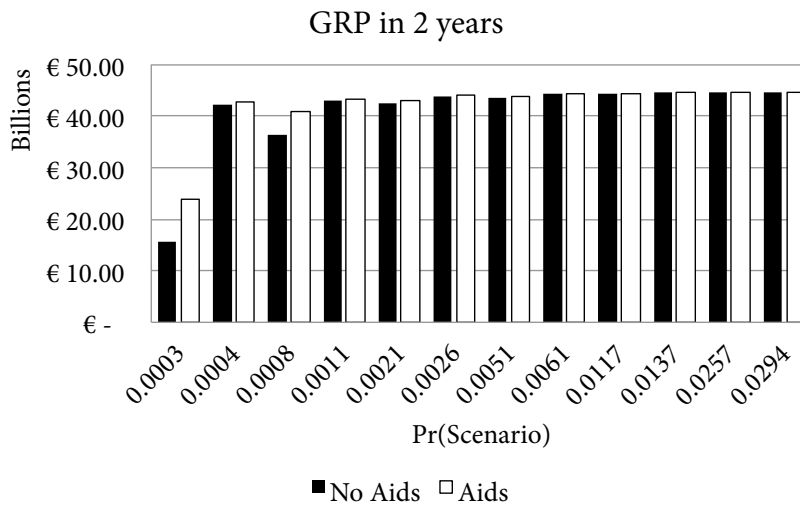


Figure 3.26: Contribution to GRP of the productive area #1: Treviso in two hypotheses of financial aids, and without. The difference between the two set of bars is the positive contribution of financial aids.

Under current hypotheses the financial aids helps to get a increase of 2.7 billions of EUR in 2 years of analysis, as shown in figure 3.27. The break-even point for the reconstruction cost is 225 EUR/m². The reconstruction cost is a key value in the decision process because the general profitability of the operation is strictly related to this assumption. In that area the value of 225 EUR/m² is quite low for industrial building. This observation suggest that unitary reconstruction cost must be accurately defined.

Although further researches are needed, it appears that the government financial help, from the societal point of view helps to reduce the the losses of gross regional product induced by earthquakes.

The transferring the risk to the insurance market can be profitable for the state because it helps in saving 2.8 billion of EUR of financial aids.

It's important to remember that the present analysis doesn't account the positive externalities of the operation, like the feeling of security of population, the increase of jobs offers, etc. if these parameter will be included in the econometric model could drastically change the judgement on the opportunity of the operation because more value will be added on the "benefit side" of the Benefit Cost equation.

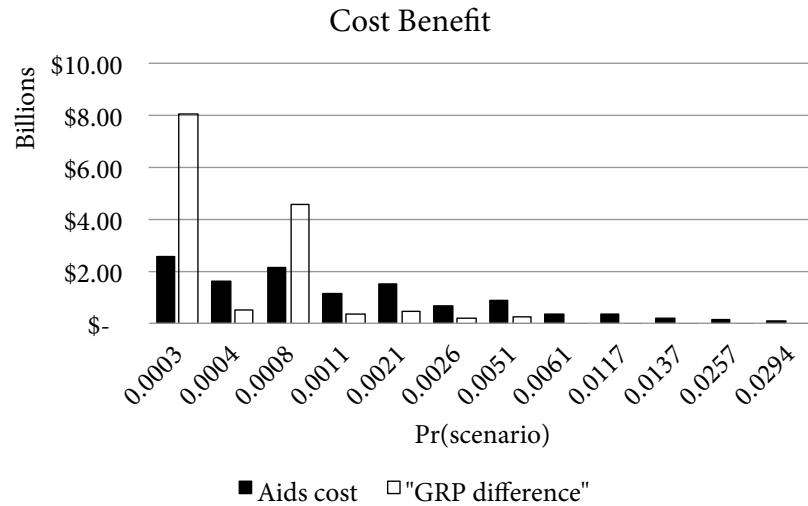


Figure 3.27: Cost benefit analysis. If the increase in GRP bar is higher than the aids cost bar, the operation is cost effective.

3.7 RELATION BUSINESSES–TRANSPORTATION SYSTEM

After the 1994 Northridge earthquake 43% of the firms that reported any loss due to earthquake stated that some portion of the losses was generated by transportation damage and the related issues. The firms also stated that 39% was the average loss connected with disruption to transportation system[6]. The firm self-reported an average loss of 85'026 USD. An interesting remark on the same paper is about the severity of transportation impacts to the businesses; in table 3.9 are reported the consequences on a scale ranging from 1 to 5 as perceived by the participants to the survey. The reported commutes employees that experienced higher time reaches up to 40% of them. In the paper the authors estimate that the 6.5 billion USD indirect losses caused by earthquake damage a 1.5 billion contribution was due to transportation system damage.

According to Gordon et al. 1998[16] the four types of transport related interruption(i.e. commuting, inhibited customer access, shipping and supply disruption) caused a job loss of more than 15'700 person-year.

The strong connection between business damage and transportation network damage has been shown after historical earthquakes. It's importation to focus on the connection between the two systems. Now it's crucial to investigate the relation between the business damage and the gross regional product.

The schema of the analysis procedure has been shown by authors in [7] and [30]. In figure 3.28 is reported the transportation simulation module schema.

The transportation network has a spatial extension of approximately 100 km x 100 km. The topological model has been represented using 11'149 link, 5'924 nodes. The network has 41 bridges that are in shaded area of figure 3.29 . Transportation system has been simulated using Frank and Wolfe algorithm, with a BRP cost function for links.

Earthquake-Related Impact	Average score on 1 to 5 scale	% of scores 4 or 5
Customer Access to Business	1.52	8.63%
Employee Access to Business	1.60	8.87%
Shipping Delays To Business	1.94	11.80%
Shipping Delays From Business	1.72	10.02%
Building Damage	1.38	4.48%
Utility Cut-Offs	1.69	10.99%
Higher Costs for Goods	1.32	3.96%
Inventory Loss or Damage	1.56	9.31%
Repair (not in Bldg. Damage)	1.70	10.84%
Seismic Retrofit (not in above)	1.21	2.34%

Table 3.9: Damage reported by firms after the 1994 Northridge earthquake due to transportation system.

For the simulation of the consequences to transportation system some hypotheses are assumed.

3.7.1 Hypotheses

To represent the connection between the activity system and the transportation system some hypotheses are assumed.

The idea is to simulate the relation with a damaged network and a demand that varies due to earthquake damage to activity system. The present model doesn't represent the damage to residential system. One should note that the freight demand is directly related to business disruption while the car demand is affected by business damage only for its business component.

In general terms the model is:

$$OD_{business} = f(BD) \quad (75)$$

where:

$OD_{business}$ is the transportation demand in general terms
 BD is the business damage.

The above observation are translated into the following hypotheses:

- The transportation demand from centroid i to centroid j is reduced as:
 - freight demand has a linear relationship
 - light vehicles demand is reduced by a factor 0.5
- The transportation network (supply side of the problem), is damaged by earthquake according to model in paragraph 2.6.4 .

The equation (75) can be particularized to account the hypotheses as:

$$OD_{eq, freight} = OD_{0, ij} \cdot BRF \quad (76)$$

$$OD_{eq, light} = OD_{0, ij} \cdot (0.5 + 0.5 \cdot BRF) \quad (77)$$

where:

$OD_{eq, freight}$ is the transportation demand of trucks
 $OD_{eq, light}$ is the transportation demand of cars
 $OD_{0, ij}$ is the pre-earthquake transportation demand
 BRF is the business residual functionality.

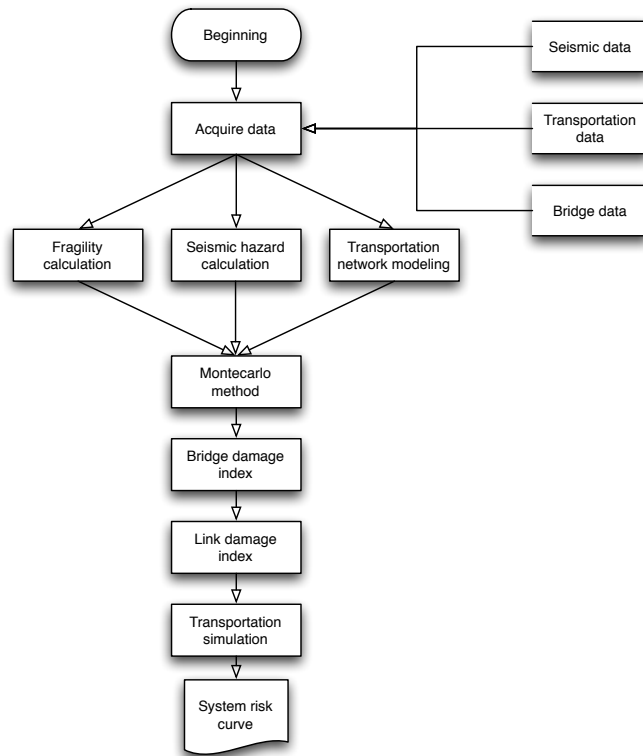


Figure 3.28: Transportation module analysis schema.

In figure 3.30 there's a representation of the analyzed business areas, in yellow squares, and the centroids of the network represented as red diamonds. To complete the model it's necessary to produce a correspondence matrix from the business areas to the related centroids.

The relation from the damaged business areas and the related centroids is expressed with an incidence table:

$$I(BU_n; \text{Centroid}) \tag{78}$$

where:

I is the incidence table where each row is composed as follows:

BU_n is the n-th business area

Centroid is the centroid.

In figure 3.31 the graphical representation that shows this relation table. The correspondence between each productive area and the centroids is based on data from the census. With more data available the discretization of the business area can be the one of each census tract, so the correspondence table is no longer needed.

The resulting risk curve from the transportation analysis is given in figure 3.32 .

3.8 GENERAL LOSS MODEL

The general loss model is:

$$\text{Loss} = D + I \tag{79}$$

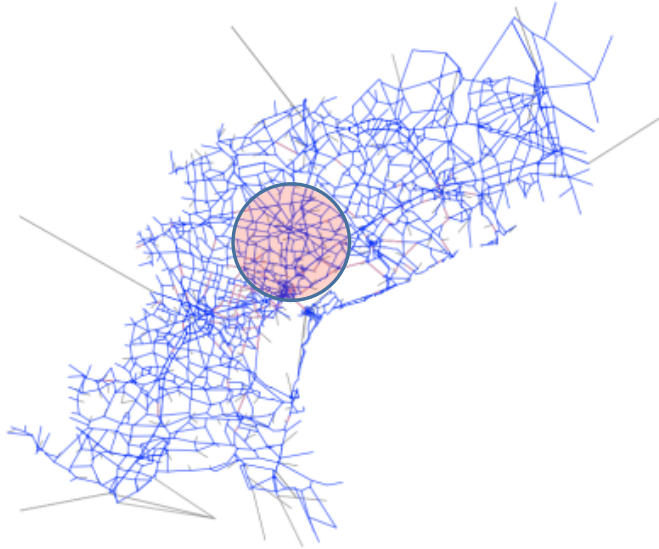


Figure 3.29: The partial Veneto transportation network topological model. The shaded area represents the analysis area where the earthquake scenarios are made and bridges damage are simulated.

$$D = BU + Br \quad (80)$$

$$I = \text{Time} + \text{Product} \quad (81)$$

where:

D	Direct Losses
I	Indirect losses
Bu	Direct losses connected to reconstruction cost in buildings
Br	Direct losses in term of bridge reconstruction or rehabilitation cost
Time	The increase in transportation network time can be monetized 15.00 EUR per hour
Product	Loss of production due to earthquake damage to industrial facilities.

Direct losses are computed as the direct cost of replacement or repair of industrial building as described in section 3.6 ; for bridges direct losses are related to the cost of reconstruction or repair, and are parametrized to the square footage of decking.

Indirect losses are defined as the reduction of productivity for businesses with respect to baseline, that is the condition pre-earthquake. Indirect losses related to transportation network are defined as the increase of total network time with respect to baseline condition, i.e. with network un-damaged and demand as pre-earthquake

3.9 NOTES ON PARALLELIZATION

Since the code requires several calculations to obtain data on several business and bridges, all the calculation have been performed in parallel, parallelizing the for cycles when data was already available.

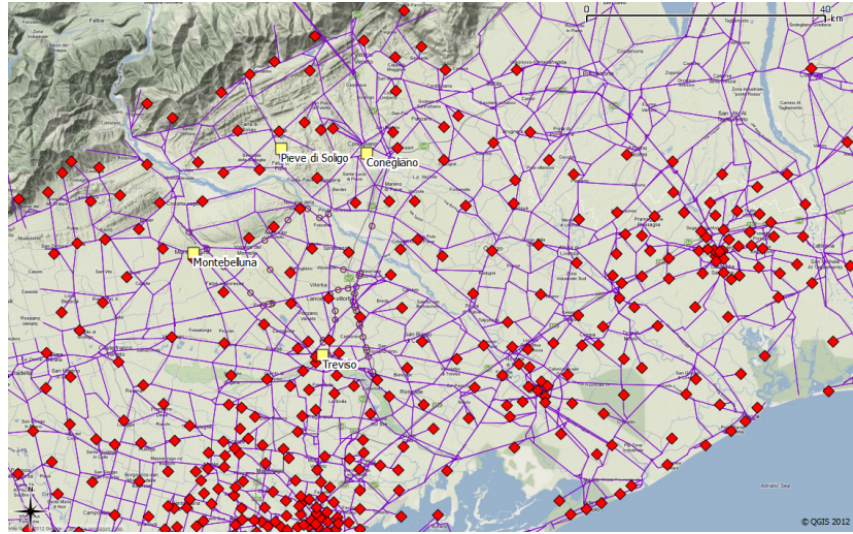


Figure 3.30: The figure represents the centroids in the transportation network in red diamonds. The yellow squares are the productive zones. The purple lines are the link of the transportation network.

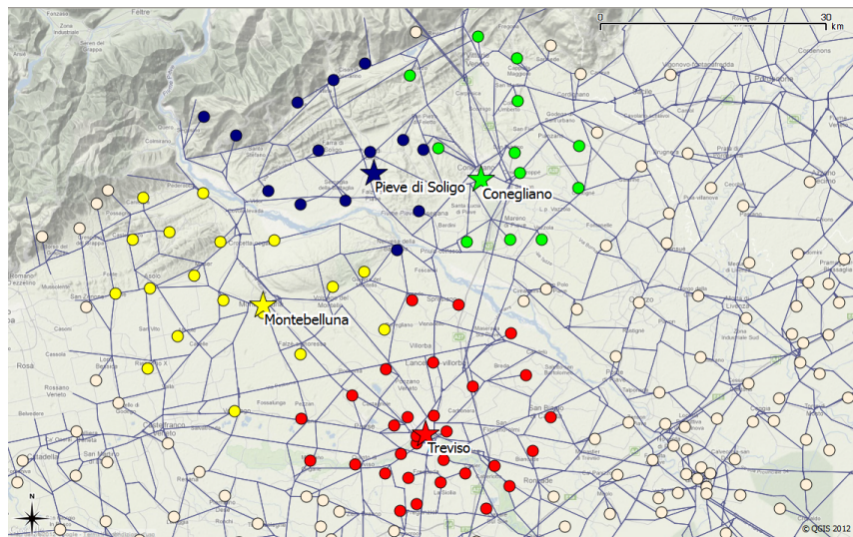


Figure 3.31: The figure shows the relation between the productive areas, as stars, and the centroids of the transportation model. The colors match the productive areas and the centroids.

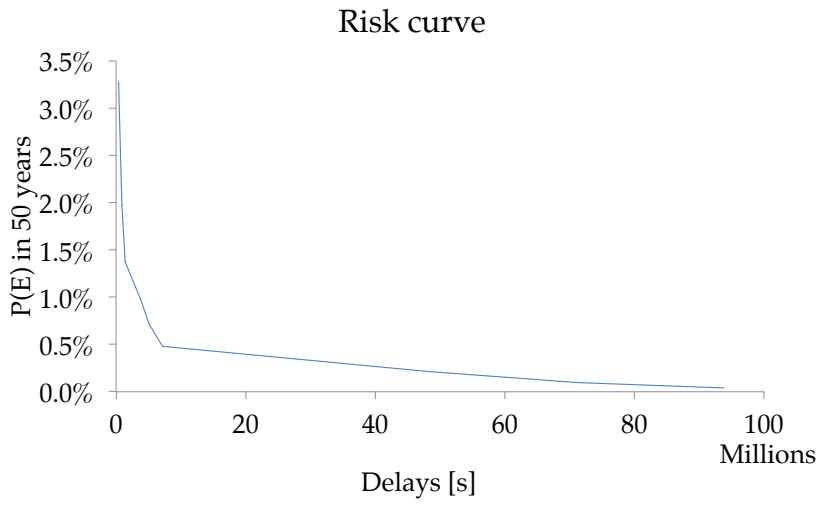


Figure 3.32: Risk in transportation network as delay due to damages to network.

4 | DISCUSSION

CONTENTS

4.1	Conclusions	81
4.2	Future work	82

4.1 CONCLUSIONS

In this thesis an innovative procedure, using seismogenic zones, for earthquake scenario generation has been proposed. The proposed method can be generalized for different areas and different seismogenic sources.

As set of hazard consistent scenario earthquakes for northeast Italy has been generated. These scenario earthquakes can be used also for further studies.

A model to describe residual functionality for productive buildings starting from fragility description has been proposed. The model can be calibrated using historical data, if available.

A novel model for the recovery process of businesses has been proposed and used to evaluate the process of recovery in time dimension.

The effects of external financial aids, e.g. funded by government after catastrophes, have been investigated and a funding priority has been explored. The study expressed the need of caution in the assumption of input parameters since the response of the model is directly related to that.

The relation between transportation system and production system has been investigated and a relation model has been proposed and tested.

The possible applications of the proposed procedure in insurance and re-insurance market is the use of the proposed procedure to price products, to improve portfolios of risks, to better understand emerging markets, to get a fast post-event estimation of future expenses, etc.

In the field of community planning; for industrial association, the model can be used to test the resilience of productive areas to extreme hazardous events; government agencies can use the results of the presented tool as a decision support system that helps in evaluating different policies and evaluate possible losses of revenues from tax collection. Government agencies could utilize the results to plan retrofitting interventions and decide how financial helps should be allocated.

Civil protection agencies can use the present tool to map the risk of buildings, to determine, after an event, the number of injured people and the buildings that require an assessment of their safety. The outcomes can be used also to plan the emergency by defining the best paths to reduce intervention times, if streets are congested or bridges collapsed.

4.2 FUTURE WORK

1. Using energy instead of a seismic demand parameter the proposed procedure can be extended to be multi-perils, accounting for earthquakes, hurricanes, tsunamis, wildfires, etc.
2. Extend the damage to bridges accounting effects of liquefaction, landslide.
3. Extend the damage to transportation network accounting the damage to roads caused by the permanent ground displacement and accounting the loss of transit-ability due to debris on the road (especially inside the town center where building collapsing may invade the road site).
4. Account the directionality of the earthquake, improve the seismic module using physic modeling and simulation by mean of f.e. software of the faulting mechanism and wave propagation. The stochastic earthquake models adequately represent the distribution of event sizes and frequency and, hence, are widely used in the estimation of hazard. However, the incorporation of mechanistic approach into a stochastic model would provide a better understanding of seismic processes underlying earthquakes.
5. Explore the economic effectiveness of financial aids for retrofitting instead of ex-post funding for reconstruction.
6. Improve the accuracy of the economic analysis using more detailed data for the economic modeling of the productive system.
7. Improve the transportation module using a generation model. This implementation will allow the model to simulate if the phenomena of demand surge will happen or not.
8. Improve the fragility description model including a simulation of each bridge usign a f.e. model and non linear time history analysis.
9. Test the proposed procedure with data from insurance market to explore a new field of applicability.

BIBLIOGRAPHY

- [1] AA.VV. (wikipedia entry) list of earthquakes: Property damages caused by earthquake.
- [2] AA.VV. Hazards u.s. - multi-hazard (hazus-mh). Technical report, Federal Emergency Management Agency (FEMA), 2012.
- [3] N. N. AMBRASEYS, K. A. SIMPSON, and J. J. BOMMER. Prediction of horizontal response spectra in europe. *Earthquake Engineering and Structural Dynamics*, 25(4):371–400, 1996.
- [4] BBCNews. Italy’s earthquake history.
- [5] D. Bindi, F. Pacor, L. Luzi, R. Puglia, M. Massa, G. Ameri, and R. Paolucci. Ground motion prediction equations derived from the italian strong motion database. *Bulletin of Earthquake Engineering*, 9:1899–1920, 2011.
- [6] Marlon G. Boarnet. Business losses, transportation damage and the northridge earthquake. Technical report, The University of California Transportation Center, 1996.
- [7] Federico Carturan, Carlo Pellegrino, Riccardo Rossi, Massimiliano Gastaldi, and Claudio Modena. An integrated procedure for management of bridge networks in seismic areas. *Bulletin of Earthquake Engineering*, pages 1–17, 2012.
- [8] Stephanie E. Chang, Masanobu Shinozuka, and James E. Moore. Probabilistic earthquake scenarios: Extending risk analysis methodologies to spatially distributed systems. *Earthquake Spectra*, 16(3):557–572, August 2000.
- [9] Sungbin et al. Cho. *Integrating transportation network and regional economic models to estimate the costs of a large earthquake*. University of Southern California, 2000.
- [10] C. Allin Cornell. Engineering seismic risk analysis. *Bulletin of the Seismological Society of America*, 58(5):1583–1606, 1968.
- [11] Sleijko D. and Rebez A. Probabilistic seismic hazard assessment and deterministic ground shaking scenarios for vittorio veneto (n.e. italy), 2002.
- [12] Gruppo di Lavoro. Redazione della mappa di pericolosità sismica prevista dall’ordinanza pcm 3274 del 20 marzo 2003. rapporto conclusivo per il dipartimento della protezione civile. Technical report, INGV, 2004.
- [13] R. T. Eguchi. Real-time loss estimation as an emergency response decision support system: the early post-earthquake damage assessment tool (epedat), 1997.
- [14] Karaka Erdem. *Regional earthquake loss estimation: Role of transportation network, sensitivity and uncertainty, and risk mitigation*. PhD thesis, Massachusetts Institute of Technology, 2005.

Bibliography

- [15] Marguerite Frank and Philip Wolfe. An algorithm for quadratic programming. *Naval Research Logistics Quarterly*, 3(1-2):95–110, 1956.
- [16] Peter Gordon, W. Richardson, Harry, and Bill Davis. Transport-related impacts of the northridge earthquake. *Journal of Transportation and Statistics*, 1(2):21–36, 1998.
- [17] William T. Holmes and Robert Reitherman. Preface. *Earthquake Spectra*, 22(S2):3–9, April 2006.
- [18] Nirmal Jayaram and Jack W. Baker. Efficient sampling and data reduction techniques for probabilistic seismic lifeline risk assessment. *Earthquake Engineering and Structural Dynamics*, 39(10):1109 – 1131, 2010. Efficient simulation;Importance sampling;K-means clustering;Lifeline;Seismic risk;Transportation network;.
- [19] Róbert Jelínek and Elisabeth Krausmann. Approaches to tsunami risk assessment. Technical report, Joint Research Center, 2008.
- [20] Victoria Kim. Japan damage could reach usd 235 billion, world bank estimates. *Los Angeles Times*, April 2011.
- [21] AnneS. Kiremidjian, Evangelos Stergiou, and Renee Lee. Seismic risk assessment of transportation networks. In KyriazisD. Pitolakis, editor, *Earthquake Geotechnical Engineering*, volume 6 of *Geotechnical, Geological and Earthquake Engineering*, pages 461–480. Springer Netherlands, 2007.
- [22] S.L.A. Kramer. *Geotechnical Earthquake Engineering*. Prentice-Hall Civil Engineering & Engineering Mechanics Series. Prentice Hall, 1996.
- [23] MATLAB. *version 7.14.0 (r2012a)*. The Mathworks, Inc., 2012.
- [24] N Metropolis and S Ulam. The monte carlo method. *Journal of the American statistical Association*, 44(247):335–341, 1949.
- [25] James E. Moore, Richard G. Little, Sungbin Cho, and Shin Lee. Using regional economic models to estimate the costs of infrastructure failures: The cost of a limited interruption in electric power in the los angeles region. *Public Works Management and Policy*, 10(3):256–274, 2006.
- [26] Pierre Mouroux and BenoîtLe Brun. Presentation of risk-ue project. *Bulletin of Earthquake Engineering*, 4:323–339, 2006.
- [27] Basoz Nesrin and Kiremidjian Anne. *Risk Assessment for Highway Transportation Systems*. Phd dissertation, Department of Civil Engineering, Stanford University, 1996.
- [28] A. Peresan, E. Zuccolo, F. Vaccari, A. Gorshkov, and G.F. Panza. Neodeterministic seismic hazard and pattern recognition techniques: Time-dependent scenarios for north-eastern italy. *Pure and Applied Geophysics*, 168:583–607, 2011.
- [29] L. Reiter. *Earthquake Hazard Analysis: Issues and Insights*. Columbia University Press, 1990.
- [30] Riccardo Rossi, Massimiliano Gastaldi, Federico Carturan, Carlo Pellegrino, and Claudio Modena. Planning and management of actions on transportation system to address extraordinary events in post-emergency situations. a multidisciplinary approach. *European Transport Trasporti Europei*, 3(51), 2012.

- [31] F. Sabetta and A. Pugliese. Estimation of response spectra and simulation of nonstationary earthquake ground motions. *Bulletin of the Seismological Society of America*, 86(2):337–352, 1996.
- [32] M. Shinozuka, M. Feng, J. Lee, and T. Naganuma. Statistical analysis of fragility curves. *Journal of Engineering Mechanics*, 126(12):1224–1231, 2000.
- [33] E. C. Stergiou and Anne S. Kiremidjian. *Treatment of uncertainties in seismic risk analysis fo Transportation systems*. PhD thesis, Department of Civil Engineering, Stanford University, 2006.
- [34] S.D. Werner, United States. Federal Highway Administration, and Multidisciplinary Center for Earthquake Engineering Research (U.S.). *REDARS 2 methodology and software for seismic risk analysis of highway systems*. Special report. Multidisciplinary Center for Earthquake Engineering Research, 2006.